BioMed Research International

Scaffolds Reinforced by Fibers or Tubes for Tissue Repair

Guest Editors: Xiaoming Li, Nicholas Dunne, Xiaowei Li, and Katerina E. Aifantis

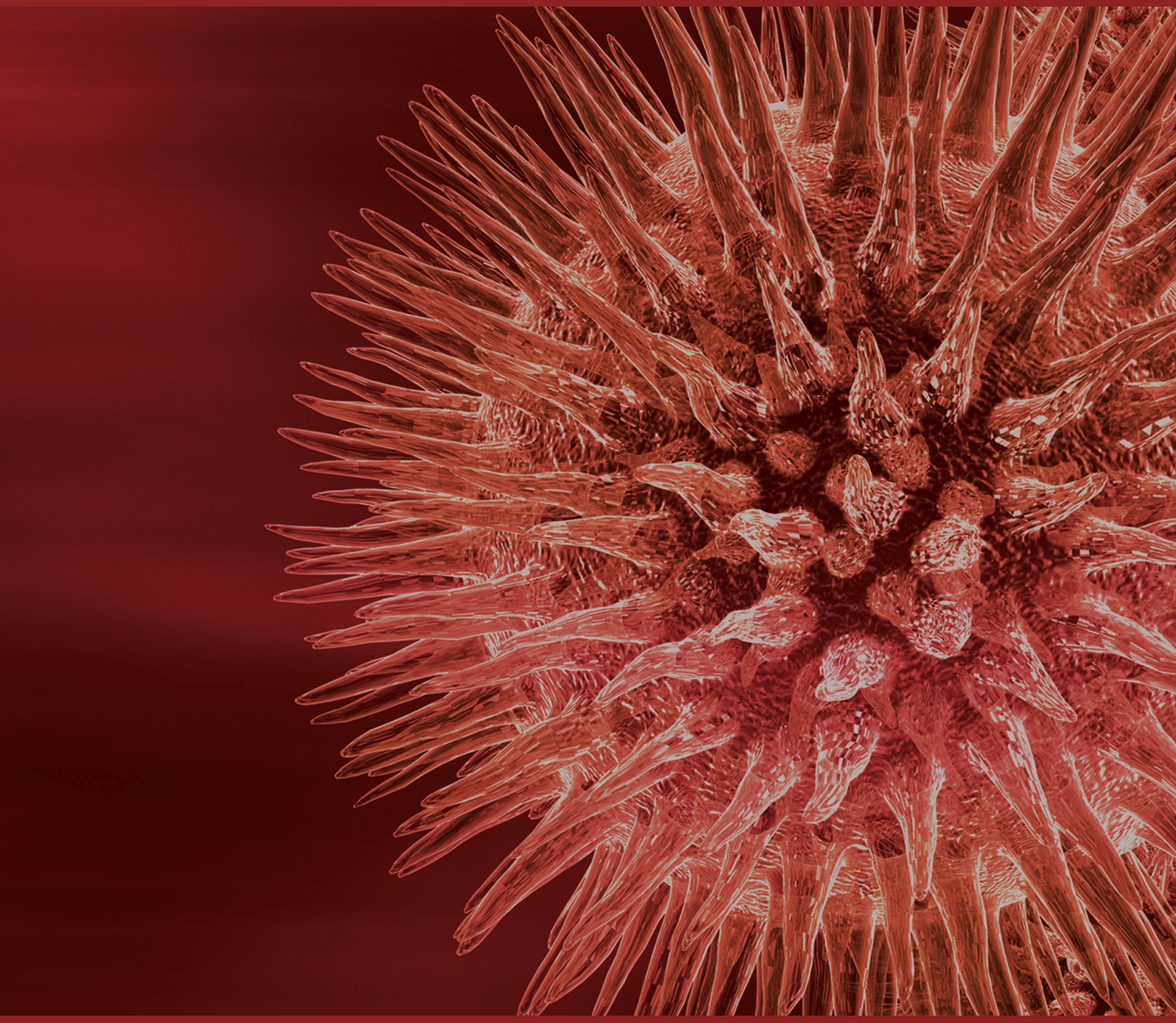

Scaffolds Reinforced by Fibers or Tubes for Tissue Repair

BioMed Research International

Scaffolds Reinforced by Fibers or Tubes for Tissue Repair

Guest Editors: Xiaoming Li, Nicholas Dunne, Xiaowei Li, and Katerina E. Aifantis

Copyright © 2014 Hindawi Publishing Corporation. All rights reserved.

This is a special issue published in "BioMed Research International." All articles are open access articles distributed under the Creative Commons Attribution License, which permits unrestricted use, distribution, and reproduction in any medium, provided the original work is properly cited.

Contents

Scaffolds Reinforced by Fibers or Tubes for Tissue Repair, Xiaoming Li, Nicholas Dunne, Xiaowei Li, and Katerina E. Aifantis
Volume 2014, Article ID 501275, 2 pages

Resin Composites Reinforced by Nanoscaled Fibers or Tubes for Dental Regeneration, Xiaoming Li, Wei Liu, Lianwen Sun, Katerina E. Aifantis, Bo Yu, Yubo Fan, Qingling Feng, Fuzhai Cui, and Fumio Watari
Volume 2014, Article ID 542958, 13 pages

Application of Ultrasound on Monitoring the Evolution of the Collagen Fiber Reinforced nHAC/CS Composites *In Vivo*, Yan Chen, Yuting Yan, Xiaoming Li, He Li, Huiting Tan, Huajun Li, Yanwen Zhu, Philipp Niemeyer, Matin Yaega, and Bo Yu
Volume 2014, Article ID 418302, 9 pages

Carbon Nanotubes Reinforced Composites for Biomedical Applications, Wei Wang, Yuhe Zhu, Susan Liao, and Jiajia Li
Volume 2014, Article ID 518609, 14 pages

The Use of Fiber-Reinforced Scaffolds Cocultured with Schwann Cells and Vascular Endothelial Cells to Repair Rabbit Sciatic Nerve Defect with Vascularization, Hongyang Gao, Yang You, Guoping Zhang, Feng Zhao, Ziyi Sha, and Yong Shen
Volume 2013, Article ID 362918, 7 pages

The Application of Fiber-Reinforced Materials in Disc Repair, Bao-Qing Pei, Hui Li, Gang Zhu, De-Yu Li, Yu-Bo Fan, and Shu-Qin Wu
Volume 2013, Article ID 714103, 10 pages

Vascularized Bone Tissue Formation Induced by Fiber-Reinforced Scaffolds Cultured with Osteoblasts and Endothelial Cells, Xinhui Liu, Guoping Zhang, Chuanyong Hou, Hua Wang, Yelin Yang, Guoping Guan, Wei Dong, Hongyang Gao, and Qingling Feng
Volume 2013, Article ID 854917, 7 pages

Hindawi Publishing Corporation
BioMed Research International
Volume 2014, Article ID 501275, 2 pages
http://dx.doi.org/10.1155/2014/501275

Editorial

Scaffolds Reinforced by Fibers or Tubes for Tissue Repair

Xiaoming Li,[1] Nicholas Dunne,[2] Xiaowei Li,[3] and Katerina E. Aifantis[4]

[1] *Key Laboratory for Biomechanics and Mechanobiology of Ministry of Education, School of Biological Science and Medical Engineering, Beihang University, Beijing 100191, China*
[2] *School of Mechanical & Aerospace Engineering, Queen's University of Belfast, Belfast BT7 1NN, Northern Ireland*
[3] *Translational Tissue Engineering Center and Whitaker Biomedical Engineering Institute, Johns Hopkins University, Baltimore, MD 21218, USA*
[4] *College of Engineering, University of Arizona, Tucson, AZ 85721, USA*

Correspondence should be addressed to Xiaoming Li; x.m.li@hotmail.com

Received 13 April 2014; Accepted 13 April 2014; Published 18 August 2014

Copyright © 2014 Xiaoming Li et al. This is an open access article distributed under the Creative Commons Attribution License, which permits unrestricted use, distribution, and reproduction in any medium, provided the original work is properly cited.

The final purpose of tissue engineering is to regenerate or repair defective/damaged tissues and organs. One of vital approaches is to use the various porous scaffolds to simulate the extracellular matrix (ECM) for cellular attachment, proliferation, and differentiation. On the other hand, scaffold materials not only offer mechanical support for embedded cells, but also create a three-dimensional environment for special cells at the same time, which contributes to the repair of tissues and organs. So scaffolds have been an increasingly hot research field because its huge potential in tissue repair engineering [1–3]. Ideal scaffolds are expected to have excellent mechanical properties and biomimetic effect.

In addition to porous and stereo structure, good biocompatibility and biodegradation, and the chance to offer appropriate space environment for cell division and tissue growth, the cracking strength is the essential condition for an ideal scaffold, especially in the condition of tissue implantation [4, 5].

However, generally speaking, considering the mechanical properties of various scaffolds, substantial scaffold materials could not provide enough mechanical support for embedded cells; that is to say, lack of strength restricts the use of scaffolds to great extent. In a sense, the strength of scaffolds determines the scope of its application.

Currently, kinds of fibers or tubes alternatives have been employed to reinforce the scaffolds for repairing specific tissues, such as ceramic fibers/tubes and polymer fibers/tubes [6]. For example, biodegradable synthetic and natural polymers are currently widely used to fabricate tissue engineering scaffolds. Synthetic PLA is a nontoxic, biocompatible, and biodegradable material widely used in tissue engineering [7, 8]. However, the mechanical properties of PLA scaffolds were much lower than that of natural bone. Furthermore, along with the degradation of the scaffold, the overall strength decreases too fast. So, it is adverse for repairing large defect and keeping the restoration for a long time. On the other hand, chitosan is a unique cationic polysaccharide with many attractive properties, including hydrophilicity, nontoxicity, and cell affinity [9–12]. To reinforce PLA scaffold, chitosan fibers are used to be natural reinforced phase; for example, Jiao et al. reported that coating chitosan on a microscale PLA scaffold could improve its mechanical strength and cell compatibility [13]. Similarly, calcium phosphates are commonly used materials for the restoration of bone defects with excellent biocompatibility and bioactivity. However, brittleness and low flexural/tensile strength so far limit their application to nonload bearing areas. Reinforcement of calcium phosphate cements with fibers can substantially improve its strength and toughness and has been one major strategy to overcome the present mechanical limitations of calcium phosphate cements. Fiber reinforced calcium phosphate cements thus bear the potential to facilitate the use of degradable bone substitutes in load bearing applications. There are lots of cases like the above examples; we will not introduce one by one; in one word, although three-dimensional porous scaffolds posses outstanding biocompatibility, biodegradability and also have huge promising application in different tissue regeneration, to meet different needs

of clinical applications, mechanical properties of desirable scaffolds should be further improved by means of addition of different appropriate fibers or tubes. However, a new problem emerges simultaneously, for the purpose of reinforcing the scaffold truly, on how we disperse the reinforcing phase into matrix uniformly, thus acquiring a homogeneous structure and component scaffolds.

In most cases, the interaction of fillers and matrix determines the reinforcing effect directly. Some measures could be taken to increase the bonding force between fillers and matrix, such as disperse fibers or tubes well as far as possible and functionalize the surface of fillers in order to enhance the scaffold. What is more, additional studies are required for making a better understanding of how the fibers or tubes influence the strength and biocompatibility of the scaffolds.

In this special issue, several articles are mainly focus on some specific applications of scaffolds reinforced by fibers or tubes, a few novel fibers or tubes with excellent performance, and the interactions between fibers or tubes and matrix as well as mechanisms of reinforcement of fibers or tube. Not only up-to-date reviews and application about scaffolds reinforced by fibers or tubes for tissue repair could be found, but also the impact of fibers or tubes on the biocompatibility and biodegradability of the scaffolds in this issue. Besides, it will make you have a good understanding of the chemical functionalization of different fibers or tubes and different kinds of link force, such as chemical bond, Van der Waals' force, and physical force. All in all, the issue will give a brief presentation about scaffolds reinforced by fibers or tubes, and most importantly, it will provide a general guide for the fabrication of more desirable scaffolds.

Xiaoming Li
Nicholas Dunne
Xiaowei Li
Katerina E. Aifantis

References

[1] L. Pang, Y. Hu, Y. Yan et al., "Surface modification of PLGA/β-TCP scaffold for bone tissue engineering: hybridization with collagen and apatite," *Surface and Coatings Technology*, vol. 201, no. 24, pp. 9549–9557, 2007.

[2] X. Li, C. A. van Blitterswijk, Q. Feng, F. Cui, and F. Watari, "The effect of calcium phosphate microstructure on bone-related cells in vitro," *Biomaterials*, vol. 29, no. 23, pp. 3306–3316, 2008.

[3] X. Li, H. Liu, X. Niu et al., "The use of carbon nanotubes to induce osteogenic differentiation of human adipose-derived MSCs in vitro and ectopic bone formation in vivo," *Biomaterials*, vol. 33, no. 19, pp. 4818–4827, 2012.

[4] J. H. Shepherd, S. Ghose, S. J. Kew, A. Moavenian, S. M. Best, and R. E. Cameron, "Effect of fiber crosslinking on collagen-fiber reinforced collagen-chondroitin-6-sulfate materials for regenerating load-bearing soft tissues," *Journal of Biomedical Materials Research A*, vol. 101, pp. 176–184, 2013.

[5] X. Li, L. Wang, Y. Fan, Q. Feng, F. Cui, and F. Watari, "Nanostructured scaffolds for bone tissue engineering," *Journal of Biomedical Materials Research A*, vol. 101, no. 8, pp. 2424–2435, 2013.

[6] X. Li, R. Cui, W. Liu et al., "The use of nano-scaled fibers or tubes to improve biocompatibility and bioactivity of biomedical materials," *Journal of Nanomaterials*, vol. 2013, Article ID 728130, 16 pages, 2013.

[7] X. Wang, G. Song, and T. Lou, "Fabrication and characterization of nano-composite scaffold of PLLA/silane modified hydroxyapatite," *Medical Engineering & Physics*, vol. 32, no. 4, pp. 391–397, 2010.

[8] H. Seyednejad, A. H. Ghassemi, C. F. van Nostrum, T. Vermonden, and W. E. Hennink, "Functional aliphatic polyesters for biomedical and pharmaceutical applications," *Journal of Controlled Release*, vol. 152, no. 1, pp. 168–176, 2011.

[9] E. Zakhem, S. Raghavan, R. R. Gilmont, and K. N. Bitar, "Chitosan-based scaffolds for the support of smooth muscle constructs in intestinal tissue engineering," *Biomaterials*, vol. 33, no. 19, pp. 4810–4817, 2012.

[10] W. Wei, P. P. Lv, X. M. Chen et al., "Codelivery of mTERT siRNA and paclitaxel by chitosan-based nanoparticles promoted synergistic tumor suppression," *Biomaterials*, vol. 34, no. 15, pp. 3912–3923, 2013.

[11] X. Li, Q. Feng, X. Liu, W. Dong, and F. Cui, "Collagen-based implants reinforced by chitin fibres in a goat shank bone defect model," *Biomaterials*, vol. 27, no. 9, pp. 1917–1923, 2006.

[12] S. Pattnaik, S. Nethala, A. Tripathi, S. Saravanan, A. Moorthi, and N. Selvamurugan, "Preparation, characterization and antimicrobial activity of a bio-composite scaffold containing chitosan/nano-hydroxyapatite/nano-silver for bone tissue engineering," *International Journal of Biological Macromolecules*, vol. 49, no. 2, pp. 188–193, 2011.

[13] Y. Jiao, Z. Liu, and C. Zhou, "Fabrication and characterization of PLLA-chitosan hybrid scaffolds with improved cell compatibility," *Journal of Biomedical Materials Research A*, vol. 80, no. 4, pp. 820–825, 2007.

Hindawi Publishing Corporation
BioMed Research International
Volume 2014, Article ID 542958, 13 pages
http://dx.doi.org/10.1155/2014/542958

Review Article

Resin Composites Reinforced by Nanoscaled Fibers or Tubes for Dental Regeneration

Xiaoming Li,[1] Wei Liu,[1] Lianwen Sun,[1] Katerina E. Aifantis,[2] Bo Yu,[3] Yubo Fan,[1] Qingling Feng,[4] Fuzhai Cui,[4] and Fumio Watari[5]

[1] *Key Laboratory for Biomechanics and Mechanobiology of Ministry of Education, School of Biological Science and Medical Engineering, Beihang University, Beijing 100191, China*
[2] *College of Engineering, University of Arizona, Tucson, AZ 85721, USA*
[3] *Department of Orthopedics, Zhujiang Hospital of Southern Medical University, Guangzhou 510282, China*
[4] *State Key Laboratory of New Ceramics and Fine Processing, Tsinghua University, Beijing 100084, China*
[5] *Department of Biomedical Materials and Engineering, Graduate School of Dental Medicine, Hokkaido University, Sapporo 060-8586, Japan*

Correspondence should be addressed to Xiaoming Li; x.m.li@hotmail.com, Bo Yu; gzyubo@gmail.com and Yubo Fan; yubofan@buaa.edu.cn

Received 30 November 2013; Accepted 4 March 2014; Published 27 May 2014

Academic Editor: Xiaowei Li

Copyright © 2014 Xiaoming Li et al. This is an open access article distributed under the Creative Commons Attribution License, which permits unrestricted use, distribution, and reproduction in any medium, provided the original work is properly cited.

It has been stated clearly that nanofillers could make an enhancement on the mechanical performances of dental composites. In order to address current shortage of traditional dental composites, fillers in forms of nanofibers or nanotubes are broadly regarded as ideal candidates to greatly increase mechanical performances of dental composites with low content of fillers. In this review, the efforts using nanofibers and nanotubes to reinforce mechanical performances of dental composites, including polymeric nanofibers, metallic nanofibers or nanotubes, and inorganic nanofibers or nanotubes, as well as their researches related, are demonstrated in sequence. The first purpose of current paper was to confirm the enhancement of nanofibers or nanotubes' reinforcement on the mechanical performances of dental restorative composite. The second purpose was to make a general description about the reinforcement mechanism of nanofibers and nanotubes, especially, the impact of formation of interphase boundary interaction and nanofibers themselves on the advanced mechanical behaviors of the dental composites. By means of the formation of interface interaction and poststretching nanofibers, reinforced effect of dental composites by sorts of nanofibers/nanotubes has been successfully obtained.

1. Introduction

In the past few decades, as a result of safety and esthetic consideration, dental composites have been generally accepted to substitute conventional "dental amalgams." The curing mode of dental composites is free radical polymerization induced by light. Generally speaking, we usually take Camphorquinone as common photoinitiator and ethyl-4-(dimethylamino) benzoate (4EDMAB) (Figure 1) as common coinitiator. Due to the excellence of dental restorative material in safety, esthetics, operation, and workability compared with amalgam, dental resin composites can be used extensively as dental restorative material for recent decades. 2,2′-Bis-[4-(methacryloxypropoxy)-phenyl]-propane (Bis-GMA) (Figure 1) is absolutely the most commonly used polymer monomer for dental resin composites [1, 2]. In order to increase the processing performance of Bis-GMA, we usually add extra polymer monomer such as tri (ethylene glycol) dimethacrylate (TEGDMA) (Figure 1) to dilute the viscosity of resin composites. So in this multiphase resin system, Bis-GMA plays a vital role in reducing volumetric shrinkage (created in the course of the photopolymerization), boosting reactivity of the composites and increasing conversion rate of double bond to some extent [3]. Small polymerization shrinkage, good processing operation, fatigue resistance, high fracture toughness and compressive strength, low heat conduction coefficient, and the capacity to meet the requirements

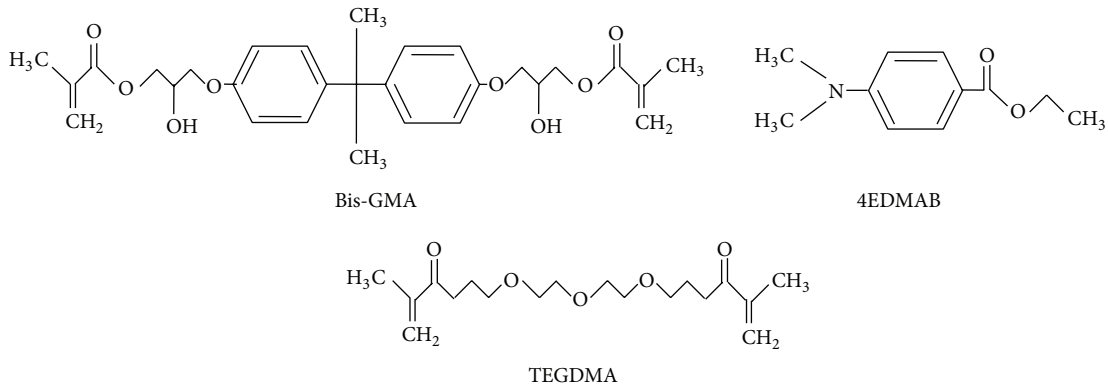

Figure 1: The molecular formula of common dental monomers and initiator.

of the aesthetics for the teeth are some vital characteristics for desired dental composites. According to a report in 2005, the percentage of all anterior tooth direct restorations and all posterior tooth direct restorations fabricated by the dental composites accounts for more than 95% and 50%, respectively [4]. Although comprehensive performances of dental resin composites have already improved evidently, high polymerization shrinkage and lack of fracture toughness restrict the applications of dental resin composites to a great extent. What is more, it is just for the above reasons that the service life of dental resin composites is relatively shorter compared with amalgam [4–7]. To some extent, amalgam could be replaced by dental resin composites. For example, high copper amalgam and light-cured resin composites were studied on the effect of repairing the defects of posterior tooth by Li and Liu. They selected 58 subjects at age from 28 to 64 and obtained 130 posterior teeth totally. Then they classified these teeth into 2 groups: silver amalgam fillings (68 teeth) and resin material fillings (62 teeth). Experiment method was to fill the teeth in regular ways and check the filling effect after a year. Clinical results showed that light-cured resin composites outperformed in the terms of color, artistcity, and preventing microleaking [8]. Qin and Zhu made a research on 218 teeth (with different cavities) from 69 old people. They classified these teeth into two groups: P60 resin composite fillings (109 teeth) and traditional amalgam fillings (109 teeth). Two years later, they made a comparison on the effect. Results showed that repairing success rate of P60 resin composite fillings reached 94.5% and that of traditional amalgam filling reached 83.5%. In conclusion, the overall repair effect of P60 resin composite on the I and II cavities is fully satisfactory [9]. Generally speaking, the fillers in size of several microns are applied to strengthen dental resin composites. However, when dental resin composites strengthen by fillers in level of micron are under high stress circumstances, such as in case of replacement of cusps, it is these defects of dental composites that make them unsuitable for broader use. So the deficiency in intensity and service life of the composites has restricted their uses seriously [10]. The necessary condition of fillers which are added into dental composites to reinforce the material shall possess three intrinsic performances. Firstly, the fillers are substantially tougher compared with resin matrices. When the dental composites are under stress, most of the stress transfers to the resins matrices by means of kinds of specific fillers. Moreover, uniform dispersion of fillers throughout the matrices is needed. Provided that the shape of fillers immersed in resin matrices is in ordinance, the odd of appearance of stress concentration tends to be larger in the body of dental composites, and such case inclines to produce microcracks all around the fillers, thus making the dental composites weakened. Fillers highly aligned along certain orientation could impede the growth of crack, which boost up the mechanical properties of dental resin composites, thereby reinforcing the dental composites. Most importantly, in the course of preparing composite materials, what we should consider most is the interactions between fillers and resin matrix, namely, interfacial adhesion force. In the case of filler-strengthened dental composites, interfacial properties have a crucial impact on the performances of resulting dental composites. High fillers surface area could raise the extent of entanglement between various fillers and surrounding dental resins and the best case is the formation of the mutual permeating structure in the middle of fillers and the dental matrix. At the same time, powerful interfacial binding force between different phases is prospected to be produced, and then corresponding mechanical performances of resultant dental composites will be reinforced.

In the academia and industry, nanofibers and nanotubes have already been employed to strengthen dental composites. Introduction of nanofibers or nanotubes allows obtaining targeted materials with high performance in various fields. Nanofillers are very different from traditional fillers due to their large specific surface area, high aspect-ratio and unique microstructure [11]. Additionally, many researchers have proved that the application of nanotechnology could greatly improve the mechanical performances of dental composites [12, 13]. In order to offset the existing shortcomings of traditional dental composites, nanofibers or nanotubes fillers with low contents are broadly regarded as ideal candidates to greatly increase mechanical performances of dental composites. Nanofillers in the form of nanofibers/nanotubes are perfect media to disperse in the matrix uniformly [14]. Huge surface area and interfacial gliding of nanofillers in

the resin matrix may give a relatively good interpretation on mechanism of damping enhancement [15–17]. Moreover, nanofillers have great potential to interact intensively with ambient polymer chains as a result of nanofillers' surface activity [18]. Also, it is known that nanofibers/nanotubes possess specific interfacial properties, which is of great importance to improve the performances of dental composite materials [12, 19]. In spite of reinforcement of natural nanofillers [20–23], we mainly consider common and feasible nanofibers/nanotubes in this paper.

Based on the above information, for the sake of satisfying increasingly high requirement for dental resin composites' mechanical performances, the research was conducted to make a further confirmation about the enhanced effects of nanofillers in forms of nanofibers/nanotubes. In this review, the methods using nanofibers and nanotubes to reinforce mechanical performances of dental composites are demonstrated in sequence, including inorganic nanofibers/nanotubes, polymeric nanofibers/nanotubes, and metallic nanofibers. The first purpose of current paper is to confirm the enhancement of nanofibers or nanotubes' reinforcement on the mechanical performances of dental restorative composite. The second purpose is to make a general description about the reinforcement mechanism of nanofibers and nanotubes, especially, the influence of formation of the mutual permeating structure and nanofibers themselves on the mechanical performances of the dental composites.

2. Reinforcement of Nanofibers

2.1. Inorganic Nanofibers

2.1.1. Glass Nanofibers. Generally, inorganic fillers with a certain mass proportion are usually employed to reinforce the dental resin composites. Among lots of inorganic fillers, glass is the most usually used inorganic fibers during the reinforcement of dental composites. The following factors may interpret the reason why glass is most usually used. Firstly, the most essential demands of dental restoration composites could be satisfied by addition of appropriate amounts of glass. Secondly, glass possesses an index of refraction very close to that of the dental resins, equipping the resultant composites with semitransparent surfaces. Also, it is just for the reason of index of refraction mismatch with dental resins that crystalline SiO_2 is unfitted to be reinforcing filler in dental composites. In general, when glass fillers in scale from dozens of nanometers to few microns are employed to reinforce the dental composites, the corresponding dental resin composites strengthen by micron-scaled glass fillers are unsuitable for broader uses under high stress circumstances, such as in case of replacement of cusps. Researchers have made a study about the enhancement of dental composites using certain glass fibers (with diameters of about ten microns) [24]; however, mainly because of poor interfacial adhesion, the mechanical properties of corresponding dental composites were indeed increased but finitely.

Both polymeric and inorganic nanofibers (with diameters of a few nanometers) can be fabricated feasibly and conveniently by means of established electrospinning technique, and we name these nanofibers "electrospun nanofibers" usually [25]. By way of electrospinning the amorphous silica and subsequently splitting at 800°C, glass nanofibers with diameters of 500 nm, homogeneous structure, and well-distributed morphology can be successfully obtained [26, 27]. It has demonstrated that when we substitute traditional dental glass filler with glass nanofibers partially, the strength and toughness of the corresponding resin composites will enhance greatly [28].

In terms of enhancement of dental composites, the nanoscaled glass fibers are believed to be so much better than conventional micron-scaled glass particles/fibers. It is the characteristics of electrospun nanofibers (such as petty diameter, huge surface area, tremendous aspect ratio, enormous strength, and modulus) that enable nanoscaled glass fibers to assume wanted structure, morphology, and performances. The following mechanism may explain the reason why small content of nanoscaled glass fibers can reinforce the dental composites drastically. When dental resin composites are under external pressure or three-body friction, microcracks are easily tended to be produced in the body of dental matrix. Although the cracks are formed, the gap between crack planes is not a vacuum and thin and long glass fibers exist in the middle section bearing load constantly, until glass fibers are broken completely. So, we can make an easy understanding that crack expansion is inhibited by the fibers, and meanwhile the matrix will become more powerful. In comparison with micron-scaled glass fibers, the nanoscaled glass fibers are thinner and also have substantial surface Si–OH groups which could interact with various silane coupling agents. Consequently, the interfacial adhesion force between the nanoscaled silanized glass fiber and the dental resin matrix will go more powerful.

In many of electrospun inorganic nanofibers, great attention has been given to glass nanofibers by researchers owing to well-understood pretreatment and extensive applications in various aspects [29]. Chen et al. [30] added electrospun glass nanofibers (with diameters of about 400 nm) into dental resin for strengthening and toughening. They concluded that electrospun glass nanofibers greatly excelled traditional glass fibers in both tension and impact tests as well as the enhancement in strength and toughness at content of 0.5% and 1%. In comparison with pure epoxy resin, the addition of electrospun glass nanofibers could raise the tensile strength, Young's modulus, and work of fracture by 12%, 33%, and 52%, respectively. Electrospun glass nanofibers with uniform morphology and irregular structure have been successfully fabricated by Chen et al., and even though glass nanofibers undergo violent ultrasonication, they can still maintain fiber morphology unchanged. Gao et al. [28] brought about the treated glass nanofibers into Bis-GMA/TEGDMA dental resin composites and subsequently confirmed the supposition whether the incorporation of glass nanofibers could cause tremendous enhancement on mechanical performances. Gao et al. demonstrated the small content substitutions of traditional dental filler with the treated nanoscaled glass nanofibers. The flexural strength and modulus improved obviously increased as much as 44% and 29%, respectively. In the end, Gao et al. hold the viewpoint

that if only chemical constitution and treatment ways of nanofibers could be further optimized, the mechanical performances of dental resin composites would be increased to a higher level.

In addition, even if electrospun glass nanofibers suffer from powerful ultrasonic violence, the whole morphology of electrospun glass nanofibers could be well maintained indicating that the glass nanofibers possess both natural morphology and structure. So we have every reason to believe that the electrospun glass nanofibers can be the most promising candidate in the reinforcement of dental resin composites.

2.1.2. Hydroxyapatite Nanofibers. Hydroxyapatite (HAP), tetracalcium phosphate, and dicalcium phosphate anhydrous are typical and biocompatible calcium phosphates fillers [31–36]. For releasing mineral into dental resin composites, calcium phosphates fillers above are generally added at some content. Also many researchers have shown that calcium phosphates are nontoxic [36]. Mechanical performances of dental resin composites could be reinforced significantly by means of introducing inorganic fibers with high toughness. Chen et al. divided the targeted dental resin composites into two groups, namely, Bis-GMA/TEGDMA dental resin composites containing silica filler at different loading content and without silica filler [37]. Moreover, the reinforcement of hydroxyapatite nanofibers with huge slenderness ratios on the targeted dental resins was seriously studied. By means of chemical approaches, hydroxyapatite nanofibers with slenderness ratios from 600 to 800 were smoothly fabricated. Owing to HAP nanofibers possessing sufficiently high slenderness ratios and relatively long and thin structure, a lot of bonding points could be created readily in the interface of nanofibers and other matrix. So in terms of mechanical performance, nanofibers are ideal reinforcing materials compared with other particles, since more stress transfer could be offered by interaction between nanofibers and matrix. Meanwhile, polymerization shrinkage could be cut down by the addition of HAP nanofibers. In brief, when the composites suffer from huge pressure, tremendous stress could be transferred from composites matrix to tough HAP nanofibers. Thus, substantial increase will be obtained in mechanical properties of dental composites finally. Chen et al. proved that biaxial flexural strength of corresponding dental resin composites could be improved drastically in the presence of hydroxyapatite nanofibers with different loading content. For instance, in terms of biaxial flexural strength, the dental resins without filling HAP nanofibers were at 100.3 MPa, and the dental resins with 10 wt% HAP nanofibers loading were at around 122.3 MPa. Obviously, biaxial flexural strength of filled dental resins raised by 22.2%. They drew a conclusion that when the loading content reached a certain point, mechanical performances of corresponding dental composites did not continue to increase any more with the growth of loading content, what is worse, some performances of corresponding dental composites would decrease greatly, for example, when the dental resins were loaded with HAP nanofibers at 40 wt%, the biaxial flexural strength will decrease to around 41.7 MPa. Hence, when such a situation above happens, we believe it has reached the percolation threshold of hydroxyapatite nanofibers. Finally, Chen et al. demonstrated that the biaxial flexural strength will be enhanced obviously at the condition of uniform dispersion of hydroxyapatite nanofibers, and the loading content is generally not too high. The improvement of dental resins composites will decline seriously, while loading content of hydroxyapatite nanofibers outnumbers percolation threshold. Since excessively high loading content of nanofibers prone to make reinforcing nanofibers into drawbacks and this will damage dental composites' mechanical performances greatly.

2.1.3. Fibrillar Silicate. Lots of single crystals in level of nanometers make up fibrillar silicate. palygorskite, whose reserve is the largest in China and America, is the most rich fibrillar silicate minerals in all types of fibrillar silicate minerals in the natural world. Silicate single crystals (about 100–3000 nm in length and 10–25 nm in diameter) are the most basic components of fibrillar silicate and micron-scaled particles can be formed by stacking mentioned single crystals [38, 39]. Highly aligned structure and extraordinary mechanical performances are the greatest characteristics of single crystals. In terms of absolute strength, the single crystals in scale of nanometers (more than 50 GPa) are over ten times as high as that of most of microscaled fibers [38]. Although montmorillonite and fibrillar silicate are both composed of nanoscale units, the largest distinction between them is the different degrees of difficulty to totally segregate into nanoscaled silicate layers and to evenly spread in dental resin composites. A larger room among stacked single crystals in fibrillar silicate than that of montmorillonite may account for the reason why there is a difference between them. Just for the reason above, the interaction of silicate layers in montmorillonite is more powerful than that of silicate layers in fibrillar silicate. Consequently, just because of this microstructure of fibrillar silicate, we could easily split fibrillar silicate into nanoscale single crystals just by way of dissolution in polar solvent and physical stirring, and this easy separation contributes to distribute uniformly in the dental resins, thus enhancing the dental composites [39]. Besides, extremely rich Si–OH groups, which could have a good interaction with diversified silane coupling agents, exist on the surface of nanoscaled single crystals. Precisely because of existence of these Si–OH groups, the interaction between silanized single crystal exfoliated by fibrillar silicate and dental composites could be tremendously powerful. The silanization of nanoscaled single crystals could contribute to distribute uniformly in the dental matrix and make an increase on the mechanical performance accordingly. Specifically, when dental composites are under tremendous pressure suddenly, they tend to create cracks in the body of composites; meanwhile, fibrillar silicate single crystals could continue to function across the cracks and restrain the expansion of cracks. So the inhibition of crack-extending and increased interaction between single crystals and matrix result in the reinforcement on the final mechanical property of the resin. Moreover, the enhancement of Bis-GMA/TEGDMA dental resins with and without traditional filler was studied by Tian et al.

[40]. Three dispersal approaches were employed to scatter nanoscaled single crystals into dental matrices evenly. Results showed that when the resin was loaded with 1 wt% nanoscaled fibrillar silicate, the modulus of elasticity, bending strength, and work of fracture increased by 16.7%, 40%, and 78.4%, respectively. Tian et al. drew a conclusion that the mechanical performances of dental resins/composites were improved tremendously when small content of nanoscaled single crystals was introduced into Bis-GMA/TEGDMA dental resins/composites. Also, the mechanical performances would not be enhanced and even would be damaged severely when greater content of nanoscaled single crystals was introduced. However, it is very difficult to distribute nanoscaled fibrillar silicate into dental composites evenly. In a word, an enhanced effect or weakened effect almost completely depends on the dispersion of nanofibrillar silicate into dental composites.

2.2. Reinforcement of Polymeric Nanofibers

2.2.1. Electrospun Nylon 6 Nanofibers. The most commonly used method to prepare kinds of ultrafine nanofibers is electrospinning because of its convenience and simplicity [41–44]. The basic principle of electrospinning can be described in the following way: the polymer solution drop was charged in the electric field, and electrical force drives the spray of polymer solution drop via a syringe needle.

In the course of preparing nylon 6 nanofibers by electrospinning [45], accelerated drawing in an irregular way enables polymer solution drop to stretch astonishingly in a very short time (about elongation of 100,000 times in less than 1/10 s). It is because of such substantial draw that conformations of polymer chains and microstructure of polymer are altered. Hence, the strength of the polymer nanofibers prepared by electrospinning will be very powerful. At the same time, the interfacial linking force between nylon 6 nanofibers and dental matrix will be very solid for the reason of high specific surface area of nanofibers. As everyone knows, the intensity of interfacial linking force between nanofillers and matrix has a decisive influence on the strength of overall dental composites. Therefore, we believe that the nylon 6 (diameters in the range from 100 to 600 nm) nanofibers could enhance the dental resin composites. The enhancement of nylon 6 nanofibers on Bis-GMA/TEGDMA dental composites was investigated by Fong [46]. They dissolved the nylon 6 nanofibers into hexafluoroisopropanol solution and obtained nanofibers by electrospinning. The tiny size of nanofibers possesses high specific surface area which may increase the interfacial adhesion between nylon 6 nanofibers and the resin matrix and lead to the improvement of performances of dental resins to a higher level. Fong also proved that the microcracks will be prevented efficiently in the presence of nanofibers. They found lots of fracture lines which were initiated in the course of fracture process on the break surface. These phenomena show that when nanofibers are arrayed along the fracture direction, it will consume huge amounts of energy in the course of complete tear. In other words, when high pressure force was imposed on the dental composites, owing to powerful forces between nylon 6 nanofibers and dental matrix, it will be extremely hard to form microcracks firstly, even if microcracks appeared, nylon 6 nanofibers will prevent the expansion of cracks. What is more, lots of energy will be consumed in the course of being torn for nanofibers, thus leading to the substantial improvement of resin composites' FS and work of fracture. However, they found no existence of residual resin in the terminal of extracted nanofibers by SEM. Little existence of residual resin demonstrates interfacial linking force between the BIS-GMA/TEGDMA dental resin and nylon 6 nanofibers that remain to be enhanced for boosting dental restorative composite. Tian et al. [47] considered that addition of fibrillar silicate (with well distribution and high arrangement) into nylon 6 nanofibers could enhance the whole mechanical performances of composite nanofibers, and the impregnation of the composite nanofibers could reinforce the dental composite efficiently. Tian et al. demonstrated that the mechanical performances of dental resin composites will be raised tremendously via small content of addition of composites nanofibers. Nevertheless, wanted reinforced effect does not appear in the case of larger content of addition of composites nanofibers. They considered that existence of flaws inside the matrix, finite mechanical performances of composite nanofibers, and low strength of interfacial linking in the interface of nanofibers and the dental matrix were main reasons. What is more, when dental resin composites are under high loading environment, microcracks will be created in the body of composites, and the nanofibers exist in the middle of cracks planes sustaining the heavy burden owing to the continuation of electrospun nanofibers. Consequently, continuous nanofibers play a critical role in inhibition of crack growth. For the purpose of acquiring ideal enhanced effects, electrospun nanofibers with high alignment rather than random distribution are needed. In addition, Dodiuk-Kenig et al. [48] studied the enhancement of electrospun nanofibers on the dental composites with the modification of hyperbranched polymer. The appearance of new functionalized nanofillers opens a door to the formation of the latest composites and the substantial increase in the mechanical performances of dental composites. Dodiuk-Kenig et al. discussed the reinforcement of nylon 6 nanofibers with different contents and different surface treatment on dental resin composites, and they considered that the reinforcement lies in the close linking between resin matrix nanofibers. Similarly, bad performances connect with poor interfacial adhesion. And it can be completely proved by the enhancement of treated nanofibers and untreated nanofibers.

2.2.2. PAN-PMMA Nanofibers. Variety of nanofibers can be fabricated successfully by means of electrospinning technique. Generally speaking, nozzle is connected with positive electrode, and the collector is usually linked with cathode. The polyacrylonitrile/poly (methyl methacrylate) (PAN/PMMA) membrane was smoothly prepared by electrospinning by Lin et al. [49]. By way of the characterization of transmission electron microscope, they confirm the PAN-PMMA nanofibers (with an outer diameter about 290 nm) and the result of an energy dispersive spectroscopy is in accord with above claim. The formation of partial interpenetrating network in the interface of

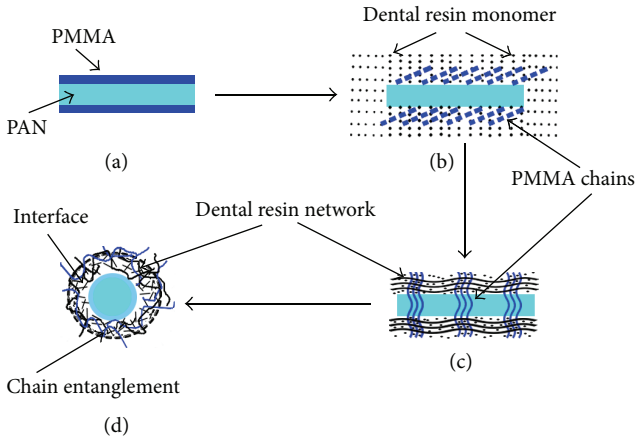

Figure 2: Diagram of formation of composites' partial interpenetrating network. (a) Nanofibers with core-shell structure. (b) Nanofibers surrounded by resin matrix. (c) Formation of partial interpenetrating network. (d) Formation of tanglement between PMMA and dental resin in the interface.

nanofibers/matrix produces drastically powerful interfacial linking force which functions mainly in the enhancement of composites (Figure 2).

Some shortcomings still exist in nonwoven nanofibers (diameters in the range of 500–800 nm) as reinforcing filler in spite of a few achieved accomplishments. Report said that irregular alignment of nanofibers leads to a decreased crystallinity and thus influencing the intensity of nanofibers membranes seriously [50]. At the same time, irregular alignment of nanofibers caused by their excessive pore and bad orientation will cause the enhancement effect to fade [51].

Lately, for the sake of raising the strength of electrospun nanofibers, much attention has been focused on the poststretching handling of nanofibers (diameters in the range of 300–500 nm) [52, 53]. It is considered that the extent of crystallization and regular alignment directly determines the properties of nanofibers itself. Also, that extent could be raised by the poststretching handling. For satisfying the higher requirements in terms of mechanical performances, the PAN/PMAA nanofibers with special structure and corresponding dental resin composites were investigated by Sun et al. [54]. A cylinder rod with high-speed rotation was employed to collect the electrospun nanofibers, thus acquiring nanofibers membranes arranged in parallel. After that, poststretching handling is a great choice to raise the extent of crystallization and regular alignment and then increase the strength of nanofibers accordingly. Sun et al. showed that the tensile performances and the extent of parallel alignment in nanofibers membranes were enhanced obviously via poststretching handling. The mechanical performance of Bis-GMA/TEGDMA dental composites was boosted indeed with the impregnation of PAN-PMMA nanofibers. For instance, with the increase of nanofibers content within certain limits, the mechanical performance of dental resin composites, such as flexural modulus and strength, maintains growing. Compared with untreated nanofibers, the reinforcement of poststretching nanofibers on dental composites is much better, especially in the terms of flexural performances. Moreover, better interfacial linking force exists in the dental resin enhanced by poststretching nanofibers via examining break surface using scanning electron microscopy.

So, we can completely consider that mechanical performance (especially tensile properties) of electrospun nanofibers membranes can be enhanced clearly by the process of poststretching treatment. Furthermore, compared with normal electrospun PAN/PMMA nanofibers, dental composites strengthened by poststretching nanofibers possess better mechanical performance (such as flexural properties and fracture energy). Ultimately, Sun et al. believed that formation of partial interpenetrating network in the interface and enhanced strength of poststretching nanofibers are the biggest reason why the mechanical performances (especially tensile properties) of Bis-GMA dental composites can be intensified by poststretching PAN/PMMA nanofibers with special structure.

2.2.3. Other Nanofibers. By means of electrospinning which is a convenient, simple, and practical technique, we can prepare various nanofibers in the scale from some micrometers to nanometers (generally less than 500 nm). But, owing to relatively low mechanical properties of natural nanofibers, they are usually not used as fillers to reinforce dental composites [55–60]. Through the development of recent decades, electrospinning technique has acquired substantial progress, and the corresponding nanofibers have been applied to lots of fields. Besides nylon 6 nanofibers and polyacrylonitrile/poly methyl methacrylate nanofibers, electrospun polyvinyl alcohol (PV–OH) nanofibers could also boost the mechanical performances of dental composites. Dodiuk-Kenig et al. [48] investigated the enhancement of PV–OH nanofibers (with a diameter of 250 nm and aspect ratio of about 1000) on the dental formulations modified by other special polymers. They regarded PV–OH nanofibers as an enhancement factor into the composites, and added the enhancement factor with and without surface treatment into the composites with a very small content. In Dodiuk-Kenig's paper, they character the corresponding dental composites enhanced by PV–OH nanofibers via several methods, and these characterizations (especially SEM images of composites section) facilitate our understanding on the mechanism of reinforcement of PV-OH nanofibers on dental composites. In a word, they considered the reinforcement consisted in the tight linking between resin matrix and nanofibers. Similarly, bad performances connect with poor interfacial adhesion, and it can be completely proved by the enhancement effect of treated nanofibers and untreated nanofibers. They concluded that addition of 0.05 wt% PV–OH nanofibers with a diameter of 250 nm into composites could increase the compressive strength by 30% and decrease the shrinkage by 50%. While little enhancement can be obtained by nanofibers with another diameter, what is worse, the addition of nanofibers with another diameter even brought about a loss of performance.

As we know, polymer nanofibers take on lots of advantages, such as wide range of scale, distinctive structure, super-high specific aspect ratio, and outstanding mechanical performances. Selection of diverse polymer species, mix of

different polymers, various treatment ways of nanofibers, and other factors could have a substantial influence on the structure, composition, and performance of electrospun nanofibers. By electrospinning technique, we enable sorts of nanofillers (such as kinds of inorganic nanoparticles) to impregnate the body of composites uniformly. For example, we could put multiwalled carbon nanotubes (MWCNT) to dissolve in the particular polymer solutions, and then we could obtain continuous nanofibers containing carbon nanotubes which can be used as nanofiller by electrospinning technique. Chronakis [61] successfully fabricated MWCNT-PAN nanofibers using electrospinning. Nanofibers with special properties also could be achieved via all kinds of advanced preparation technology [62, 63]. Additionally, natural polymer is also a good candidate reinforcing filler; for example, some researchers made a deep study about reinforcement of collagen-based scaffold chitin nanofibers for bones [64].

The simplicity of modification on both surface and internal of polymer nanofibers is another reason why we focus on the polymer nanofibers [65]. Various functionalizations of polymer nanofibers after the synthesis are easy to realize. Moreover, for preparing nanofibers with special structures and morphology, it is very likely to regulate and control the structures of nanofibers as we designed [66]. Consequently, polymer nanofibers are considered to be ideal candidate nanofillers in reinforcing the mechanical performances of dental composites.

2.3. Ceramic Nanofibers. Despite dental resin composites are broadly applied to restore tooth. The service life of composites is far shorter than that of amalgams because of inner cracks and fracture [67]. In order to raise the mechanic performances and decrease inner cracks and fracture, many kinds of special fibers have been employed to increase overall strength of composites. However, most of these materials are unsuitable because of behavior, stabilization, and aesthetic requirements. It is reported that composites boosted by glass nanofibers assume weaker mechanical performances after absorbing water [68]. Ceramic materials possess many advantages, such as outstanding physical performance, stabilization in high temperature, and excellent compatibility. By means of fusing, we acquire ceramic fillers in the form of single crystal whiskers, and the existence form of whiskers favors the better silanization of themselves. In general, ceramic fillers possess huge aspect ratio (with a diameter and length of approximately 0.5 mm and 5 mm, resp.) [69, 70]. Moreover, ceramic nanofillers are in the form of single crystal whiskers which take on a tremendous tensile strength at about 50 GPa compared with glass fibers at about 3 GPa [71]. The small size and relatively excellent structure of ceramic whiskers could provide a sensational distribution in the dental matrix, which facilitates the increase of interbonding between ceramic whiskers and matrix. Just because of various advantages of single crystal whiskers above, when dental composites suffer from enormous pressure, ceramic whiskers have a great potential to inhibit the emergence of microcracks and prevent its enlargement. That is to say, huge external pressure will be largely resisted by ceramic whiskers, which contributes to greatly increase the mechanical properties of the resin composites. Also, it was said that the strength and toughness of thermal-curing composites doubled with suitable addition of tremendously strong Si_3N_4 and SiN ceramic whiskers [72–74]. Since there exists mismatch between whiskers' refractive and resins' refractive, it will restrict composites' application severely. Some ceramic nanofibers, such as zirconia-yttria-silica, zirconia-yttria, and zirconia-silicia, can be successfully obtained by Xu et al. by electrospinning way and following sintering [75]. Particularly, due to slippery surfaces and special configuration of zirconia-silicia and zirconia-yttria-silica nanofibers (with diameters from 100–300 nm), it is very possible to apply them in the enhancements of dental composites. The enhanced effect of zirconia-silicia and zirconia-yttria-silica on dental composites was studied by Guo et al. [76]. The reason why they choose zirconia-silicia or zirconia-yttria-silica as addition to enhance composites is because of their super-high strength, excellent stabilization, biocompatibility, and low light scattering. Heat curing and light curing are applied in the course of fabricating the control composites and experimental composites. Finally, they drew a conclusion that overall properties could be increased obviously (such as flexural strength and modulus and fracture energy) with impregnation of zirconia-silicia and zirconia-yttria-silica nanofibers at content of 2.5% and 5.0%, respectively. If they continued to raise the amount of zirconia-silicia nanofibers up to 7.5%, reversely, main performances decreased clearly. All dental composites enhanced by zirconia-silicia possess obviously higher fracture toughness than the control. In order to put the strength of dental composites to a completely new level with increasing nanofibers, we need new-fashioned and effective nanofibers. Consequently, other ceramic nanofibers and smaller content of zirconia/silica are being studied. Of course, we should try to work out innovative ways to make the mechanic performances of the composite stronger and their service life longer, and this is the long-term target that we have been pursuing.

3. Reinforcement of Nanotubes

3.1. Inorganic Nanotubes

3.1.1. Halloysite Nanotubes. In terms of strength and service life, dental amalgams are far better than that of composites enhanced by majority of inorganic fillers. The applications of dental composites strengthened by much of inorganic fillers are restricted seriously just because of reason above [77–79]. Currently, the dental composites on the market can only meet essential demand of filling tooth but fail to be employed in high pressure-assuming positions. Moreover, in contrast to the life of dental amalgams, the service life of dental composites is one-third of that of dental amalgams. The mechanical intensification of dental composites could be boosted drastically by means of addition of fibers/whiskers with micrometer scale [80, 81]. For instance, Xu et al. [82] thought that the mechanic strength and toughness of dental composites doubled when certain content of tremendously strong ceramic fibers/whiskers was added into composites.

Moreover, the ability to polish and handle was improved partially [83–85].

Being different from fibers in scale of microns, nanoscaled crystals make up hallosite [84]. Halloysite is a very commonly used natural mineral as a result of halloysites' wide source, simple purification steps, and high cost performance [85]. The length of halloysite nanotubes (with diameters of dozens of nanometers) are generally in the scope from 200 nm to 1 μm and Young's modulus of halloysite nanotubes is in the scope from 230 to 340 GPa. Moreover, safety, biocompatibility, and easy handling are also the characteristics of halloysites. Compared with montmorillonite, halloysite is more easy to exfoliate into single halloysite nanotubes (HNTs) and to scatter in the dental composites evenly.

The room among stacked layers may account for the reason. The room among silicate layers in montmorillonite is smaller than that of hallosite; hence, the interaction of montmorillonite is more powerful than that of hallosite. Hence, as to hallosite, it is not necessary to replace metal ions with special reagent at all. The halloysite nanotube in halloysite can be split fully in the presence of polar solvents and mechanical agitation. Moreover, as a result of existence of rich Si–OH group on the external of halloysite nanotubes (HNTs), the silanized halloysite nanotube could be closely connected with dental resin matrix via tremendously powerful interfacial linking force. The enhancement of Bis-GMA/TEGDMA dental resins or composites boosted by various contents of HNTs was studied by Chen et al. [86]. For splitting the halloysite into halloysite nanotubes and scattering evenly in dental composites, three approaches were employed. They came to a conclusion that introduction of low content of the silanized HNTs into dental resins/composites brought about a clear enhancement. But, high content of addition did not cause improvement on the mechanic performances. Briefly, the reinforcement of halloysite nanotubes almost entirely depends on the dispersion effect in the matrix. Excellence dispersion facilitates reinforcing the dental resins/composites; halloysite nanotubes are strengthening phase. On the contrary, halloysite nanotubes will become harming phase, thus damaging the overall performance of dental resins/composites. For the mechanical performances of dental resins/composites could increase tremendously by the addition of well-distributed halloysite nanotubes at appropriate content. Halloysite nanotubes have huge potential to be effective strengthening filler in enhancement for dental composites.

3.1.2. Carbon Nanotubes and Boron Nitride Nanotubes. As everyone knows, carbon nanotubes possess astonishing mechanical performances and excellent biocompatibility [86–88]. For instance, the modulus of carbon nanotubes is ten times stronger than that of steel; exactly, single-walled carbon nanotubes (SWCNTs, with a high aspect ratio at around 500–1000) possess outstanding mechanical performance. For instance, it takes on a tensile strength at 50–100 GPa which is five times higher than that of steel, but the weight of the steel is six times than that of carbon nanotubes [89–93]. Given the remarkable physical performances and ultrahigh specific surface area, single-walled carbon nanotubes are really very promising in the reinforcement of dental composites and very likely to replace glass fiber fillers. Single-walled carbon nanotubes have been used for hard-tissue application, such as the regeneration and repair of bones and teeth, and have a good biocompatibility in general case [94, 95]. The improved effect of dental composites is restricted for the reason of carbon nanotubes' gathering and weak interfacial linking with composites. Nanotubes prefer gathering together and the condition of nanotubes' distribution in polymer solution becomes extremely important for enhancement [96]. Generally, nanotubes are prone to agglomeration, so it is very difficult to disperse evenly. Moreover, the surface of nanotubes is so smooth that it will affect the interfacial adhesion force between the nanotubes and composites. If agglomeration happens, the nanofillers will be drawn out from the dental composites instead of breaking and nanotubes' function is restricted to large extent. Zhang et al. [95] gained a well-distributed effect in the dental composites by way of coating single-walled carbon nanotubes with modified nano-SiO_2. Eventually, what we hope is excellent scattering and substantial bonding force of single-walled carbon nanotubes after addition into the dental composites, and we also expect that the performances could be enhanced tremendously. The impregnation of modified single-walled carbon nanotubes indeed brings about enhancement of dental resin composites obviously by the statistical analysis. Moreover, other researchers indeed demonstrated that the carbon nanotubes could be a very promising scaffold material for dental materials [97].

Boron nitride nanotubes, which possess tremendous tensile strength, have a similar structure to carbon nanotubes [98]. Exactly, they exhibit extraordinary tensile strength at about 30 GPa and Young's modulus at about 900 GPa; moreover, the oxidizing temperature may reach as high as 800°C. Boron nitride nanotubes gained so much attention because of its ultrahigh performances in strengthening effect. By the means of hot pressing, BNNTs/alumina composites were prepared by Wang et al. [99] and the reinforced effect of Boron nitride nanotubes on the mechanic performances of alumina matrix was studied. They concluded that the flexure strength would be raised with the introduction of Boron nitride nanotubes at higher temperature.

3.2. Metallic Nanotubes

Titania Nanotubes. The appearance of nanomaterials provides an opportunity to advance the mechanical performances of dental composites and bone cements to a new level [100, 101]. Khaled et al. gained a very good enhancement effect of poly methyl methacrylate by way of addition of titania nanofibers [102]. Nanotubes (average diameter is 200 nm) have a high ratio of length to diameter and super-high specific area as good as nanofibers. Precisely because of above characteristics, it is very possible to heighten the physical performances obviously. Furthermore, the effect of extra intertwining (both internal and external interlinking of nanotubes) can be obtained entirely due to tubular structure of titania nanotubes. Khaled et al. [103] carried out a research

for the purpose of boosting the physical performances of common acrylic cement via addition of late-model titania nanotube which acts as a strengthening phase. The main purpose is to procure the enhancement of dental cements via the addition of strengthening phase and compare with enhanced effect of current fillers. And they concluded that pressure could be transformed easily and efficiently via extremely powerful interface, because there exists powerful interfacial adhesion between treated TiO_2 nanotubes and dental matrix. Certainly, this late-fashioned nanofiller coupled with the current fillers could be employed together to strengthen flowable and usual dental composites with no damage in biocompatibility.

Generally speaking, the nanofibers take on the shape long and thin and possess diameters at hundreds of nanometers. Nanotubes have the tubular structure and slightly bigger diameters. As with surface properties, lots of functional groups exist on the surface of nanofibers, such as –OH group, but these groups do not exist on the nanotubes commonly, so we should conduct a treatment on the nanotubes before their usage. Owing to distinctive structure of nanotubes, they usually have relatively high strength than nanofibers, but it does not mean that nanotubes are better fillers than nanofibers. For reinforcement of dental composites, it mostly depends on the condition of nanofillers themselves and their status in the matrix, such as dispersion, interbonding, and other influence factors. As long as we take full and reasonable advantage of these nanofillers, the substantial increase on mechanical performance of dental composites will be acquired definitely [104].

4. The Potential Reinforcement Mechanism

Through the study of so many cases of enhancement of nanotubes/nanofibers, a reinforcing mechanism could be seen clearly. Namely, under high external pressure, microcracks tend to be created in the body of dental composites. However, the room of cracks is not empty, nanofibers or nanotubes still exist in the middle of cracks plane and function across planes. Thereby, cracks are prevented via the remaining fillers. Hence, much of the stress is transmitted through the fillers into the resins, and that is the reason why the nanofillers must be largely tougher than the resin matrices. Of course, the Van der Waals' force via physical entanglement and chemical bonding between nanofillers and matrix lays the theoretical foundation for the improvement of dental composites' performance. The enhanced performances of composites boosted by post-stretching PAN/PMMA nanofibers are the best example of previous viewpoint. So, powerful mechanical performances and ultrasmall scale are the necessary condition for valid bridging fillers.

Another strengthening mechanism is that uniform dispersion of fillers throughout the matrices is needed. Supposing that the immersed parts of fillers are irregular in appearance, it will tend to form the stress concentration easily. Also, stress concentration is the main reason for creating small cracks in the matrix, thus damaging the properties of composites. Therefore, to produce the biggest effect of chemical bond, nanofillers should be dispersed as uniform as possible. The nanofillers which are highly aligned along some orientation (such as across the cracks) could impede the growth of crack, thus raising the mechanical behavior of dental resin and reinforcing the dental composites.

Last strengthening mechanism but most importantly is the interaction between nanofillers and composites. In the course of preparing composite materials, what we should consider most is the interactions between fillers and resin matrix, namely, interfacial adhesion. In the condition of filler-strengthened dental composites, interfacial properties have a crucial impact on the performances of resulting dental composites. High fillers surface area could raise the extent of entanglement between various fillers and surrounding dental resin and the best case is the formation of the mutual permeating structure in the middle of fillers and the dental matrix, which bring about a specific interface in the nanometer scale. At the same time, powerful interfacial binding force between different phases aimed to hinder the movement of polymer chains is prospected to be produced, and then corresponding mechanical performances of resultant dental composites will be reinforced. For the purpose of enhancing the interfacial chemical binding, various measurements will be taken, such as functioning of nanofillers. As to this strengthening mechanism, extremely strong chemical bond between nanofillers and matrix is the most vital factor for reinforcing.

So, in my opinion, the potential reinforcement mechanism is that extreme toughness nanofibers and nanotubes are fabricated. Provided that immersed parts of fillers are irregular in appearance, it will tend to form the stress concentration easily. Also, stress concentration is the main reason for generating small cracks in the matrix, thus damaging the properties of composites. Then we disperse them uniformly in the dental matrix in some direction and when the microcrack emerges. Powerful bonding between nanofibers and nanotubes will impede the growth of cracks, which will greatly facilitate the reinforcement of dental composites (Figure 3). In brief, no matter what treatment you conduct on the surface of nanofillers, chemical bond between nanofillers and matrix is always to be considered firstly. Only by means of the formation of strong chemical bonding in the composites can you could obtain reinforced dental composites. Finally, on the basis of powerful chemical bonding, we could increase Van der Waals' force electric attraction as far as possible.

5. Conclusions and Perspectives

In this review, the efforts using nanofibers and nanotubes to reinforce mechanical performances of dental composites, including polymeric nanofibers/nanotubes, metallic nanofibers, and inorganic nanofibers/nanotubes, as well as their researches related, are demonstrated in sequence. We demonstrated the use of kinds of nanofibers or nanotubes to reinforce dental composites. Addition of nanofibers or nanotubes could acquire composites materials with distinct performances in lots of areas. Nanofillers are very different from traditional fillers largely because of their scale in nanometers and special microstructure, and we can make a substantial increase on the mechanic properties of resin

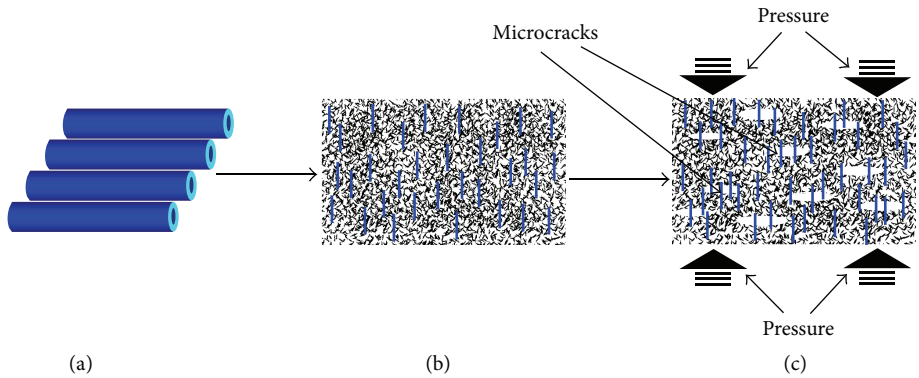

Figure 3: Diagram of reinforcement mechanism of dental composites. (a) Extremely hard nanofibers or tubes, (b) extremely hard nanofibers/tubes highly aligned along some orientation uniformly in the dental composites, and (c) when dental composite subjected to powerful pressure, nanofibers, or tubes acts as a bridge across the microcrack which impedes the growth of crack, and then dental composites will be reinforced.

composites by means of nanotechnology. On the way to conquer current flaws of traditional dental composites, fillers in forms of nanofibers or nanotubes are the most promising fillers to raise the mechanical performances of dental composites tremendously at a low content. We also make a general understating of the potential reinforce cement mechanism, the reinforcement effect which greatly depends on nanofillers' toughness, condition of nanofillers' dispersion in the body, and powerful bonding between nanofillers (in forms of nanofibers or nanotubes) and matrix. It is because we already have a broad understanding of the influence factor of reinforcement effect that we have a clear direction for the future development.

In the future, a further study on the mechanism of reinforcing the dental composites should be carried on, as well as the influence factor of reinforcement effect. Only when we master the mechanism of reinforcing the dental composites well and the influence factor of reinforcement effect can we make a further increase reinforcement of the dental composites. Additionally, more novel methods of preparing nanofibers or nanotubes will be introduced. In order to put the mechanical performances of dental resin composites to a completely new level, more tough nanofillers should be fabricated, the method of dispersing nanofillers more uniformly should be found, and interfacial adhesion between fillers and the body should be more and more powerful.

Conflict of Interests

The authors declare that they have no financial or personal relationship with any people or organization that may inappropriately influence their work. There is no professional or commercial interest of any kind in all the commercial identities mentioned in the paper.

Acknowledgments

The authors acknowledge the financial supports from the National Basic Research Program of China (973 Program no. 2011CB710901), the National Natural Science Foundation of China (nos. 31370959 and 81101348), Beijing Natural Science Foundation (no. 7142094), the Beijing Nova Program (no. 2010B011), Program for New Century Excellent Talents (NCET) in University from Ministry of Education of China, State Key Laboratory of New Ceramic and Fine Processing (Tsinghua University), Natural Science Foundation of Guangdong Province, China (nos. 10451051501004727 and 10151051501000107), Guangdong Medical Scientific Research Project (no. A2013385), the Doctoral Fund of Ministry of Education, China (20114433120004), outstanding person fund of Zhujiang Hospital, International Joint Research Center of Aerospace Biotechnology and Medical Engineering, Ministry of Science and Technology of China, and the 111 Project (no. B13003).

References

[1] R. L. Bowen, "Dental filling material comprising vinyl-silane treated fused silica and a binder consisting of the reaction product of bisphenol and glycidyl methacrylate," US Patent 3, 066, 112, 1962.

[2] R. L. Bowen, "Performances of a silica-reinforced polymer for dental restorations," *Journal of the American Dental Association*, vol. 66, pp. 57–64, 1963.

[3] B. B. Reed, K. Choi, S. H. Dickens, and J. W. Stansbury, "Effect of resin composition of kinetics of dimethacrylate photopolymerization," *Polym Preprint*, vol. 2, pp. 108–117, 1997.

[4] P. S. Stein, J. Sullivan, J. E. Haubenreich, and P. B. Osborne, "Composite resin in medicine and dentistry," *Journal of Long-Term Effects of Medical Implants*, vol. 15, no. 6, pp. 641–654, 2005.

[5] S. Rüttermann, S. Krüger, W. H.-M. Raab, and R. Janda, "Polymerization shrinkage and hygroscopic expansion of contemporary posterior resin-based filling materials—a comparative study," *Journal of Dentistry*, vol. 35, no. 10, pp. 806–813, 2007.

[6] D. C. Sarrett, "Clinical challenges and the relevance of materials testing for posterior composite restorations," *Dental Materials*, vol. 21, no. 1, pp. 9–20, 2005.

[7] T. Beazoglou, S. Eklund, D. Heffley, J. Meiers, L. J. Brown, and H. Bailit, "Economic impact of regulating the use of amalgam

restorations," *Public Health Reports*, vol. 122, no. 5, pp. 657–663, 2007.

[8] X. Z. Li and L. Z. Liu, "The curative effect observation of two fillings on posterior tooth repairing," *Medical Journal of the Northwest National Defense*, vol. 3, pp. 84–84, 2002.

[9] J. Qin and Y. l. Zhu, "The comparison of clinical effects of P60 resin composite and traditional amalgam on the I, II cavities," *Chinese Journal of Stomatology*, vol. 7, pp. 259–261, 2009.

[10] A. K. Abell, K. F. Leinfelder, and D. T. Turner, "Microscopic observations of the wear of a tooth restorative composite in vivo," *Journal of Biomedical Materials Research*, vol. 17, no. 3, pp. 501–507, 1983.

[11] T. Stober, M. Henninger, M. Schmitter, M. Pritsch, and P. Rammelsberg, "Three-body wear of resin denture teeth with and without nanofillers," *Journal of Prosthetic Dentistry*, vol. 103, no. 2, pp. 108–117, 2010.

[12] S. K. Kovvuru, V. N. Mahita, B. S. Manjunatha, and B. Sudhakar, "Nanotechnology: the emerging science in dentistry," *Journal of Orofacial Research*, vol. 2, no. 1, pp. 33–36, 2012.

[13] S. B. Mitra, D. Wu, and B. N. Holmes, "An application of nanotechnology in advanced dental materials," *Journal of the American Dental Association*, vol. 134, no. 10, pp. 1382–1390, 2003.

[14] X. M. Li, Y. Yang, Y. B. Fan, Q. L. Feng, F. Z. Cui, and F. Watari, "Biocomposites reinforced by fibers or tubes, as scaffolds for tissue engineering or regenerative medicine," *Journal of Biomedical Materials Research Part A*, vol. 102, no. 5, pp. 1580–1594, 2013.

[15] E. Özden, Y. Z. Menceloğlu, and M. Papila, "Engineering chemistry of electrospun nanofibers and interfaces in nanocomposites for superior mechanical properties," *ACS Applied Materials and Interfaces*, vol. 2, no. 7, pp. 1788–1793, 2010.

[16] A. Zucchelli, M. L. Focarete, C. Gualandi, and S. Ramakrishna, "Electrospun nanofibers for enhancing structural performance of composite materials," *Polymers for Advanced Technologies*, vol. 22, no. 3, pp. 339–349, 2011.

[17] J. Zhu, H. Peng, F. Rodriguez-Macias et al., "Reinforcing epoxy polymer composites through covalent integration of functionalized nanotubes," *Advanced Functional Materials*, vol. 14, no. 7, pp. 643–648, 2004.

[18] T. Ramanathan, A. A. Abdala, S. Stankovich et al., "Functionalized graphene sheets for polymer nanocomposites," *Nature Nanotechnology*, vol. 3, no. 6, pp. 327–331, 2008.

[19] F. Meng, Y. Zhan, R. Zhao, and X. Liu, "New strategy to reinforce and toughen composites via introducing thorns-like micro/nanofibers," *European Polymer Journal*, vol. 48, no. 1, pp. 74–78, 2012.

[20] X. Li, Q. Feng, W. Wang, and F. Cui, "Chemical characteristics and cytocompatibility of collagen-based scaffold reinforced by chitin fibers for bone tissue engineering," *Journal of Biomedical Materials Research Part B*, vol. 77, no. 2, pp. 219–226, 2006.

[21] M. A. Melo, S. F. Guedes, H. H. Xu, and L. K. Rodrigues, "Nanotechnology-based restorative materials for dental caries management," *Trends in Biotechnology*, vol. 31, no. 8, pp. 459–467, 2013.

[22] W. Höland, V. Rheinberger, E. Apel et al., "Future perspectives of biomaterials for dental restoration," *Journal of the European Ceramic Society*, vol. 29, no. 7, pp. 1291–1297, 2009.

[23] X. Li, Q. Feng, and F. Cui, "In vitro degradation of porous nano-hydroxyapatite/collagen/PLLA scaffold reinforced by chitin fibres," *Materials Science and Engineering C*, vol. 26, no. 4, pp. 716–720, 2006.

[24] G. Willems, P. Lambrechts, M. Braem, J. P. Celis, and G. Vanherle, "A classification of dental composites according to their morphological and mechanical characteristics," *Dental Materials*, vol. 8, no. 5, pp. 310–319, 1992.

[25] Y. Dzenis, "Spinning continuous fibers for nanotechnology," *Science*, vol. 304, no. 5679, pp. 1917–1919, 2004.

[26] Y. Liu, S. Sagi, R. Chandrasekar, L. Zhang, N. E. Hedin, and H. Fong, "Preparation and characterization of electrospun SiO_2 nanofibers," *Journal of Nanoscience and Nanotechnology*, vol. 8, no. 3, pp. 1528–1536, 2008.

[27] S. Wen, L. Liu, L. Zhang, Q. Chen, L. Zhang, and H. Fong, "Hierarchical electrospun SiO_2 nanofibers containing SiO_2 nanoparticles with controllable surface-roughness and/or porosity," *Materials Letters*, vol. 64, no. 13, pp. 1517–1520, 2010.

[28] Y. Gao, S. Sagi, L. Zhang et al., "Electrospun nano-scaled glass fiber reinforcement of bis-GMA/TEGDMA dental composites," *Journal of Applied Polymer Science*, vol. 110, no. 4, pp. 2063–2070, 2008.

[29] S.-S. Choi, S. G. Lee, S. S. Im, S. H. Kim, and Y. L. Joo, "Silica nanofibers from electrospinning/sol-gel process," *Journal of Materials Science Letters*, vol. 22, no. 12, pp. 891–893, 2003.

[30] Q. Chen, L. Zhang, M.-K. Yoon, X.-F. Wu, R. H. Arefin, and H. Fong, "Preparation and evaluation of nano-epoxy composite resins containing electrospun glass nanofibers," *Journal of Applied Polymer Science*, vol. 124, no. 1, pp. 444–451, 2012.

[31] X. M. Li, X. H. Liu, M. Uo, Q. L. Feng, F. Z. Cui, and F. Watari, "Investigation on the mechanism of the osteoinduction for calcium phosphate," *Bone*, vol. 43, pp. S111–S112, 2008.

[32] R. W. Arcís, A. López-Macipe, M. Toledano et al., "Mechanical properties of visible light-cured resins reinforced with hydroxyapatite for dental restoration," *Dental Materials*, vol. 18, no. 1, pp. 49–57, 2002.

[33] C. Domingo, R. W. Arcís, E. Osorio et al., "Hydrolytic stability of experimental hydroxyapatite-filled dental composite materials," *Dental Materials*, vol. 19, no. 6, pp. 478–486, 2003.

[34] X. Li, C. A. van Blitterswijk, Q. Feng, F. Cui, and F. Watari, "The effect of calcium phosphate microstructure on bone-related cells in vitro," *Biomaterials*, vol. 29, no. 23, pp. 3306–3316, 2008.

[35] C. Santos, R. L. Clarke, M. Braden, F. Guitian, and K. W. M. Davy, "Water absorption characteristics of dental composites incorporating hydroxyapatite filler," *Biomaterials*, vol. 23, no. 8, pp. 1897–1904, 2002.

[36] X. Li, H. Liu, X. Niu et al., "The use of carbon nanotubes to induce osteogenic differentiation of human adipose-derived MSCs in vitro and ectopic bone formation in vivo," *Biomaterials*, vol. 33, no. 19, pp. 4818–4827, 2012.

[37] L. Chen, Q. Yu, Y. Wang, and H. Li, "BisGMA/TEGDMA dental composite containing high aspect-ratio hydroxyapatite nanofibers," *Dental Materials*, vol. 27, no. 11, pp. 1187–1195, 2011.

[38] M. Tian, C. Qu, Y. Feng, and L. Zhang, "Structure and properties of fibrillar silicate/SBR composites by direct blend process," *Journal of Materials Science*, vol. 38, no. 24, pp. 4917–4924, 2003.

[39] M. Tian, W. Liang, G. Rao, L. Zhang, and C. Guo, "Surface modification of fibrillar silicate and its reinforcing mechanism on FS/rubber composites," *Composites Science and Technology*, vol. 65, no. 7-8, pp. 1129–1138, 2005.

[40] M. Tian, Y. Gao, Y. Liu, Y. Liao, N. E. Hedin, and H. Fong, "Fabrication and evaluation of Bis-GMA/TEGDMA dental resins/composites containing nano fibrillar silicate," *Dental Materials*, vol. 24, no. 2, pp. 235–243, 2008.

[41] M. Bognitzki, T. Frese, M. Steinhart et al., "Preparation of fibers with nanoscaled morphologies: electrospinning of polymer blends," *Polymer Engineering and Science*, vol. 41, no. 6, pp. 982–989, 2001.

[42] A. Frenot and I. S. Chronakis, "Polymer nanofibers assembled by electrospinning," *Current Opinion in Colloid and Interface Science*, vol. 8, no. 1-2, pp. 64–75, 2003.

[43] T. Subbiah, G. S. Bhat, R. W. Tock, S. Parameswaran, and S. S. Ramkumar, "Electrospinning of nanofibers," *Journal of Applied Polymer Science*, vol. 96, no. 2, pp. 557–569, 2005.

[44] R. Dersch, M. Steinhart, U. Boudriot, A. Greiner, and J. H. Wendorff, "Nanoprocessing of polymers: applications in medicine, sensors, catalysis, photonics," *Polymers for Advanced Technologies*, vol. 16, no. 2-3, pp. 276–282, 2005.

[45] D. H. Reneker, A. L. Yarin, H. Fong, and S. Koombhongse, "Bending instability of electrically charged liquid jets of polymer solutions in electrospinning," *Journal of Applied Physics*, vol. 87, no. 9 I, pp. 4531–4547, 2000.

[46] H. Fong, "Electrospun nylon 6 nanofiber reinforced BIS-GMA/TEGDMA dental restorative composite resins," *Polymer*, vol. 45, no. 7, pp. 2427–2432, 2004.

[47] M. Tian, Y. Gao, Y. Liu et al., "Bis-GMA/TEGDMA dental composites reinforced with electrospun nylon 6 nanocomposite nanofibers containing highly aligned fibrillar silicate single crystals," *Polymer*, vol. 48, no. 9, pp. 2720–2728, 2007.

[48] H. Dodiuk-Kenig, K. Lizenboim, S. Roth et al., "Performance enhancement of dental composites using electrospun nanofibers," *Journal of Nanomaterials*, vol. 2008, Article ID 840254, 6 pages, 2008.

[49] S. Lin, Q. Cai, J. Ji et al., "Electrospun nanofiber reinforced and toughened composites through in situ nano-interface formation," *Composites Science and Technology*, vol. 68, no. 15-16, pp. 3322–3329, 2008.

[50] X. Zong, S. Ran, D. Fang, B. S. Hsiao, and B. Chu, "Control of structure, morphology and property in electrospun poly(glycolide-co-lactide) non-woven membranes via post-draw treatments," *Polymer*, vol. 44, no. 17, pp. 4959–4967, 2003.

[51] J.-W. Lu, Z.-P. Zhang, X.-Z. Ren, Y.-Z. Chen, J. Yu, and Z.-X. Guo, "High-elongation fiber mats by electrospinning of polyoxymethylene," *Macromolecules*, vol. 41, no. 11, pp. 3762–3764, 2008.

[52] J. Ji, G. Sui, Y. Yu et al., "Significant improvement of mechanical properties observed in highly aligned carbon-nanotube-reinforced nanofibers," *Journal of Physical Chemistry C*, vol. 113, no. 12, pp. 4779–4785, 2009.

[53] L.-Q. Liu, D. Tasis, M. Prato, and H. D. Wagner, "Tensile mechanics of electrospun multiwalled nanotube/poly(methyl methacrylate) nanofibers," *Advanced Materials*, vol. 19, no. 9, pp. 1228–1233, 2007.

[54] W. Sun, Q. Cai, P. Li et al., "Post-draw PAN-PMMA nanofiber reinforced and toughened Bis-GMA dental restorative composite," *Dental Materials*, vol. 26, no. 9, pp. 873–880, 2010.

[55] X. M. Li, X. H. Liu, G. P. Zhang et al., "Repairing 25mm bone defect using fibres reinforced scaffolds as well as autograft bone," *Bone*, vol. 43, pp. S94–S94, 2008.

[56] E. Saiz, E. A. Zimmermann, J. S. Lee, U. G. K. Wegst, and A. P. Tomsia, "Perspectives on the role of nanotechnology in bone tissue engineering," *Dental Materials*, vol. 29, no. 1, pp. 103–115, 2013.

[57] X. Li and Q. Feng, "Porous poly-L-lactic acid scaffold reinforced by chitin fibers," *Polymer Bulletin*, vol. 54, no. 1-2, pp. 47–55, 2005.

[58] I. D. Sideridou, M. M. Karabela, and E. C. Vouvoudi, "Physical properties of current dental nanohybrid and nanofill light-cured resin composites," *Dental Materials*, vol. 27, no. 6, pp. 598–607, 2011.

[59] K. D. Jandt and B. W. Sigusch, "Future perspectives of resin-based dental materials," *Dental Materials*, vol. 25, no. 8, pp. 1001–1006, 2009.

[60] X. Li, Q. Feng, X. Liu, W. Dong, and F. Cui, "Collagen-based implants reinforced by chitin fibres in a goat shank bone defect model," *Biomaterials*, vol. 27, no. 9, pp. 1917–1923, 2006.

[61] I. S. Chronakis, "Novel nanocomposites and nanoceramics based on polymer nanofibers using electrospinning process—a review," *Journal of Materials Processing Technology*, vol. 167, no. 2-3, pp. 283–293, 2005.

[62] K. Jayaraman, M. Kotaki, Y. Zhang, X. Mo, and S. Ramakrishna, "Recent advances in polymer nanofibers," *Journal of Nanoscience and Nanotechnology*, vol. 4, no. 1-2, pp. 52–65, 2004.

[63] W. E. Teo, R. Inai, and S. Ramakrishna, "Technological advances in electrospinning of nanofibers," *Science and Technology of Advanced Materials*, vol. 12, no. 1, pp. 3002–3020, 2011.

[64] X. Li, Q. Feng, Y. Jiao, and F. Cui, "Collagen-based scaffolds reinforced by chitosan fibres for bone tissue engineering," *Polymer International*, vol. 54, no. 7, pp. 1034–1040, 2005.

[65] J. M. Deitzel, W. Kosik, S. H. McKnight, N. C. Beck Tan, J. M. DeSimone, and S. Crette, "Electrospinning of polymer nanofibers with specific surface chemistry," *Polymer*, vol. 43, no. 3, pp. 1025–1029, 2001.

[66] D. Li and Y. Xia, "Electrospinning of nanofibers: reinventing the wheel?" *Advanced Materials*, vol. 16, no. 14, pp. 1151–1170, 2004.

[67] V. Deligeorgi, I. A. Mjör, and N. H. Wilson, "An overview of reasons for the placement and replacement of restorations," *Primary Dental Care*, vol. 8, no. 1, pp. 5–11, 2001.

[68] T. M. Lastumäki, L. V. J. Lassila, and P. K. Vallittu, "Flexural properties of the bulk fiber-reinforced composite DC-Tell used in fixed partial dentures," *International Journal of Prosthodontics*, vol. 14, no. 1, pp. 22–26, 2001.

[69] H. H. K. Xu, *Crack-bridging toughening of continuous-fiber ceramic composites at ambient and elevated temperatures [Ph.D. thesis]*, University of Maryland at College Park, 1993.

[70] H. H. K. Xu, C. P. Ostertag, L. M. Braun, and I. K. Lloyd, "Short-crack mechanical properties and failure mechanisms of Si3N4-matrix/SiC-fiber composites," *Journal of the American Ceramic Society*, vol. 77, no. 7, pp. 1889–1896, 1994.

[71] H. Iwanaga and C. Kawai, "Tensile strength of silicon nitride whiskers synthesized by reacting amorphous silicon nitride and titanium dioxide," *Journal of the American Ceramic Society*, vol. 81, no. 3, pp. 773–776, 1998.

[72] H. H. K. Xu, "Dental composite resins containing silica-fused ceramic single-crystalline whiskers with various filler levels," *Journal of Dental Research*, vol. 78, no. 7, pp. 1304–1311, 1999.

[73] H. H. K. Xu, "Whisker-reinforced heat-cured dental resin composites: effects of filler level and heat-cure temperature and time," *Journal of Dental Research*, vol. 79, no. 6, pp. 1392–1397, 2000.

[74] H. H. K. Xu, J. B. Quinn, D. T. Smith, A. A. Giuseppetti, and F. C. Eichmiller, "Effects of different whiskers on the reinforcement of dental resin composites," *Dental Materials*, vol. 19, no. 5, pp. 359–367, 2003.

[75] X. Xu, G. Guo, and Y. Fan, "Fabrication and characterization of dense zirconia and zirconia-silica ceramic nanofibers," *Journal of Nanoscience and Nanotechnology*, vol. 10, no. 9, pp. 5672–5679, 2010.

[76] G. Guo, Y. Fan, J.-F. Zhang, J. L. Hagan, and X. Xu, "Novel dental composites reinforced with zirconia-silica ceramic nanofibers," *Dental Materials*, vol. 28, no. 4, pp. 360–368, 2012.

[77] K. F. Leinfelder, T. B. Sluder, J. F. F. Santos, and J. T. Wall, "Five-year clinical evaluation of anterior and posterior restorations of composite resin," *Operative Dentistry*, vol. 12, pp. 52–78, 1980.

[78] A. M. Lacy, "A critical look at posterior composite restorations," *The Journal of the American Dental Association*, vol. 114, no. 3, pp. 357–362, 1987.

[79] R. E. Jordan and M. Suzuki, "Posterior composite restorations. Where and how they work best," *The Journal of the American Dental Association*, vol. 122, no. 12, pp. 30–37, 1991.

[80] R. Giordano II, "Fiber reinforced composite resin systems," *General dentistry*, vol. 48, no. 3, pp. 244–249, 2000.

[81] M. Behr, M. Rosentritt, D. Latzel, and T. Kreisler, "Comparison of three types of fiber-reinforced composite molar crowns on their fracture resistance and marginal adaptation," *Journal of Dentistry*, vol. 29, no. 3, pp. 187–196, 2001.

[82] H. H. Xu, G. E. Schumacher, F. C. Eichmiller, and J. M. Antonucci, "Strengthening composite resin restorations with ceramic whisker reinforcement," *Practical Periodontics and Aesthetic Dentistry*, vol. 12, no. 1, pp. 111–118, 2000.

[83] E. Joussein, S. Petit, J. Churchman, B. Theng, D. Righi, and B. Delvaux, "Halloysite clay minerals—a review," *Clay Minerals*, vol. 40, no. 4, pp. 383–426, 2005.

[84] V. Vergaro, E. Abdullayev, Y. M. Lvov et al., "Cytocompatibility and uptake of halloysite clay nanotubes," *Biomacromolecules*, vol. 11, no. 3, pp. 820–826, 2010.

[85] H. Zhang and B. W. Darvell, "Mechanical properties of hydroxyapatite whisker-reinforced bis-GMA-based resin composites," *Dental Materials*, vol. 28, no. 8, pp. 824–830, 2012.

[86] Q. Chen, Y. Zhao, W. Wu, T. Xu, and H. Fong, "Fabrication and evaluation of Bis-GMA/TEGDMA dental resins/composites containing halloysite nanotubes," *Dental Materials*, vol. 28, no. 10, pp. 1071–1079, 2012.

[87] D. A. Walters, L. M. Ericson, M. J. Casavant et al., "Elastic strain of freely suspended single-wall carbon nanotube ropes," *Applied Physics Letters*, vol. 74, no. 25, pp. 3803–3805, 1999.

[88] X. Li, L. Wang, Y. Fan, Q. Feng, and F.-Z. Cui, "Biocompatibility and toxicity of nanoparticles and nanotubes," *Journal of Nanomaterials*, vol. 2012, Article ID 548389, 19 pages, 2012.

[89] O. Lourie and H. D. Wagner, "Evaluation of Young's modulus of carbon nanotubes by micro-Raman spectroscopy," *Journal of Materials Research*, vol. 13, no. 9, pp. 2418–2422, 1998.

[90] S. Kumar and R. Vijayalakshmi, "Nanotechnology in dentistry," *Indian Journal of Dental Research*, vol. 17, no. 2, pp. 62–65, 2006.

[91] X. Li, Y. Fan, and F. Watari, "Current investigations into carbon nanotubes for biomedical application," *Biomedical Materials*, vol. 5, no. 2, Article ID 022001, 12 pages, 2010.

[92] R. Andrews, D. Jacques, A. M. Rao et al., "Nanotube composite carbon fibers," *Applied Physics Letters*, vol. 75, no. 9, pp. 1329–1331, 1999.

[93] S. Jain, A. P. Jain, S. Jain, O. N. Gupta, and A. Vaidya, "Nanotechnology: an emerging area in the field of dentistry," *Journal of Dental Sciences*, pp. 1–9, 2013.

[94] X. Li, L. Wang, Y. Fan, Q. Feng, F.-Z. Cui, and F. Watari, "Nanostructured scaffolds for bone tissue engineering," *Journal of Biomedical Materials Research Part A*, vol. 101, no. 8, pp. 2424–2435, 2013.

[95] F. Zhang, Y. Xia, L. Xu, and N. Gu, "Surface modification and microstructure of single-walled carbon nanotubes for dental resin-based composites," *Journal of Biomedical Materials Research Part B*, vol. 86, no. 1, pp. 90–97, 2008.

[96] I. M. Hamouda, "Current perspectives of nanoparticles in medical and dental biomaterials," *Journal of Biomedical Research*, vol. 26, no. 3, pp. 143–151, 2012.

[97] X. Li, H. Gao, M. Uo et al., "Effect of carbon nanotubes on cellular functions in vitro," *Journal of Biomedical Materials Research Part A*, vol. 91, no. 1, pp. 132–139, 2009.

[98] X. Wei, M.-S. Wang, Y. Bando, and D. Golberg, "Tensile tests on individual multi-walled boron nitride nanotubes," *Advanced Materials*, vol. 22, no. 43, pp. 4895–4899, 2010.

[99] W.-L. Wang, J.-Q. Bi, K.-N. Sun, M. Du, N.-N. Long, and Y.-J. Bai, "Fabrication of alumina ceramic reinforced with boron nitride nanotubes with improved mechanical properties," *Journal of the American Ceramic Society*, vol. 94, no. 11, pp. 3636–3640, 2011.

[100] B. Marrs, R. Andrews, T. Rantell, and D. Pienkowski, "Augmentation of acrylic bone cement with multiwall carbon nanotubes," *Journal of Biomedical Materials Research Part A*, vol. 77, no. 2, pp. 269–276, 2006.

[101] S. P. Kotha, C. Li, S. R. Schmid, and J. J. Mason, "Fracture toughness of steel-fiber-reinforced bone cement," *Journal of Biomedical Materials Research Part A*, vol. 70, no. 3, pp. 514–521, 2004.

[102] S. M. Khaled, R. Sui, P. A. Charpentier, and A. S. Rizkalla, "Synthesis of TiO_2-PMMA nanocomposite: using methacrylic acid as a coupling agent," *Langmuir*, vol. 23, no. 7, pp. 3988–3995, 2007.

[103] S. M. Z. Khaled, R. J. Miron, D. W. Hamilton, P. A. Charpentier, and A. S. Rizkalla, "Reinforcement of resin based cement with titania nanotubes," *Dental Materials*, vol. 26, no. 2, pp. 169–178, 2010.

[104] X. M. Li, R. R. Cui, W. Liu et al., "The use of nano-scaled fibers or tubes to improve biocompatibility and bioactivity of biomedical materials," *Journal of Nanomaterials*, vol. 2013, Article ID 728130, 16 pages, 2013.

Hindawi Publishing Corporation
BioMed Research International
Volume 2014, Article ID 418302, 9 pages
http://dx.doi.org/10.1155/2014/418302

Research Article

Application of Ultrasound on Monitoring the Evolution of the Collagen Fiber Reinforced nHAC/CS Composites *In Vivo*

Yan Chen,[1] Yuting Yan,[2] Xiaoming Li,[3] He Li,[2] Huiting Tan,[2] Huajun Li,[2] Yanwen Zhu,[2] Philipp Niemeyer,[4] Matin Yaega,[4] and Bo Yu[5]

[1] *Department of Ultrasonic Diagnosis, Zhujiang Hospital of Southern Medical University, Guangzhou 510282, China*
[2] *The Second Clinical Medical College of Southern Medical University, Guangzhou 510282, China*
[3] *Key Laboratory for Biomechanics and Mechanobiology of Ministry of Education, School of Biological Science and Medical Engineering, Beihang University, Beijing 100191, China*
[4] *Department of Orthopaedic surgery and Traumatology, Freiburg University Hospital, Freiburg, Germany*
[5] *Department of Orthopedics, Zhujiang Hospital of Southern Medical University, Guangzhou 510282, China*

Correspondence should be addressed to Xiaoming Li; x.m.li@hotmail.com and Bo Yu; gzyubo@gmail.com

Received 31 October 2013; Accepted 4 March 2014; Published 14 April 2014

Academic Editor: Xiaowei Li

Copyright © 2014 Yan Chen et al. This is an open access article distributed under the Creative Commons Attribution License, which permits unrestricted use, distribution, and reproduction in any medium, provided the original work is properly cited.

To date, fiber reinforce scaffolds have been largely applied to repair hard and soft tissues. Meanwhile, monitoring the scaffolds for long periods *in vivo* is recognized as a crucial issue before its wide use. As a consequence, there is a growing need for noninvasive and convenient methods to analyze the implantation remolding process *in situ* and in real time. In this paper, diagnostic medical ultrasound was used to monitor the *in vivo* bone formation and degradation process of the novel mineralized collagen fiber reinforced composite which is synthesized by chitosan (CS), nanohydroxyapatite (nHA), and collagen fiber (Col). To observe the impact of cells on bone remodeling process, the scaffolds were planted into the back of the SD rats with and without rat bone mesenchymal stem cells (rBMSCs). Systematic data of scaffolds *in vivo* was extracted from ultrasound images. Significant consistency between the data from the ultrasound and DXA could be observed ($P < 0.05$). This indicated that ultrasound may serve as a feasible alternative for noninvasive monitoring the evolution of scaffolds *in situ* during cell growth.

1. Introduction

Cell-based bone tissue engineering has emerged as a promising alternative to traditional bone graft treatment [1]. Due to mineralized collagen fibers making up the microstructure of natural bone tissue [2], a biomimetic nanohydroxyapatite/collagen (nHA/Col) scaffold reinforced by mineralizing type I collagen fiber seems to be a very promising system for bone tissue engineering [3–5]. Hence the development of mineralized collagen fiber composites is in urgent need of a noninvasive, quantifiable, and systematic method to monitor the complex regenerate function and degradation process *in vivo* and in real time. Accurate *in vivo* data is needed for a complete understanding of the mineralized collagen fiber and guiding the scaffold design.

Developing a simple and easy-to-use method to monitor regeneration process of the scaffolds is critical for bone tissue engineering research. Current approaches for acquiring precise bone mineral density (BMD) value are mostly by dual-energy X-ray absorptiometry (DXA) or computed tomography (CT) [6]. However, for one thing, the scanning and image reconstruction procedures are of complex operations, in high consumption and with strong radiation. Thus it is difficult to meet the need of a long-term evaluation of dynamic tracking. For another, DXA and CT could only provide morphological information and are unable to achieve the exploration of bone microstructure, which is the determining factor of bone function independently of BMD [7, 8]. To date, measurements on bone constructs and some desired mechanical parameters mainly rely on destructive and time-consuming histological and biochemical assay [9]. The substantial animal use, low repeatability, and difficulty of *in vivo* examination limit its application. There are also some budding nondestructive technologies. MR elastography (MRE)

could make an assessment of mechanical properties, but it is limited by a poor spatial resolution at 5 mm [10]. Optical coherence tomography (OCT), with high spatial resolution but low penetration capacity, was mainly used in evaluation of vascular scaffold currently [11]. Microcomputed tomography (μCT) could evaluate the scaffolds systematically, but its use was limited by its high expense and equipment requirement [12].

Hence, there remains a significant need for noninvasive techniques to sequentially monitor the progress of tissue construct evolution *in vivo* without periodic animal sacrifice. Since the report about ultrasonic speed and attenuation in bone in 1975 [13], ultrasound was gradually developed to be a noninvasive, nonradiative diagnostic tool of bone. Physical parameters tested by ultrasound were capable of reflecting bone density, quality, and some other mechanical factors of cancellous bone [14, 15]. Consequently, ultrasonic technology has been widely used in analyzing children's bone condition and osteoporosis in recent years and reveals a promising application [16]. However, ultrasound is rarely reported to evaluate scaffolds in bone tissue engineering. Recently, ultrasound elasticity imaging (UEI) has been found to be an available tool for characterizing mechanical changes of the implanted scaffold with high resolution and substantial detecting depth, but it is at expenses of higher cost, more specific hardware, and not easily accessible to most research groups [17, 18]. In our study, we attempted to establish a noninvasive, comprehensive, and convenient bone repair monitoring system based on diagnostic ultrasound.

Appropriate scaffolds capable of providing suitable structural and biological constructs are of great importance for cellular ingrowth [19]. In our preliminary study, an injectable thermo sensitive hydrogel composite based on CS, HA, and Col was demonstrated with great biocompatibility and excellent osteogenesis performance [20, 21]. In current research, we reshaped it as a mineralized collagen fiber reinforced solid scaffold (nHAC/CS) to obtain a stable initial mechanical strength. Moreover, to explore how rBMSCs affect the bone repair process, we added rBMSCs into the scaffold and made the comparison with the simple nHAC/CS group. The ultimate goal is to innovatively excavate diagnostic ultrasound to monitor the real-time remodeling information for the long cultivation period of the two scaffold groups. Systematic *in vivo* indexes were extracted from ultrasonic images, such as bone mass, BMD, calcification rate, degradation rate, and uniformity of inner structure, and were compared with the analyzed indexes of DXA. The feasibility of diagnostic ultrasound was illustrated as a direct tool to evaluate the evolution of constructs online for tissue engineers.

2. Material and Method

2.1. Fabrication of Scaffold Materials

2.1.1. Preparation of Thiolated Chitosan. Chitosan (800 mg) was dissolved in acetum solution (400 mL, 1%). Iminothiolane hydrochloride (80 mg) was added after stirring for 5 hours. The pH of the solution was adjusted to 6.0 by adding sodium hydroxide (5 M). Dialysis with hydrogen chloride (5 M) was repeated 3 times. Thiolated-chitosan sample was prepared after freeze-drying.

2.1.2. Synthesis of nHAC/CS Scaffold. The synthesis of nHA/Col (nHAC) powder has been reported previously [22]. It was assembled with nanofibrils of mineralized collagen and sterilized by X-ray irradiation. Thiolated-chitosan sample (200 mg) was dissolved in sodium hydroxide (10 mL, 0.1 M) and nHAC powder (200 mg) was added into the solution. Then the solution was stirred and dispersed evenly by ultrasonic wave. We removed the solution into 96-well plates carefully, and the sample was freeze-dried at room temperature.

2.2. Cell Isolation and Culture. Bone marrow was obtained from 12-week-old male SD rats. Briefly, femurs were aseptically removed and broken. The Bone marrow was absorbed by an injector, and then rat mesenchymal stem cells (rBMSCs) were isolated to the culture flask after centrifugation at 1500 RPM for 5 min. The rBMSCs were cultured in DMEM/F-12 medium and allowed to adhere for 24 hours. Nonadherent cells were then removed. After that, the cells were cultured at 37°C in 95% humidity and 5% carbon dioxide, and the medium was changed regularly every 3 days. After 3 weeks, adherent cells were detached by trypsin-EDTA (0.5 to 0.2 g/L, Invitrogen) and used for the *in vivo* experiments.

2.3. Implantation Experiment in SD Rats. All the animals were operated in the light of the guidelines for animal experiments. In this study, 18 healthy SD female rats (150 g on average), supplied by the Animal Research Center of Guangdong Province, were divided into two groups equally (A, B). After induction with midazolam, the rats were anesthetized by the 0.3 mL/kg mixture of xylazine and ketamine (2 : 1). Then the rats were placed in the prone position, depilated, and sterilized from *arcus costarum* to hip joint. An incision was made close to erector spinae. We performed blunt dissection on superficial fascia and created three muscular pockets in the back. For each rat, two scaffolds of the same type were implanted. The columnar scaffold (nHAC/CS) was implanted with 0.5 mL concentrated solution of rBMSCs (5×10^6) in the rats of group A, and in group B the same scaffold was implanted together with 0.5 mL normal saline (NS) as a control. The administration of antibiotics as prophylactic measure was carried out. All animals survived to the designated time without any major complications. The design of the study was displayed in Figure 1.

2.4. Ultrasonic Examination. Ultrasound images were taken with an ALOKA prosound α-10 premier diagnostic ultrasound system (1.1 mechanical index, 80 transmission gain) equipped with a 12 MHZ probe for all scans. Each group was performed a detection at week 0, week 1, week 2, week 4, week 6, week 8, week 10, and week 12. Rats were anesthetized in prone position with the inspection area exposed. Then we put the probe above the muscular pockets in order to observe the evolution of the scaffold constructs.

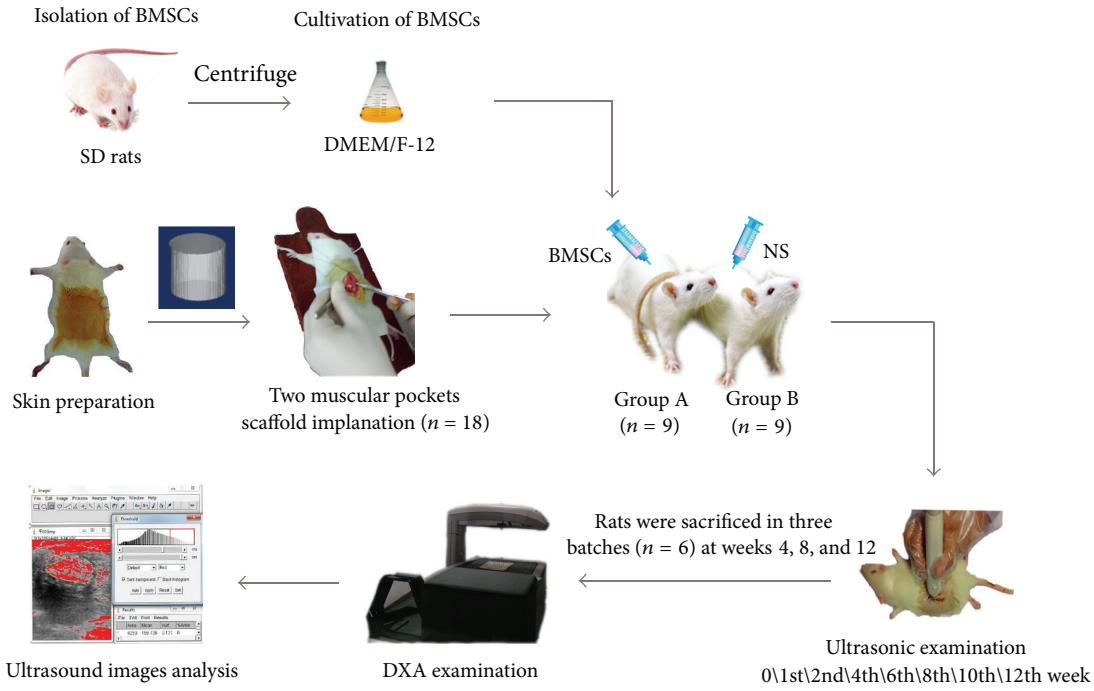

Figure 1: Schematic showing design of the study.

2.5. Ultrasound Images Analysis. The ultrasonic backscattered signal is displayed as a gray-scale array with values ranging from 0 to 255, and 0 denotes a negligible difference in resistance from the surrounding medium; the development of an ultrasound signal over time was interpreted as an increase in stiffness that may due to the solidifying development of materials. Gray-scale value, calcification rate, degradation rate, and homogeneous degree were measured and BMD was estimated by analyzing ultrasound images.

2.6. DXA. The rats were sacrificed in three batches ($n = 6$) at weeks 4, 8, and 12 with their affiliated tissue constructs harvested. And then each scaffold was scanned twice by a Lunar Prodigy DXA bone densitometer (GE Healthcare, Madison, WI, USA). BMD was used to evaluate the scaffolds' ability of heterotopic osteogenesis, which can be analyzed by LunarenCORE software (ver. 10.0, standard-array mode). All the measurements were executed by the same technologist who had received professional training.

2.6.1. Gray-Scale Value. The gray-scale value (GV) was analyzed by measuring the mean GV of the implant area over time by the method of histogram echo intensity. The measurements from the six images were averaged together for each implant, reported as mean ± standard deviation.

2.6.2. Calcification Rate and Degradation Rate. All images were analyzed by *ImageJ software* to measure calcification rate and degradation rate. Implant region was set as region of interest (ROI). According to the GV ("Min"-"Max") of material tested in one hour after operation, GV ranging from "Max" to 255 was regarded as the region of calcification and the other was noncalcified region. Similarly gray-scale value ranging from 0 to "Min" and "Max" to 255 was regarded as the region of degradation and the other was no degradation region. Thus the calcification rate and degradation rate were estimated.

2.6.3. Homogeneous Degree. Implant region was set as ROI. Homogeneous degree was calculated by applying the index "kurtosis" in *ImageJ*.

2.6.4. BMD Estimation. According to the BMD and GV of radius, femur, tibia, pelvis, 7th cervical vertebrae, and 1st, 2nd, and 3rd lumbar vertebra in rats, regression curve was calculated. On the basis of this curve, BMD corresponding with each GV was estimated by the software of Origin 8.0. Finally, we carried out agreement analysis between estimated BMD and actual measured BMD by DXA.

2.7. Statistics. The correlation between two continuous variables, GV by ultrasound and BMD by DXA, was quantified with a Pearson correlation coefficient. Bland-Altman plots were used to assess the agreements between estimated BMD by ultrasound and actual measured BMD by DXA. The regression of the average and the difference between the two indicators were analyzed. All experimental data were reported as the mean ± standard deviation ($n = 6$). Levene homoscedasticity test and independent-samples t-test were used to identify any significant differences between the different groups. A P value of $<0.05^{*}$ and $<0.01^{**}$ was considered statistically significant. Statistical analyses were

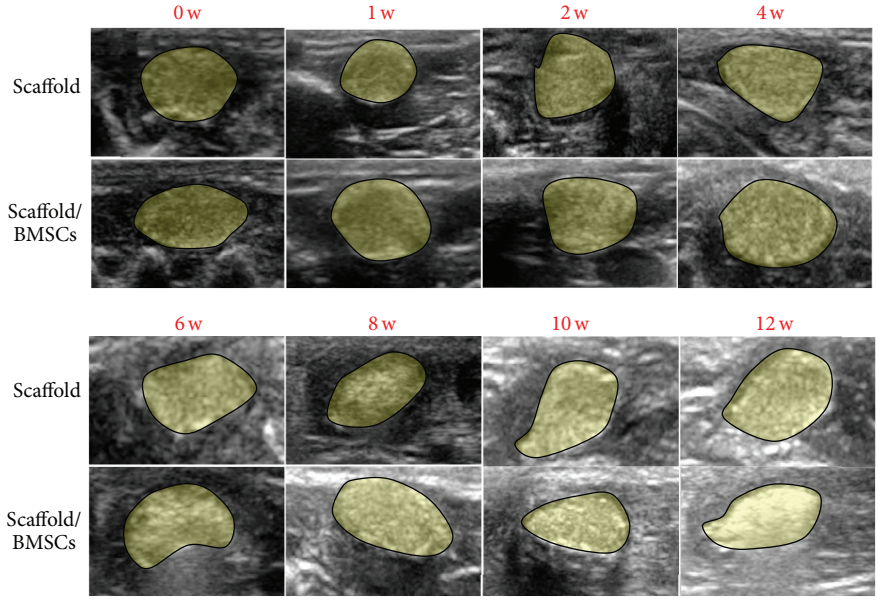

Figure 2: Ultrasound images of implanted scaffold over time, showing the evolution of constructs of the two groups (scaffold or scaffold/rBMSCs). The ROIs were signed by translucent yellow overlays.

performed with SPSS19.0 software (SPSS Inc., Chicago, IL, USA).

3. Results and Discussion

3.1. The Mean Echo Intensity and Bone Formation. Ultrasound images of the implanted scaffolds with or without cells over time were displayed in Figure 2. It was obviously observed that the outline of implant was legible at each time point and the echo intensity of implanted site showed noticeable rise with time. Ultrasonic wave is largely attenuated through cancellous bone, and it was reported that attenuation of ultrasound propagating and acoustic velocity in bone is used widely for bone assessment [18, 23]. Gray-scale value (GV), which could digitize the mean echo intensity, is an indicator of acoustic impedance in implant site and has connection with medium density and sound velocity [24]. Thus, several researchers attempted to utilize GV to assess the tissue stiffness and mechanical properties [25–27]. Kreitz et al. [28] proposed GV as a good parameter to evaluate the collagen formation with a high correlation with hydroxyproline content ($r = 0.98$). In our study, to quantitatively analyse the changes of mean echo intensity among different time points and different groups, computer-assisted GV was measured in Table 1. A significant increase of GV over time was presented in Figure 3, probably representing the trend of bone mineral deposition and implanted scaffold calcification with respect to bone formation. The mean echo intensity of implant together with cells was enhanced from the fourth week ($P < 0.05$). The performance of rBMSCs may stimulate osteoblast differentiation as a result of GV level overtopping the control group. At 12 weeks after implanting, the GV of implant site jumped to 177 and 201, respectively, as high as the level of cancellous bone according to Table 4.

Table 1: Experimental data values for gray-scale value of the scaffold group and scaffold/rBMSCs group over time.

	GV		
Time (w)	Scaffold (mean ± SD)	Scaffold/BMSCs (mean ± SD)	*P* value
0	63.85 ± 7.7	62.07 ± 5.49	0.655
1	82.88 ± 5.04	87.73 ± 7.17	0.205
2	99.29 ± 2.13	105.23 ± 14.03	0.35
4	111.85 ± 6.76	122.53 ± 6.03	0.016*
6	127.23 ± 6.35	140.93 ± 6.57	0.004**
8	144.99 ± 10.31	165.08 ± 5.95	0.011*
10	155.44 ± 8.51	173.09 ± 11.14	0.016*
12	176.62 ± 13.75	200.99 ± 12.39	0.009**

*$P < 0.05$, **$P < 0.01$.

The outcome indicated that the ultrasonic echo intensity (gray-scale brightness from images) could be a potential parameter assessing mechanical function *in vivo*. The GV indicator reflected a high consistency with the process of osteogenesis constructs, and the correlativity with BMD would be verified in the following sections.

3.2. The Process of Calcification and Degradation. In cell-based tissue engineering, the regeneration performance of scaffolds largely relies on their degradability. Current methods for quantifying degradation process are histological examination and direct sample measurements with animal sacrifice and scaffold destruction. Ultrasound is potentially to be applied as a noninvasive technique to obverse consequent scaffold degradation of the same specimen [29]. The degradation process results in different acoustical properties

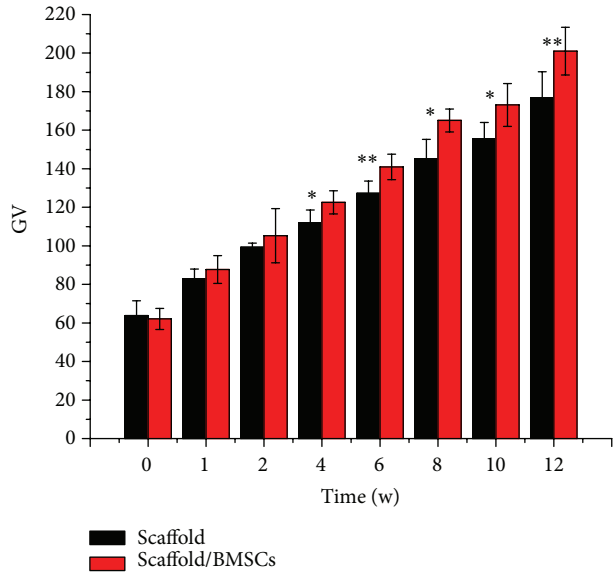

Figure 3: Ultrasound outcome indicating mean echo intensity (GV) of implant site for week 0, 1, 2, 4, 6, 8, or 10 postsurgery ($n = 9$ in each group). Results were expressed as mean ± SD ($n = 9$).

Table 2: Calcification and degradation characteristics of scaffolds at each time point.

Time (w)	Calcification rate (%) (mean ± SD)			Degradation rate (%) (mean ± SD)			Calcification rate/degradation rate		
	Scaffold	Scaffold/BMSCs	*P* value	Scaffold	Scaffold/BMSCs	*P* value	Scaffold	Scaffold/BMSCs	*P* value
1	4.07 ± 0.4	4.43 ± 0.9	0.389	8.41 ± 1.1	8.84 ± 0.7	0.445	0.49 ± 0.02	0.5 ± 0.08	0.688
2	6.36 ± 1.4	7.97 ± 2.2	0.157	14.94 ± 2.4	13.21 ± 2.6	0.258	0.42 ± 0.04	0.62 ± 0.18	0.042*
4	13.76 ± 3.6	15.96 ± 0.8	0.201	25.1 ± 4.3	20.91 ± 3.3	0.09	0.55 ± 0.1	0.78 ± 0.12	0.004**
6	18.55 ± 4.5	27.27 ± 2	0.001**	35.21 ± 2.6	35.68 ± 7.5	0.888	0.52 ± 0.11	0.78 ± 0.12	0.003**
8	31.16 ± 8.5	42.83 ± 7.3	0.023*	54.44 ± 6.8	56.49 ± 1.7	0.504	0.57 ± 0.11	0.76 ± 0.13	0.021*
10	40.69 ± 7.2	55.25 ± 8.3	0.009**	67.32 ± 2.7	64.3 ± 4.4	0.636	0.61 ± 0.11	0.83 ± 0.12	0.007**
12	55.65 ± 6	66.23 ± 7.2	0.02*	75.59 ± 5.3	76.89 ± 4.3	0.649	0.74 ± 0.05	0.86 ± 0.1	0.02*

*$P < 0.05$, **$P < 0.01$.

Table 3: The kurtosis coefficient showing internal uniformity of scaffold at each time point.

Time (w)	Ultrasonic kurtosis coefficient		*P* value
	Scaffold (mean ± SD)	Scaffold/BMSCs (mean ± SD)	
0	9.89 ± 0.89	10.55 ± 0.72	0.187
1	3.8 ± 1.2	5.15 ± 1.24	0.084
2	0.69 ± 1.52	3.08 ± 1.31	0.016*
4	−0.14 ± 1.18	0.83 ± 1.35	0.961
6	−0.39 ± 1.9	4.34 ± 1.15	0.001**
8	1.35 ± 2.48	3.14 ± 1.18	0.142
10	1.07 ± 1.24	5.93 ± 2.3	0.002**
12	5 ± 1.21	12.9 ± 3.43	0.002**

*$P < 0.05$, **$P < 0.01$.

of the implantation site and could be detected by ultrasound as diminishing echo intensity [30, 31]. Chitosan was interfused in our scaffold to obtain better degradation property. The degradation of implanted scaffold could result in two conditions: for one, bone mineral deposition and calcified tissue ingrowth exactly at the degradation area; for another, the new bone formation is not as fast as the degradation of material and consequent cavitation or porosity could be observed *in situ*. Hence, the stable degradation rate of scaffold, which would exactly match the calcification rate, has a critical impact on the internal architecture and load-bearing capability. Calcification rate versus degradation rate could be a valuable indicator for scaffold assessment.

The measurement results via ultrasound are listed in Table 2. The calcification rate of scaffolds with cells was much better than the control group (Figure 4(a)), while no statistically significant differences could be found between the two groups in degradation rate (Figure 4(b)), which indicated stem cells played an important role in calcification process and displayed no help in facilitating degradation. The scaffold/rBMSCs group possessed a higher value of the ratio (calcification rate versus degradation rate), which was a representative of better internal structure and more reliable mechanical support at its early stage. Ultrasound

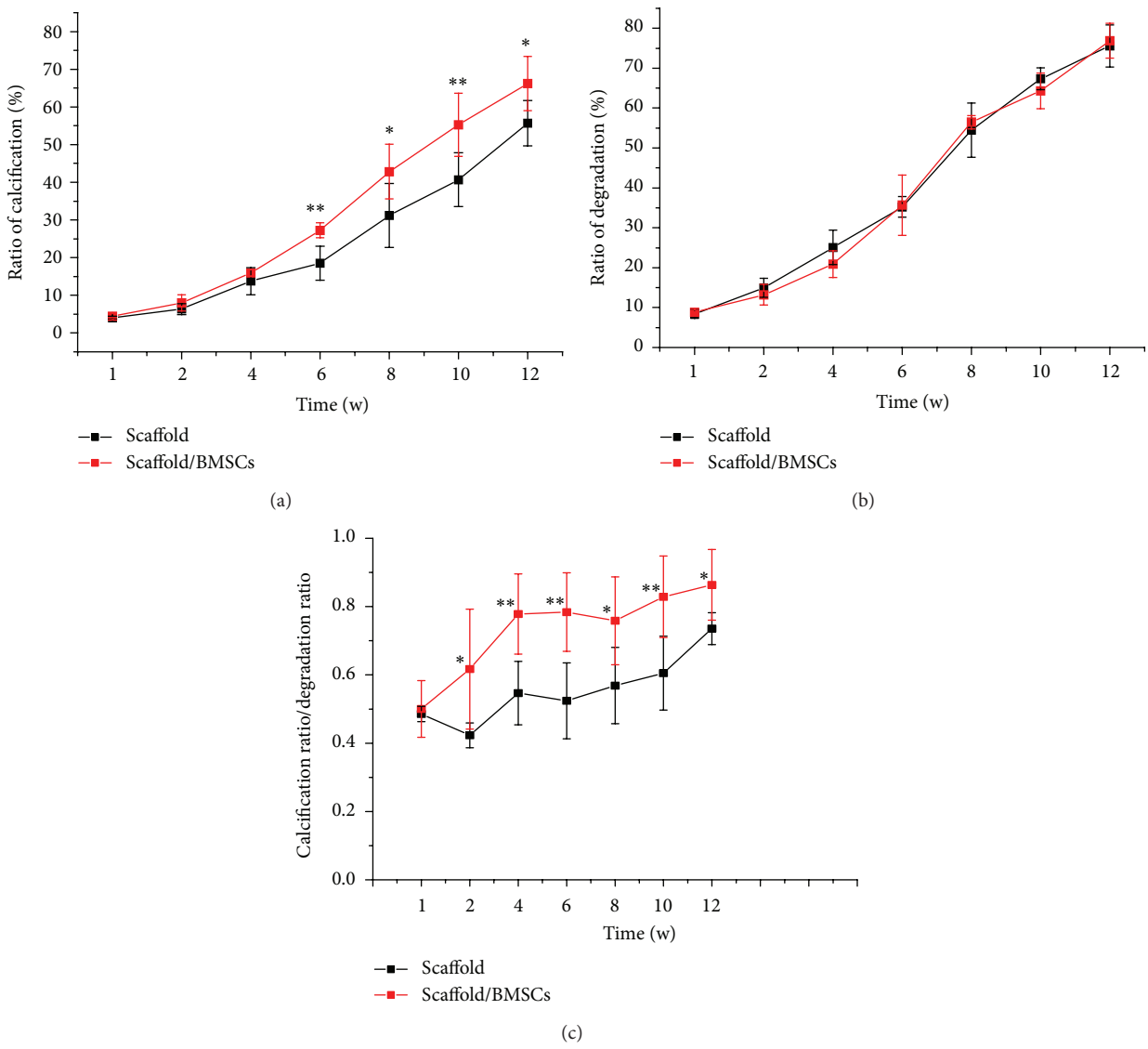

FIGURE 4: Regeneration property (a) and degradation property (b) of implant via ultrasound over time. Calcification rate versus degradation rate was calculated (c). Results were expressed as mean ± SD ($n = 9$); $^*P < 0.05$ as compared to control group with no cells added.

technique, as a noninvasive measure of monitoring the scaffold degradation and regeneration process, will greatly help tissue engineers improve the design process.

3.3. Homogeneous Degree of Implantation Area. Because the osteoporosis is thought to be largely determined by the combined effects of low bone content and poor microframework, the assessment of bone microstructure quality is of equal importance to BMD measure in bone tissue engineering. A systematic and ideal technique could assess the microstructure of scaffold noninvasively, which may have considerable impact on the mechanical indicator of fragility, stress, or strength. In our study, we attempted to utilize ultrasonic kurtosis coefficient to monitor the homogeneity of implantation area. Kurtosis is used to reflect the sharpness or flatness of the frequency distribution curve. Here, we calculated kurtosis coefficient as the concentration of GV near the mean as compared with the normal distribution. Therefore, the higher the value of kurtosis is, the more centralized the GV of implant site would be; that is, excessive calcification or excessive degradation region would not arise inside the implanted materials. Inversely, if the kurtosis coefficient of implant site is low or even negative, it is indicated that the frequency distribution curve of GV is relatively flat, which represents the heterogeneity of internal structure.

Table 3 presented the kurtosis coefficient of GV in implant site at each time point. The homogeneous degree decreased in the first month after the implant operation and dropped to the lowest point at week 4 or so (Figure 5). It may be due to the rapid degradation rate in the early phase, which could give rise to the structural instability. Then with the constant calcification of scaffold, the voids were filled with new-born bone and the evenness index increased. Until 3 months,

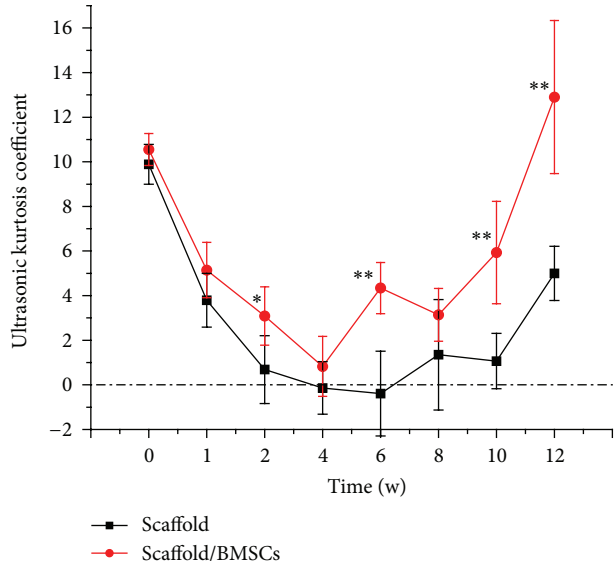

Figure 5: Graph of ultrasonic kurtosis coefficient of scaffold group and scaffold/rBMSCs group over time. Results were expressed as mean ± SD ($n = 9$); $^*P < 0.05$ as compared to control group with no cells added.

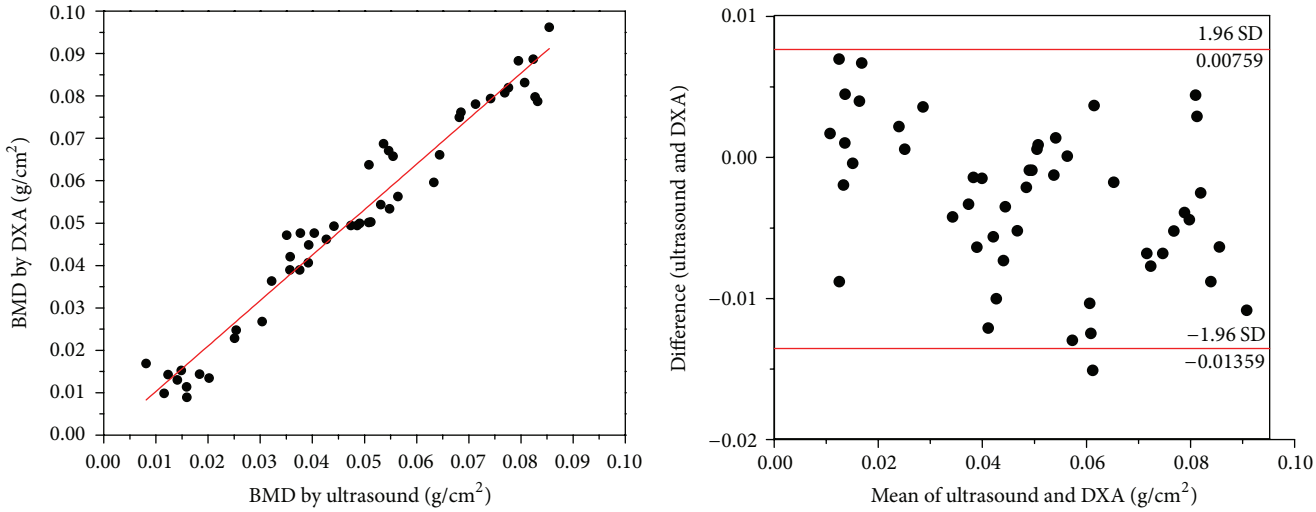

Figure 6: Linear regression plots (solid lines) of estimated BMD by ultrasound versus the measurements by DXA at different implant sites (a). Bland-Altman plots for agreement of data by ultrasound and DXA (b).

calcification was quite homogeneous and almost reached the internal morphology of cancellous bone as a result of a high kurtosis coefficient of GV. From the graph, the kurtosis coefficient of scaffold/rBMSCs group showed significantly higher than the control group up to 3 months after implanting ($P < 0.01$). It may be interpreted to be the effect of stem cells in modulating the microstructure of internal scaffold. Nevertheless, in the scaffold group without cells, kurtosis coefficient was less than 0 for approximately one month, which demonstrated a quite unstable internal structure with poor mechanical property and the implant area might cause more frequently collapse or distortion. Hence, it is of crucial importance to monitor the bone quality and material internal microstructure in real time in bone tissue engineering.

3.4. Comparison between the GV by Ultrasound and the BMD by DXA. In recent researches, ultrasound technique has been gradually concerned with quantitative assessment of the scaffold constructs in animal studies [32, 33]. In order to demonstrate the feasibility of this approach for bone tissue engineering, some scholars made comparisons between ultrasound results and the traditional technique, such as histology or direct mechanical test, and a strong linear

Table 4: Measured GV by ultrasound and BMD by DXA of radius, femur, tibia, pelvis, 7th cervical vertebrae, 1st & 2nd & 3rd lumbar vertebra in rats. Average values were calculated and recorded for each measurements ($n = 5$).

Detection part	GV by ultrasound	BMD ($g \cdot cm^{-2}$) by DXA
Radius	182	0.075
Femur	250	0.106
Tibia	197	0.088
Pelvis (ilium)	255	0.111
Vertebrae C7	190	0.089
Vertebrae LI	204	0.091
Vertebrae L2	213	0.098
Vertebrae L3	225	0.099

relationship was exhibited in their studies [17, 28, 34]. Measurement of BMD by DXA is generally considered to be the golden standard technique [35]. The relevant relationships between ultrasonic parameters and actual measurement by DXA was explored in our research. We first measured the radius, femur, tibia, pelvis, 7th cervical vertebrae, and 1st, 2nd, and 3rd lumbar vertebra of rats, and the data of GV by ultrasound and BMD by DXA was extracted in Table 4. The relationship between the two continuous variables was assessed with a bivariate correlation method (Pearson's test). Significant linear correlation between these two indicators was found to be the following: actual BMD = 5.34^{-4} GV–0.02 ($P < 0.05$; $r = 0.96$). According to the formula, we could estimate BMD of implant site based on the measured GV at different points in time (Table 1). Linear regression plot of estimated BMD by ultrasound parameters and direct measurements of BMD by DXA at different implant sites were presented in Figure 6(a). Then, Bland-Altman test was used to assess the agreements between the BMD measured by ultrasound and DXA. The regression of the mean and the difference was analyzed (Figure 6(b)). High consistency of estimated BMD and actual measured value was confirmed ($P < 0.05$). This is the key finding of our study and suggests that the ultrasonic techniques described in this paper can be a feasible alternative to invasively monitor the evolution of constructs online of tissue engineered scaffolds during cell growth.

4. Conclusions

This study established the validity of ultrasound as a noninvasive method to assess tissue transformation of the mineralized collagen fiber reinforced scaffold *in vivo* and in real time. We attempted to utilize ultrasound technology for providing accurate information of osteogenesis, degradation, and calcification process and homogeneity of the internal structure of the scaffolds without periodic animal sacrifice. An improvement in calcification rate and structural homogeneity with the growth of rBMSCs was observed by ultrasound, and the ultrasound findings matched direct BMD measurements by DXA distinctly. This study illustrated the potential of medical diagnosis ultrasound equipment for nondestructively monitoring the evolution of constructs online in bone tissue engineering. Also further research would be necessary to clarify this application before it is widely used.

Conflict of Interests

The authors declare no conflict of interests regarding the publication of this paper.

Authors' Contribution

Yuting Yan and Yan Chen contributed equally to this paper.

Acknowledgments

The authors are grateful for the financial support from the National Basic Research Program of China (973 Program, no. 2011CB710901), National Natural Science Foundation of China (nos. 81101348, 31000431, 81371931, and. 81301240), Natural Science Foundation of Guangdong Province, China (nos. 10451051501004727 and 10151051501000107), Guangdong Medical Scientific Research Project (A2013385), Doctoral Fund of Ministry of Education, China (20114433120004), the Beijing Nova Program (no. 2010B011), Program for New Century Excellent Talents (NCET) in University from Ministry of Education of China, and the outstanding person fund of Zhujiang Hospital.

References

[1] G. J. Meijer, J. D. De Bruijn, R. Koole, and C. A. van Blitterswijk, "Cell-based bone tissue engineering," *PLoS Medicine*, vol. 4, no. 2, pp. 260–264, 2007.

[2] S. Liao, M. Ngiam, C. K. Chan, and S. Ramakrishna, "Fabrication of nano-hydroxyapatite/collagen/osteonectin composites for bone graft applications," *Biomedical Materials*, vol. 4, no. 2, Article ID 025019, 2009.

[3] C. Du, F. Z. Cui, Q. L. Feng, X. D. Zhu, and K. de Groot, "Tissue response to nano-hydroxyapatite/collagen composite implants in marrow cavity," *Journal of Biomedical Materials Research*, vol. 42, no. 4, pp. 540–548, 1998.

[4] X. Niu, Q. Feng, M. Wang, X. Guo, and Q. Zheng, "Porous nano-HA/collagen/PLLA scaffold containing chitosan microspheres for controlled delivery of synthetic peptide derived from BMP-2," *Journal of Controlled Release*, vol. 134, no. 2, pp. 111–117, 2009.

[5] Z. Huang, J. Tian, B. Yu, Y. Xu, and Q. Feng, "A bone-like nano-hydroxyapatite/collagen loaded injectable scaffold," *Biomedical Materials*, vol. 4, no. 5, Article ID 055005, 2009.

[6] H. K. Genant, C. Libanati, K. Engelke et al., "Improvements in hip trabecular, subcortical, and cortical density and mass in postmenopausal women withosteoporosis treated with denosumab," *Bone*, vol. 56, no. 2, pp. 482–488, 2013.

[7] E. Dall'Araa, B. Luisiera, R. Schmidtb et al., "DXA predictions of human femoral mechanical properties depend on the load configuration," *Medical Engineering & Physics*, vol. 35, no. 11, pp. 1564–1572, 2013.

[8] W. Sun, A. Darling, B. Starly, and J. Nam, "Computer-aided tissue engineering: overview, scope and challenges," *Biotechnology and Applied Biochemistry*, vol. 39, no. 1, pp. 29–47, 2004.

[9] E. L. Hedberg, H. C. Kroese-Deutman, C. K. Shih et al., "Methods: a comparative analysis of radiography, microcomputed tomography, and histology for bone tissue engineering," *Tissue Engineering*, vol. 11, no. 9-10, pp. 1356–1367, 2005.

[10] P. Garteiser, S. Doblas, J. Daire et al., "MR elastography of liver tumours: value of viscoelastic properties for tumour characterisation," *European Radiology*, vol. 22, no. 10, pp. 2169–2177, 2012.

[11] M. J. Grundeken, R. P. Kraak, D. M. de Bruin, and J. J. Wykrzykowska, "Three-dimensional optical coherence tomography evaluation of a left main bifurcation lesion treated with ABSORB bioresorbable vascular scaffold including fenestration and dilatation of the side branch," *International Journal of Cardiology*, vol. 168, no. 3, pp. e107–e108, 2013.

[12] J. M. Deuerling, D. J. Rudy, G. L. Niebur, and R. K. Roeder, "Improved accuracy of cortical bone mineralization measured by polychromatic microcomputed tomography using a novel high mineral density composite calibration phantom," *Medical Physics*, vol. 37, no. 9, pp. 5138–5145, 2010.

[13] P. N. Wells, "Absorption and dispersion of ultrasound in biological tissue," *Ultrasound in Medicine and Biology*, vol. 1, no. 4, pp. 369–376, 1975.

[14] T. Otani and Takahiko, "Quantitative estimation of bone density and bone quality using acoustic parameters of cancellous bone for fast and slow waves," *Japanese Journal of Applied Physics B*, vol. 44, no. 6, pp. 4578–4582, 2005.

[15] E. Bossy, M. Talmant, M. Defontaine, F. Patat, and P. Laugier, "Bidirectional axial transmission can improve accuracy and precision of ultrasonic velocity measurement in cortical bone: a validation on test materials," *IEEE Transactions on Ultrasonics, Ferroelectrics, and Frequency Control*, vol. 51, no. 1, pp. 71–79, 2004.

[16] S. Nayak, M. S. Roberts, and S. L. Greenspan, "Cost-effectiveness of different screening strategies for osteoporosis in postmenopausal women," *Annals of Internal Medicine*, vol. 155, no. 11, pp. 751–761, 2011.

[17] J. Yu, K. Takanari, Y. Hong et al., "Non-invasive characterization of polyurethane-based tissue constructs in a rat abdominal repair model using high frequency ultrasound elasticity imaging," *Biomaterials*, no. 3411, pp. 2701–2709, 2013.

[18] K. Hattori, Y. Takakura, Y. Morita, M. Takenaka, K. Uematsu, and K. Ikeuchi, "Can ultrasound predict histological findings in regenerated cartilage?" *Rheumatology*, vol. 43, no. 3, pp. 302–305, 2004.

[19] Y. Wen, M. R. Gallego, L. F. Nielsen, L. Jorgensen, E. H. Moler, and H. M. Nielsen, "Design and characterization of core—shell mPEG—PLGA composite microparticles for development of cell—scaffold constructs," *European Journal of Pharmaceutics and Biopharmaceutics*, no. 85, pp. 87–89, 2013.

[20] Y. Chen, Z. Huang, X. Li et al., "*In Vitro* biocompatibility and osteoblast differentiation of an injectable Chitosan/Nano hydroxyapatite/Collagen scaffold," *Journal of Nanomaterials*, vol. 2012, Article ID 401084, 6 pages, 2012.

[21] Z. Huang, Q. Feng, B. Yu, and S. Li, "Biomimetic properties of an injectable chitosan/nano-hydroxyapatite/ collagen composite," *Materials Science and Engineering C*, vol. 31, no. 3, pp. 683–687, 2011.

[22] W. Zhang, S. S. Liao, and F. Z. Cui, "Hierarchical self-assembly of nano-fibrils in mineralized collagen," *Chemistry of Materials*, vol. 15, no. 16, pp. 3221–3226, 2003.

[23] H. Asai, H. Kanai, and N. Chubachi, "Noninvasive method for measuring velocity of leaky surface skimming compressional wave propagating on bone surface," *Electronics Letters*, vol. 32, no. 24, pp. 2290–2291, 1996.

[24] R. R. Scholten, S. Pillen, A. Verrips, and M. J. Zwarts, "Quantitative ultrasonography of skeletal muscles in children: normal values," *Muscle and Nerve*, vol. 27, no. 6, pp. 693–698, 2003.

[25] C. S. Chamberlain, S. E. Duenwald-Kuehl, G. Okotie et al., "Temporal healing in rat achilles tendon: ultrasound correlations," *Annals of Biomedical Engineering*, vol. 41, no. 3, pp. 477–487, 2013.

[26] K. Mizushige, H. Morita, S. Senda, and H. Matsuo, "Evaluation of arterial wall histological and physical characteristics using intravascular echography," *Japanese Circulation Journal*, vol. 56, no. 6, pp. 565–571, 1992.

[27] S. Duenwald, H. Kobayashi, K. Frisch, R. Lakes, and R. Vanderby, "Ultrasound echo is related to stress and strain in tendon," *Journal of Biomechanics*, vol. 44, no. 3, pp. 424–429, 2011.

[28] S. Kreitz, G. Dohmen, S. Hasken, T. Schmitz-Rode, P. Mela, and S. Jockenhoevel, "Nondestructive method to evaluate the collagen content of fibrin-based tissue engineered structures via ultrasound," *Tissue Engineering C: Methods*, vol. 17, no. 10, pp. 1021–1026, 2011.

[29] K. Kim, C. G. Jeong, and S. J. Hollister, "Non-invasive monitoring of tissue scaffold degradation using ultrasound elasticity imaging," *Acta Biomaterialia*, vol. 4, no. 4, pp. 783–790, 2008.

[30] S. Brugaletta, J. Gomez-Lara, P. W. Serruys et al., "Serial *in vivo* intravascular ultrasound-based echogenicity changes of everolimus-eluting bioresorbable vascular scaffold during the first 12 months after implantation: insights from the ABSORB B trial," *JACC: Cardiovascular Interventions*, vol. 4, no. 12, pp. 1281–1289, 2011.

[31] N. Bruining, S. De Winter, J. R. T. C. Roelandt et al., "Monitoring *in vivo* absorption of a drug-eluting bioabsorbable stent with intravascular ultrasound-derived parameters: a feasibility study," *JACC: Cardiovascular Interventions*, vol. 3, no. 4, pp. 449–456, 2010.

[32] J. Yu, K. Takanari, Y. Hong et al., "Non-invasive characterization of polyurethane-based tissue constructs in a rat abdominal repair model using high frequency ultrasound elasticity imaging," *Biomaterials*, vol. 34, no. 11, pp. 2701–2709, 2013.

[33] J. Gómez-Lara, S. Brugaletta, B. D. Gogas et al., "Agreement and reproducibility of gray-scale intravascular ultrasound and optical coherence tomography for the analysis of the bioresorbable vascular scaffold," *Catheterization and Cardiovascular Interventions*, vol. 79, no. 6, pp. 890–902, 2012.

[34] D. Dutta, K.-W. Lee, R. A. Allen et al., "Non-invasive assessment of elastic modulus of arterial constructs during cell culture using ultrasound elasticity imaging," *Biomechanics and Modeling in Mechanobiology*, vol. 10, no. 4, pp. 529–538, 2011.

[35] S. P. Väänänen, H. Isaksson, P. Julkunen, J. Sirola, H. Kröger, and J. S. Jurvelin, "Assessment of the 3-D shape and mechanics of the proximal femur using a shape template and a bone mineral density image," *Biomechanics and Modeling in Mechanobiology*, vol. 10, no. 4, pp. 529–538, 2011.

Hindawi Publishing Corporation
BioMed Research International
Volume 2014, Article ID 518609, 14 pages
http://dx.doi.org/10.1155/2014/518609

Review Article

Carbon Nanotubes Reinforced Composites for Biomedical Applications

Wei Wang,[1] Yuhe Zhu,[1] Susan Liao,[2] and Jiajia Li[1]

[1] *Department of Prosthodontics, School of Stomatology, China Medical University, Shenyang 110002, China*
[2] *School of Materials Science and Engineering, Nanyang Technological University, Singapore 639798*

Correspondence should be addressed to Wei Wang; yuhe740442@hotmail.com

Received 28 December 2013; Accepted 17 January 2014; Published 24 February 2014

Academic Editor: Xiaoming Li

Copyright © 2014 Wei Wang et al. This is an open access article distributed under the Creative Commons Attribution License, which permits unrestricted use, distribution, and reproduction in any medium, provided the original work is properly cited.

This review paper reported carbon nanotubes reinforced composites for biomedical applications. Several studies have found enhancement in the mechanical properties of CNTs-based reinforced composites by the addition of CNTs. CNTs reinforced composites have been intensively investigated for many aspects of life, especially being made for biomedical applications. The review introduced fabrication of CNTs reinforced composites (CNTs reinforced metal matrix composites, CNTs reinforced polymer matrix composites, and CNTs reinforced ceramic matrix composites), their mechanical properties, cell experiments *in vitro*, and biocompatibility tests *in vivo*.

1. Introduction

Carbon is an important element to various sciences, from physics, chemistry, and materials science to life science, but conventional carbon formulation in the micron scale may not be the optimal implant material [1]. Then the nanomaterials such as the carbon nanotubes (CNTs), with unique electrical, mechanical, and surface properties, have captured the attention and aroused the interest of many scientists, since CNTs were discovered by Iijima in 1991 and up to now appear well suited as a biomaterial [2–7]. CNTs are substances with cylindrical structure of about 1 nm diameter and 1–10 μm length, consisting of only carbon atoms. In general, CNTs contain single-wall carbon nanotubes (SWCNTs) and multiwall carbon nanotubes (MWCNTs). SWCNTs are viewed as rolled-up structures of single sheets of graphene and individual carbon structures approximately 1 nm in diameter and up to a millimeter or more in length, and MWCNTs are similar to hollow graphite fibers, except that they have a much higher degree of structural perfection, which are having a diameter of 10–200 nm [8–11]. Lu and Tsai investigated the load transfer efficiency in double-walled carbon nanotubes (DWCNTs, a hollow cylindrical structure, which contains two concentric graphene layers) using multiscale finite element modeling, and the results showed that increasing of CNTs' length can effectively improve the load transfer efficiency in the outermost layers, while the DWCNTs with incremental covalent bonds exhibit increasing load transfer efficiency in the inner layer. Besides, compared with SWCNTs, the DWCNTs still possess the less capacity of load transfer efficiency [12]. For MWCNTs, the outer graphene layers as well as the inner layers may be responsible for sustaining the applied load, and the load carrying capacity from the outermost layer to interior layers in MWCNTs associated with different interatomistic properties are waiting to be investigated thoroughly [12].

Treacy et al. measured the elastic modulus of MWCNTs to be 1TPa, on the same level of diamond. Compared with steel, the mechanical strength is 100 times higher of steel, but the density is only one sixth of the steel [13, 14]. Wang et al. studied the axial strength of MWCNTs and reported elastic modulus values ranging from 200 to 400 GPa, the bending modulus is to 14 GPa, and compression strength is about 100 GPa. The high deformation of CNTs allows it to break when tensile strength reaches 18% [15]. Iijima et al. investigated bending strength of CNTs, and their experimental results and theoretical studies have demonstrated that CNTs have extremely high tensile strengths, as high as 100 GPa

[16, 17]. Depending on the outstanding quality of the CNTs, it is possible to use CNTs for composites reinforcement. It is also believed that the incorporation of CNTs into matrix materials should lead to composites with unique properties.

Compared with conventional carbon, CNTs are stronger and more flexible and have a higher tensile strength to weight ratio [18]. Since CNTs have a density even smaller than graphite due to the tube structure, and with sufficient high strength and excellent thermal and chemical stability, the CNTs material may be used as a structural material in the biomedical field [4, 19–24]. At present, CNTs are used as carriers for drug delivery and gene therapy, and CNTs have been shown effective to reinforce scaffolds for tissue engineering and regenerative medicine [25–30]. Since CNTs have pores and the pores of SWCNTs and MWCNTs were, respectively, less than 1 nm and 4–30 nm in diameter [31, 32], SWNTs and MWNTs might be available for tissue regeneration. Besides, CNTs have been used as supports for enzyme immobilization to improve biocatalyst performances such as activity, stability, and reusability [33]. CNTs can be easily separated by simple filtration [34] and enzymes can be adsorbed [35, 36] or covalently attached [37, 38] on surface of SWCNTs and MWCNTs. The study of Prlainovic showed that lipase can be successfully adsorbed on the surface of unmodified MWCNTs, and immobilized preparations were characterized, with FT-IR spectroscopy, AFM, and cyclic voltammetry [39]. As filler materials, CNTs are used to improve the properties of polymer composites [40].

To date, various composite materials have been prepared by incorporating SWCNTs or MWCNTs into a metal matrix, a ceramic matrix, or a polymer matrix (including SiC ceramic, SiN ceramic, quartz, Al_2O_3, and mental ceramic) [41–50]. And CNTs reinforced polymer matrix composites and CNTs reinforced ceramic matrix composites may be used as a structural material in the bone cement, bone filling material, and tissue engineering scaffolds [45–50]. Webster et al. fabricated polyurethane/CNTs composite, and the composite material possessed better electrical conductivity and mechanical properties, which can be used in neural tissue and bone [51, 52]. Deng et al. studied the use of MWCNT/chitosan (CHI) scaffolds, composed of MWCNTs (up to 89 wt%) and CHI and with a well-defined microchannel porous structure, as biocompatible and biodegradable supports for cell growth [53].

This review addresses the different synthetic methods, mechanical properties, and biocompatibility of CNTs-based reinforced composites, which may indicate that CNTs-based reinforced composites appear suited as biomaterials and may become useful scaffold materials for tissue engineering.

2. Fabrication of CNTs and CNTs-Based Reinforced Composites

2.1. Fabrication of CNTs. CNTs are generally prepared using five main synthesis methods containing ARC discharge, laser ablation, chemical vapor deposition (CVD), catalyst chemical vapor deposition (CCVD), and template-directed synthesis [54, 55]. Although arc discharge is a common method for CNTs synthesis, it is difficult to control the morphology of CNTs, such as length, diameter, and number of layers. Compared with arc-discharge and laser-ablation methods, CVD is most widely used for its low set-up cost, high production yield, and ease of scale-up [56]. CCVD is the most flexible and economic method for the production of CNTs; however, since many parameters influence the producing process, it is still very complex for precisely controlled growth of CNTs [54]. In the study of Disfani, MWCNTs produced by the catalytic carbon vapor deposition (CCVD) process were then functionalized, which were designated as CNTs-COOH, CNTs-OH, and CNTs-NH2. And different functionalized CNTs, as well as nonfunctionalized CNTs, were incorporated into a phenoxy resin via a melt mixing process [57].

2.2. Fabrication of CNTs-Based Reinforced Composites

2.2.1. Fabrication of CNTs Reinforced Metal Matrix Composites. CNTs reinforced the strength, hardness, abrasion, and wear properties and thermal of stability of metal, and CNTs reinforced metal matrix composites are prepared through a variety of processing techniques, such as powder metallurgy, the melt casting, spray forming, electrochemical deposition, and other novel techniques. At present, CNTs as reinforcement in Fe-matrix, Cu-matrix, Mg-matrix, and Ni-matrix composite materials have been successfully fabricated [58–62]. Kuzumaki et al. produced CNTs reinforced aluminum (Al) composites by hot-press and hot-extrusion methods [63]. CNTs-Fe-Al_2O_3 composites have been prepared by hot pressing [64, 65].

2.2.2. Fabrication of CNTs Reinforced Polymer Matrix Composites. The common fabricating methods of CNTs/polymer composites are solution mixing, melt blending, in situ polymerization, and sol-gel method [66]. Uniform dispersion of CNTs in polymer is a fundamental challenge and several factors that influence the dispersion of CNTs in a polymer matrix have to be considered in the preparation process of CNTs/polymer composites. In recent years, many polymers, such as epoxy [67–69], PMMA [70–73], PVA [74], PVC [75], PP [76], PE [77, 78], PA12 [79], and PS [80, 81], have been employed as matrices to prepare CNTs/polymer composites.

2.2.3. Fabrication of CNTs Reinforced Ceramic Matrix Composites. Ceramic materials possess high temperature resistance, corrosion resistance, and better biocompatibility compared with metal and polymer. The poor mechanical properties of ceramic with regard to its brittleness and low fracture toughness restrict its use in load bearing applications [82–85]. Therefore, CNTs with excellent physical and chemical properties are added to enhance the mechanical properties of the ceramic matrix. The fabricating methods of CNTs/ceramic composites include hot pressing process (HP), hot isostatic pressing-sintering (Sinter-HIP), spark

plasma sintering (SPS), microwave sintering, and high-temperature extrusion molding according to the sintering process [86, 87]. SPS method is a newly developed technique used widely since 1990 [88]. During recent years, various ceramics, composites, cermets, and other materials, including Al, Ti, and functionally graded materials (FGM), have been successfully compacted by SPS [88–96]. Compared with other sintering methods, SPS method has several advantages. The SPS method can break surface oxide layer on particles and heat them up instantly by electric spark discharges under compressive pressure. In this way, it is possible to obtain fully dense samples at relatively low sintering temperature and pressure in a very short holding time [56, 95, 97]. Besides, by rapid temperature rise, grain growth of the raw material is kept to a minimum, thus making it possible to maintain the nanotube structure in the sintered bulk CNTs. Wang et al. successfully fabricated CNTs-based composites including MWCNTs/5, 20, 25% polycarbosilane (PCS), 100% MWCNTs, and MWCNTs/40% hydroxyapatite (HA) composites by using the SPS method under different sintering conditions. In addition, Yao et al. fabricated CNTs/alumina reinforced composite by a combined process of pressureless sintering and atmosphere hot-pressing sintering [96]. Ogihara et al. synthesized the CNTs/alumina composite using pressureless sintering under vacuum and hot isostatic pressing [97].

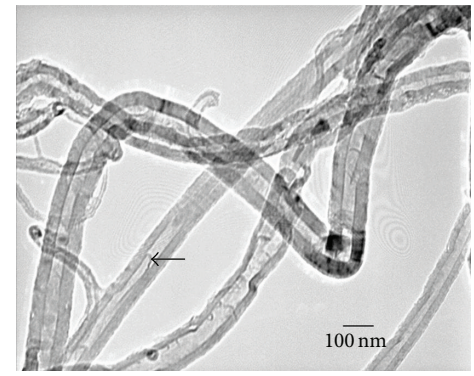

(a)

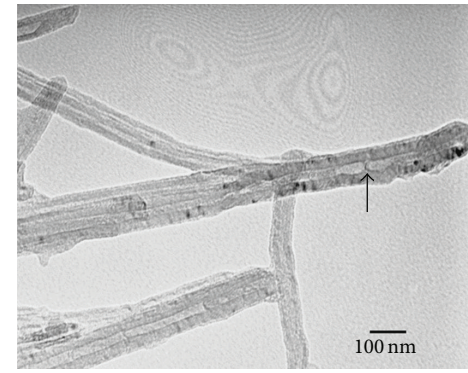

(b)

Figure 1: TEM images of MWCNTs starting powders and 100% MWCNTs monolith after SPS treatment [98]. (a) MWCNTs powders and (b) 100% MWCNTs monolith.

3. Mechanical Properties and Biocompatibility of CNTs-Based Reinforced Composites

3.1. Microstructure. CNTs have recently gained substantial interest for their potential applications in tissue engineering due to their large ratio of surface area to volume and unique microstructure. From the TEM micrographs, MWCNTs starting powders had external and internal diameters of 20–80 nm and 10–50 nm, and the 100% MWCNTs monolith basically maintained the nanosized tube microstructure and the bamboo microstructures following SPS treatment, as indicated by the hollow arrow in Figures 1(a) and 1(b) [98].

For the phenoxy/MWCNTs nanocomposites, optical microscopic images were shown as in Figure 2, from which we can see the state of CNTs dispersion in phenoxy matrix for different functionalized and nonfunctionalized MWCNTs, and compared with the other composites, the agglomerates are much bigger for CNTs-COOH (Figure 2(a)) [57]. TEM images of phenoxy/MWCNTs nanocomposites were shown as in Figure 3. The size of aggregates was in the scale of 200 nm, and the size of CNTs aggregates follows the following trend: CNT-COOH>pure-CNT>CNT-OH>CNT-NH [57].

In the sintering process of MWCNTs/5, 20, and 25% PCS, nanosized SiC particles pyrolyzed from PCS during sintering worked as the binder for MWCNTs, while HA was selected as binder to consolidate MWCNTs, which has been extensively used for maxillofacial surgery, orthopedics, and implant fabrication and is one of the most compatible biomaterials owing to its similar chemical composition and crystal structure to apatite in human hard tissue such as bone and tooth [84, 85, 99]. However, the poor mechanical properties of HA with regard to its brittleness and low fracture toughness restrict its use in load bearing applications (orthopedic/dental implant) [86, 87].

3.2. Mechanical Properties. It has been well proved that the mechanical property of matrix could be largely enhanced by the addition of CNTs [100, 101].

3.2.1. Mechanical Properties of CNTs Reinforced Metal Matrix Composites. For AZ31/CNTs composite, the maximal tensile strength and the elongation of the AZ31/CNTs composites are enhanced by 41.3% and 119.4%, respectively, and the elastic modulus and microhardness are also raised by 67.8% and 66.9%, respectively, when compared with those of the as-cast AZ31 Mg alloys [102]. Kim et al. were the first to report Cu-CNTs reinforced composites by SPS. Further rolling was performed on the composite to deform and align the CNT rich regions resulting in improved properties. SPS of Cu-CNTs nanocomposite powder, produced by molecular level mixing process, helps further improve density and mechanical properties. Enhancement in mechanical strength by 129% with addition of 5 vol% CNTs had been demonstrated [103].

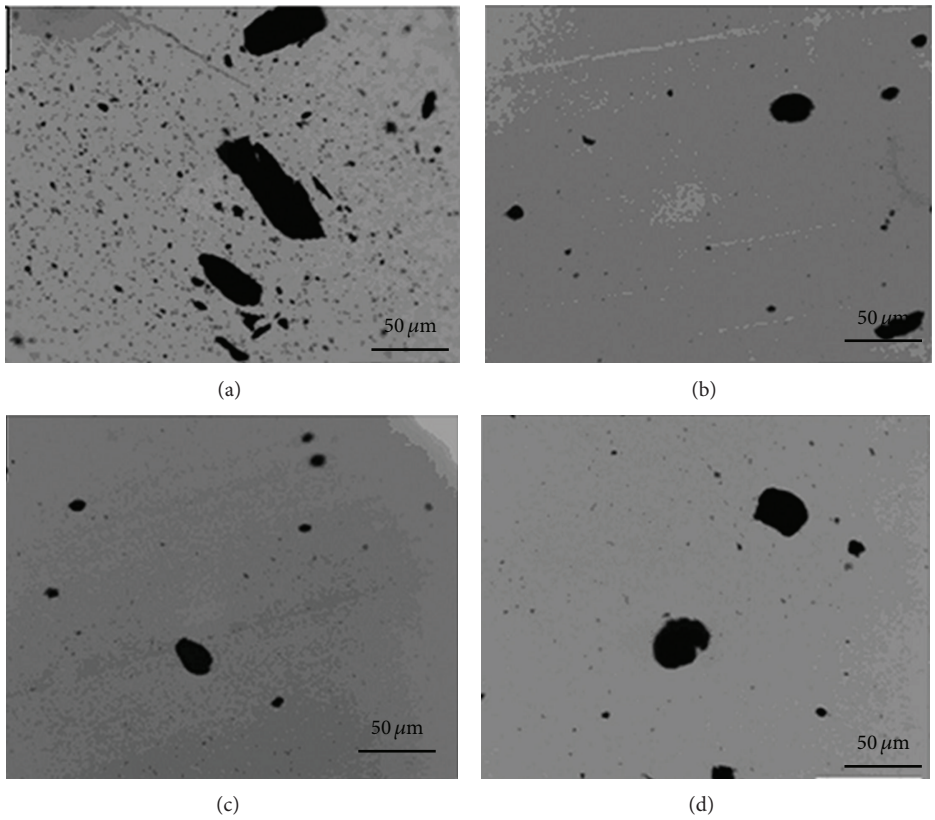

Figure 2: Optical microscopic images of phenoxy/MWCNTs nanocomposites containing (a) CNTs-COOH, (b) CNTs-OH, (c) CNTs-NH2, and (d) pure CNTs [57].

3.2.2. Mechanical Properties of CNTs Reinforced Polymer Matrix Composites. In previous study, carboxyl-functionalized MWCNTs were used as fillers in a polyamide 6 (PA6) matrix in order to change the effect of the material [104, 105]. Sun et al. reported that the addition of CNTs improved the storage modulus E' and loss modulus E'' of the PA6/CNTs composite [104]. Zomer Volpato et al. synthesized MWCNTs/PA6 composite, and incorporation of up to 2 wt% CNTs in CNTs/PA6 laminates improved the flexural stress of the laminates up to 36%, which should form hydrogen bonds between the polymer and filler or form amide bond between the free amines on the polymer and the CNTs carboxyl groups [105].

To improve the physiochemical properties of polyurethane (PU), CNTs are incorporated to add functionalities of material. For instance, Amr et al. reported that Young's modulus of CNTs/polystyrene (PS) nanocomposites was increased by 22% [106]; Jung et al. reported that the transparent PU film was incorporated with functionalized MWCNTs and found 2-fold and 10-fold increases in tensile strength and modulus, respectively, for MWCNTs/PU composite film [107]. According to the result of Tijing, the incorporation of MWCNTs increased the tensile strength and modulus of the composite nanofibers by 69% and 140%, respectively, and 62% and 78%, respectively, for composite films, and the MWCNTs/PU composites showed an improved thermal degradation behavior [108].

3.2.3. Mechanical Properties of CNTs Reinforced Ceramic Matrix Composites. Yao et al. reported that the mechanical properties of the CNTs/alumina reinforced composite can be obviously improved due to the addition of the CNTs. As the increase of mass fraction of carbon nanotubes, the tensile strength and Brinell hardness of the composite are elevated and achieve the maximum of 245 MPa and 106.66 n/mm^2, respectively, when the mass fraction of CNTs increases to 2.0 wt% [96]. Ogihara et al. synthesized the CNTs/alumina composite by direct growth of CNTs on alumina by chemical vapor deposition (CVD) and the as-grown nanocomposites were densified by SPS, and the mechanical strength was enhanced as follows: Young's modulus, 383 GPa; Vickers hardness, 19.9 GPa; Bending strength, 578 MPa [97].

For Zirconia-MWCNTs composites, the addition of MWCNTs aims to avoid the slow crack propagation and to enhance the toughness of the ceramic material used for prostheses. The sample of Zirconia MWCNTs shows higher density, lower grain size, improved toughness, and enhanced hardness, which suggested the good behavior of MWCNTs as strengthening agents for zirconia [109].

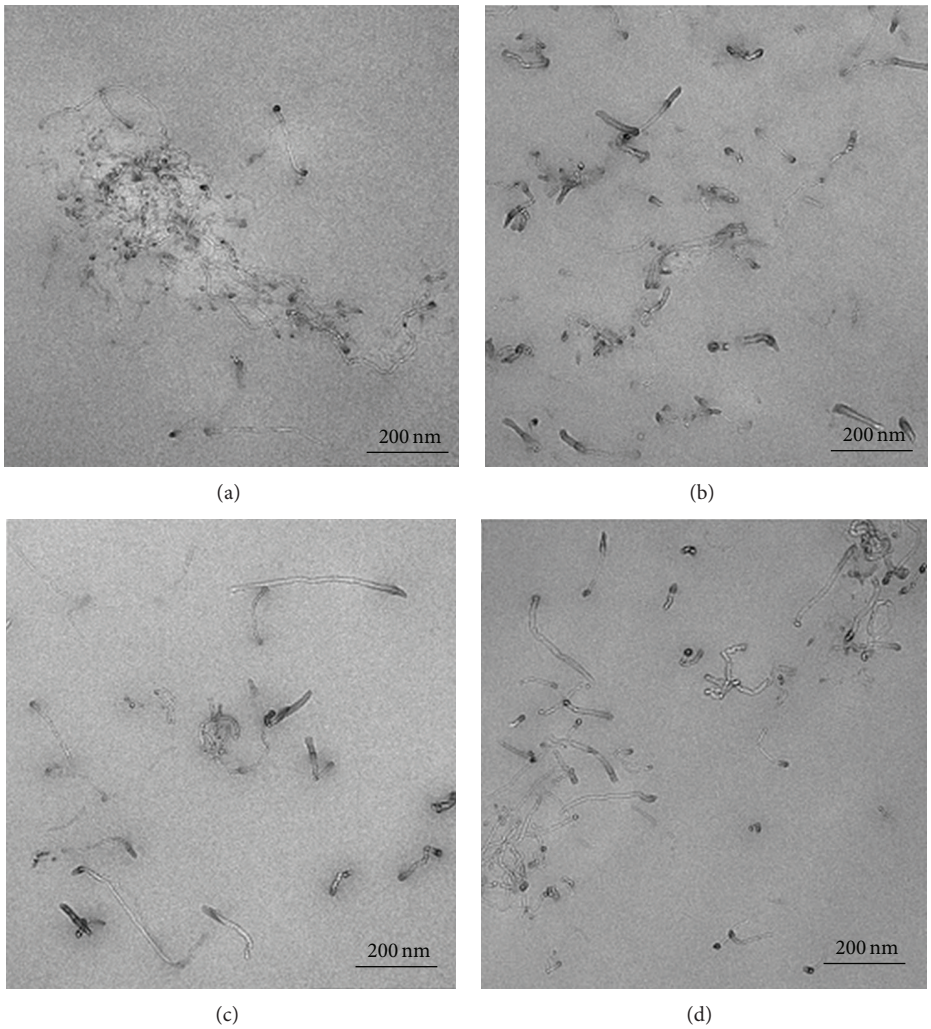

Figure 3: TEM images of phenoxy/MWCNTs nanocomposites containing (a) CNTs-COOH, (b) CNTs-OH, (c) CNTs-NH2, and (d) pure-CNTs [57].

For MWCNTs/PCS composites, it is found that PCS content and sintering pressure improved the bulk density and Vickers hardness of sintered MWCNTs, and the value of mechanical properties was highest for the MWCNTs/20% PCS. The bulk density, Young's modulus, and compressive strength of the MWCNTs/20% PCS material had the highest value of 2.13 g/cm^3, 27 GPa, and 298 MPa, which was higher than that of human bone. However, the bulk density, Young's modulus, and compressive strength of 100% MWCNTs monolith were 1.95 g/cm^3, 20 GPa, and 249 MPa, which were very closer to those of bone (1.9 g/cm^3, 19 GPa, and 150 MPa) and lower than those of other traditional implant materials: Ti (4.51 g/cm^3, 120 GPa, and 500 MPa) and HA (3.15 g/cm^3, 35 GPa, and 600 MPa) [98, 110–113]. The results showed that the 100% MWCNTs monolith could match the mechanical properties of human compact bone, which might be more suitable for implant materials than HA and Ti.

3.3. Biocompatibility. At present, carbon nanotubes have been extensively studied for use in biomedical applications, and biomaterials using CNTs are expected to be developed for clinical use [114–119]. Some studies showed that nanophase biomaterials had higher biocompatibility than similar micron-sized materials [5, 120]. Many studies *in vivo* and *in vitro* have investigated the biocompatibility of CNTs for biomedical applications. There are controversies on CNTs cytotoxicity, and CNTs might have adverse effects, which is ascribed to their physicochemical properties, such as structure, surface area, extent of oxidation, producing method, and concentration [121]. The toxicity of CNTs on the respiratory system is investigated. Lam et al. studied toxicity of CNTs by bronchial injection test, and the results of studies showed that 0.5 mg of CNTs can cause the death of part of mice, another part of the lungs in mice is characterized by damage granuloma [122]. In contrast, Miyawaki et al. investigated *in vitro* and *in vivo* the toxicities of carbon nanohorns (CNHs).

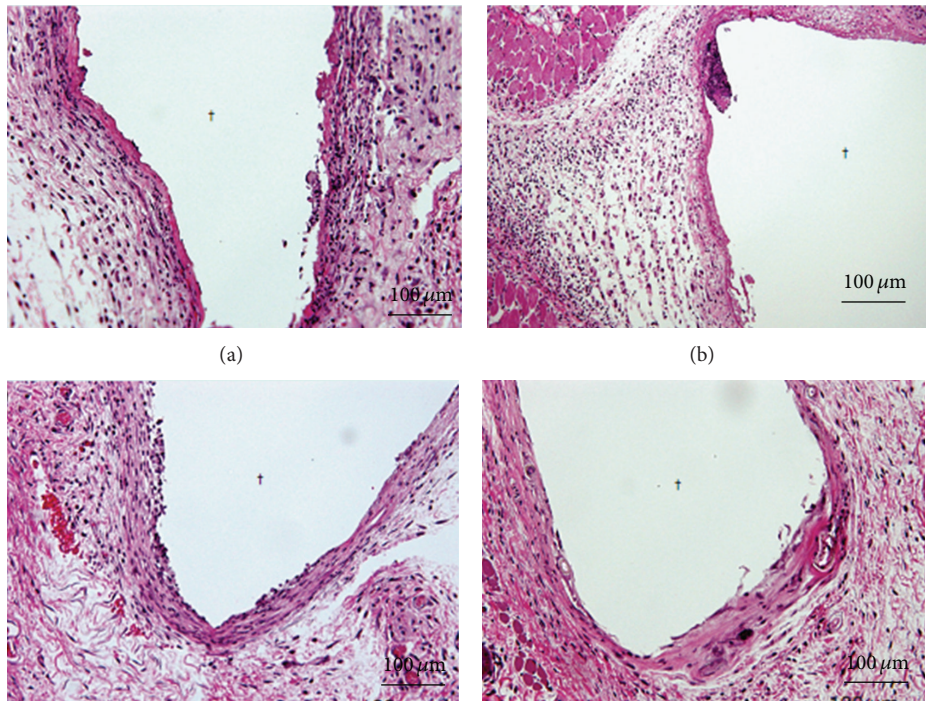

Figure 4: Tissue images around alumina ceramic and CNTs/alumina composites embedded in the subcutaneous tissue of mice: (a) alumina ceramic after 1 week, (b) CNTs/alumina after 1 week, (c) alumina ceramic after 4 weeks, and (d) CNTs/alumina after 4 weeks [97].

The CNHs were found to be a nonirritant and a nondermal sensitizer through skin primary and conjunctival irritation tests and skin sensitization test. The acute peroral toxicity of CNHs was found to be quite low; the lethal dosage for rats was more than 2000 mg/kg of body weight. Intratracheal instillation tests revealed that CNHs rarely damaged rat lung tissue for a 90-day test period, although black pigmentation due to accumulated nanohorns was observed. Yet the present results suggest that CNHs have low acute toxicities [123].

Used in the scaffold, CNTs could promote cell adhesion, and MWNTs could decrease osteoclast number to inhibit bone resorption [124, 125]. When it comes to osteoblasts, CNTs did not have cytotoxicity to osteoblasts and did not have harmful effects on osteoblast differentiation or mineralization [126–128]. In addition, nonfunctionalized SWCNTs had little toxicity to cell such as decreasing the viability and number of cells [129]. It is reported that there was no acute toxicity or adverse reaction for functionalized CNTs; however, the severe tissue deposition and inflammatory response were observed for pristine CNTs. Tang et al. modified the CNTs with macromolecules (polyethylene glycol PEG), and the results indicated that the synthesized CNTs are very biocompatible, exhibiting no differences from normal control groups, and in other words, shorter pristine and polymer functionalized MWCNTs have a significant potential for biomedical applications as efficient carriers for diagnostic, therapeutic, or cell-specific targeting molecules [130]. Ahn et al. investigated the incorporation of MWCNTs into calcium phosphate cements (CPC) and evaluated the bioactive nature of CPC-MWCNTs hybrid the osteogenic differentiation capacity as bone grafting materials, using proliferation and differentiation of MC3T3-E1 cells, the result of which showed that CPC-MWCNTs hybrid which promoted the osteogenic differentiation of osteoblasts could serve well as bone repairing graft material [131]. Zomer Volpato et al. synthesized PA6/MWCNT and investigated the effect of the addition of CNTs on the cell-material interactions and found that the proliferation and activation of MG63 cell line osteoblasts were enhanced due to surface modification caused by the filler addition compared to the purely PA6 networks [105]. The result of Ogihara et al. about cell attachment of CNTs/alumina composite indicated that CNTs/alumina composite had more favorable cell attachment properties, and CNTs at the surface of the implant did not inhibit attachment [97].

Meanwhile the subcutaneous tissue reactions and bone tissue reactions were evaluated for the alumina ceramic and CNTs/alumina composite, and found that inflammatory cells were observed around the composites after 1 week, however, severe inflammatory reactions were not observed (Figures 4(a) and 4(b)) [97]. And after 4 weeks, thin fibrous capsules attached to alumina ceramic had been formed, and the inflammatory reaction had disappeared. Similar phenomenon was observed on the CNTs/alumina composite (Figures 4(c) and 4(d)) [97].

Yokoyama et al. investigated the biological behavior of hat-stacked carbon nanofibers (H-CNFs) in the subcutaneous tissue of rats, and the results showed that H-CNFs were

englobed by fibrous connective tissue with little inflammation [27]. But Muller et al. found that CNTs have the potential to cause serious inflammatory and fibrotic reactions by studying rats exposed to respirable CNTs particles [132]. Colvin reported that the pulmonary toxicity of CNTs was not obvious as granulomas which were not commonly observed in rat lungs instilled with CNTs [133]. Additionally, the study of Kumar et al. has revealed that the chemical state of the surface of CNTs may strongly influence tissue response [134]. The influence of catalytic particles, like Fe and Ni, applied during the synthesis of CNTs on the toxicity of CNTs has been reported [30].

The inflammation of MWCNTs powders is most serious in the soft tissue, which may be due to that the dispersed powder easily caused body response. At 1 week after the implantation in the soft tissue of rats, MWCNTs powders were surrounded by granulation tissue with many macrophages and foreign body giant cells (Figure 5(a)) [110], which was consistent with the study of Warheit et al., who have demonstrated that pulmonary exposures to CNTs in rats produced multifocal granulomas that consisted of macrophage-like multinucleate, [135]. However, no severe inflammatory response was observed around MWCNTs/PCS composites with different percentage of PCS and 100% MWCNTs monolith. For the response in subcutaneous tissue, there was a difference dependent on the content of PCS in the early implant stage; the degree of inflammation was influenced by SiC pyrolyzed from PCS. At 1 week after surgery, inflammatory response around MWCNTs/5% PCS (Figure 5(c)) was milder than that around MWCNTs/25% PCS (Figure 5(e)) [110]. MWCNTs/20% PCS was covered by relatively thick fibrous connective tissue including many cells with large cytoplasm like fibroblasts, fibroblasts with spindle-shaped cytoplasm, and some inflammatory round cells (Figure 5(d)) [111], and an inflammatory reaction around the 100% MWCNTs monolith was observed at 1 week after implantation in subcutaneous tissue (Figure 5(b)) [98]. But at 4 weeks after implantation, the MWCNTs/20% PCS and 100% MWCNTs monolith were covered by loose fibrous connective tissue, and inflammation around materials was slight in comparison to that at 1 week (Figures 6(a) and 6(b)) [98, 111]. The inflammatory reaction after one-week implantation is normal for the short period that immediately follows an implantation treatment.

The images of bone tissue reactions after alumina ceramic or CNTs/alumina composite implanted in rabbit femurs were shown as Figure 7 [97]. At 12 weeks, new bone was found around the composites and the fibrous capsule between the composites and the bone was rarely observed (Figures 7(a), 7(b), 7(e), and 7(f)). At 24 weeks, the entire circumference of the specimen had attached to the bone tissue without gaps, and composites were completely incorporated into the bone and the bone defect was repaired (Figures 7(c), 7(d), 7(g), and 7(h)). These results showed that the bone tissue compatibility of CNT/alumina composite is comparable with that of alumina ceramic.

For the response in bone tissue, after implantation for 4 weeks in the femur, part of the newly formed bone attached to MWCNTs/20% PCS directly (Figure 8(a)), lamellar newly formed bone was observed around the 100% MWCNTs implant (Figure 8(b)), and a large of newly formed bone was observed around the MWCNTs/40% HA composites as shown in Figure 8(c), and the newly formed bone was attached to the implant directly [98, 111, 112]. The MWCNTs/PCS composite had very little prophlogistic effect and possessed osteoconductivity. Similar *in vitro* results were described by Elias et al. who reported that carbon fiber compacts improved the growth of osteoblasts compared to conventional carbon fiber [120]. However, the osteoconductivity was influenced by the PCS content, and the amount of the newly formed bone was least in MWCNTs/20% PCS and most in MWCNTs/40% HA. HA was added for improving the biocompatibility of MWCNTs materials. HA is widely accepted coating for orthopedic implants since 1980 due to its excellent biocompatibility and bioactivity properties [133, 136]. And many composites containing HA were fabricated and show good biocompatibility [137, 138]. MWCNTs/HA composites possessed better osseointegration than pure MWCNTs as we expected.

4. Conclusions and Perspectives

Nanoscale substances like CNTs could be potential applied in almost all the walks of life: media, entertainment, communication, transport, health, and environment, especially in the nanobiomedical field [53]. CNTs, with a range of unique properties, appear suited as biomaterials and may become useful scaffold materials for tissue engineering. Reinforcing scaffolds with CNTs has been suggested to be an effective means of developing engineering materials for tissue regeneration. These reinforced scaffolds have been largely applied for not only hard tissue but also soft tissue repair. However, their safety and effectiveness as biomaterials are still unclear. More and more interests were emerged in CNT-based composites, including the synthesis of the composites and their mechanical properties, cell experiments *in vitro*, and biocompatibility *in vivo*. From previous studies, we could find that there were many methods for composing the variable CNTs-based composites under different synthetic conditions. Those composites with adjustable mechanical properties could be used for different usages, such as tissue engineering, delivery of genes and drugs, scaffold, implant, or as filler in other composites to improve their mechanical properties. Besides, we found that the mechanical property of 100% MWCNTs monolith was most close to that of human bone. Moreover, in the animal experiments, no severe inflammatory response such as necrosis and no toxicity for soft tissue and bone regeneration were observed around most CNTs-based composites. The weak inflammatory reaction in short term after implantation was normal for the short period that immediately followed an implantation treatment, and the inflammation could be reduced with the extension of experiment time. The MWCNTs/40% HA composites possessed better osseointegration than other composites.

Although modified CNTs might not represent certain original structure and properties of CNTs, it is still possible for the modified CNTs-based composites to further

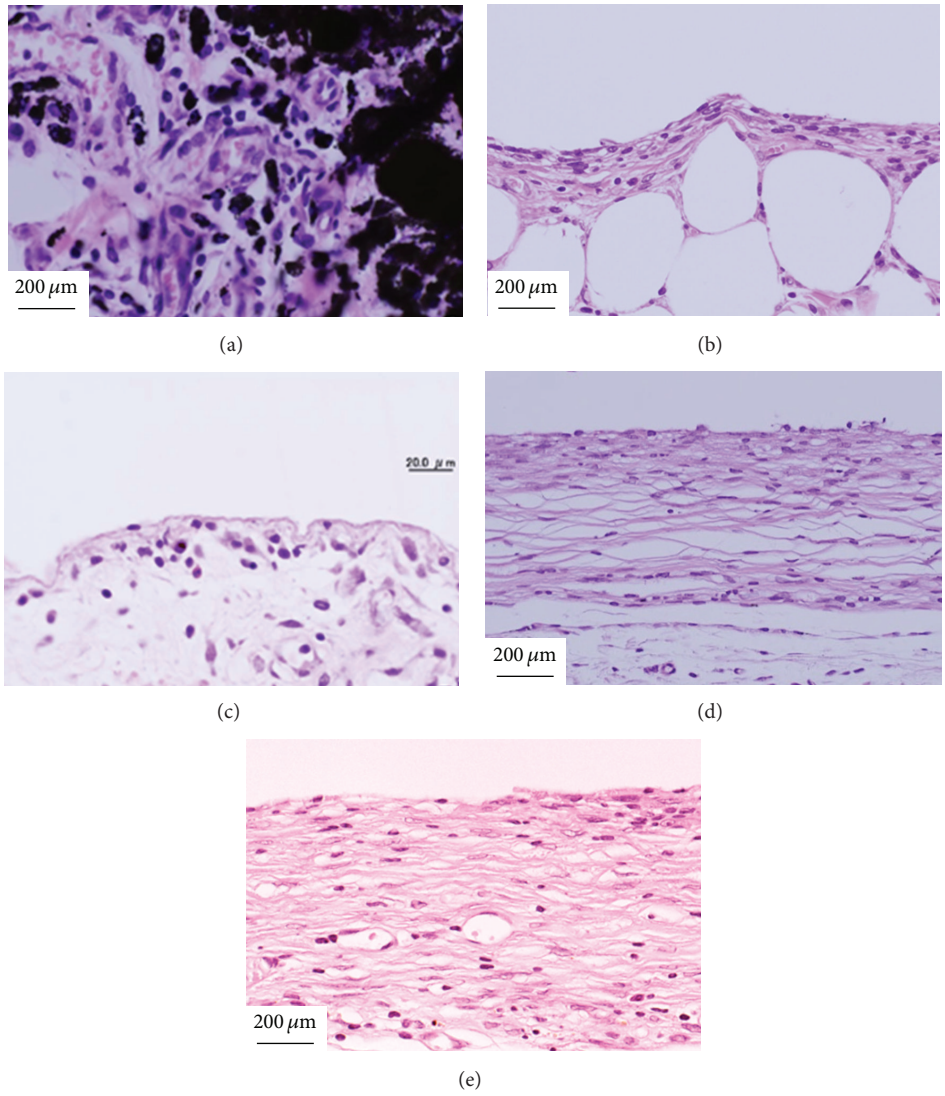

Figure 5: Tissue responses at one week after implantation [98, 110–112]. (a) MWCNTs powders, (b) 100% MWCNTs monolith, (c) MWCNTs/5% PCS, (d) MWCNTs/20% PCS, and (e) MWCNTs/25% PCS.

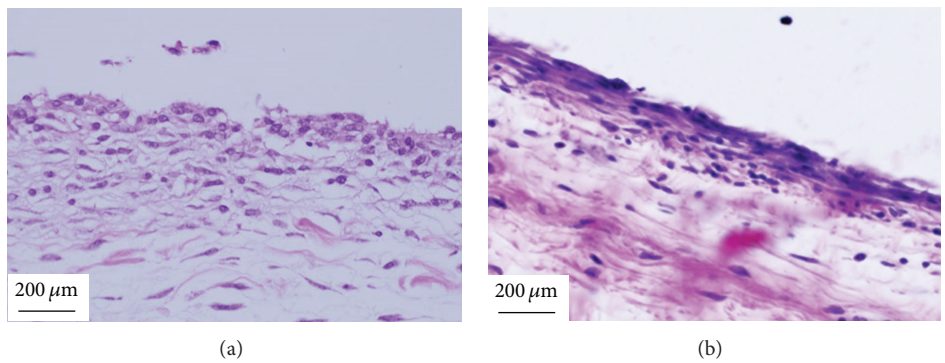

Figure 6: Tissue responses at 4 weeks after implantation [98, 111]. (a) MWCNTs/20%PCS and (b) 100% MWCNTs monolith.

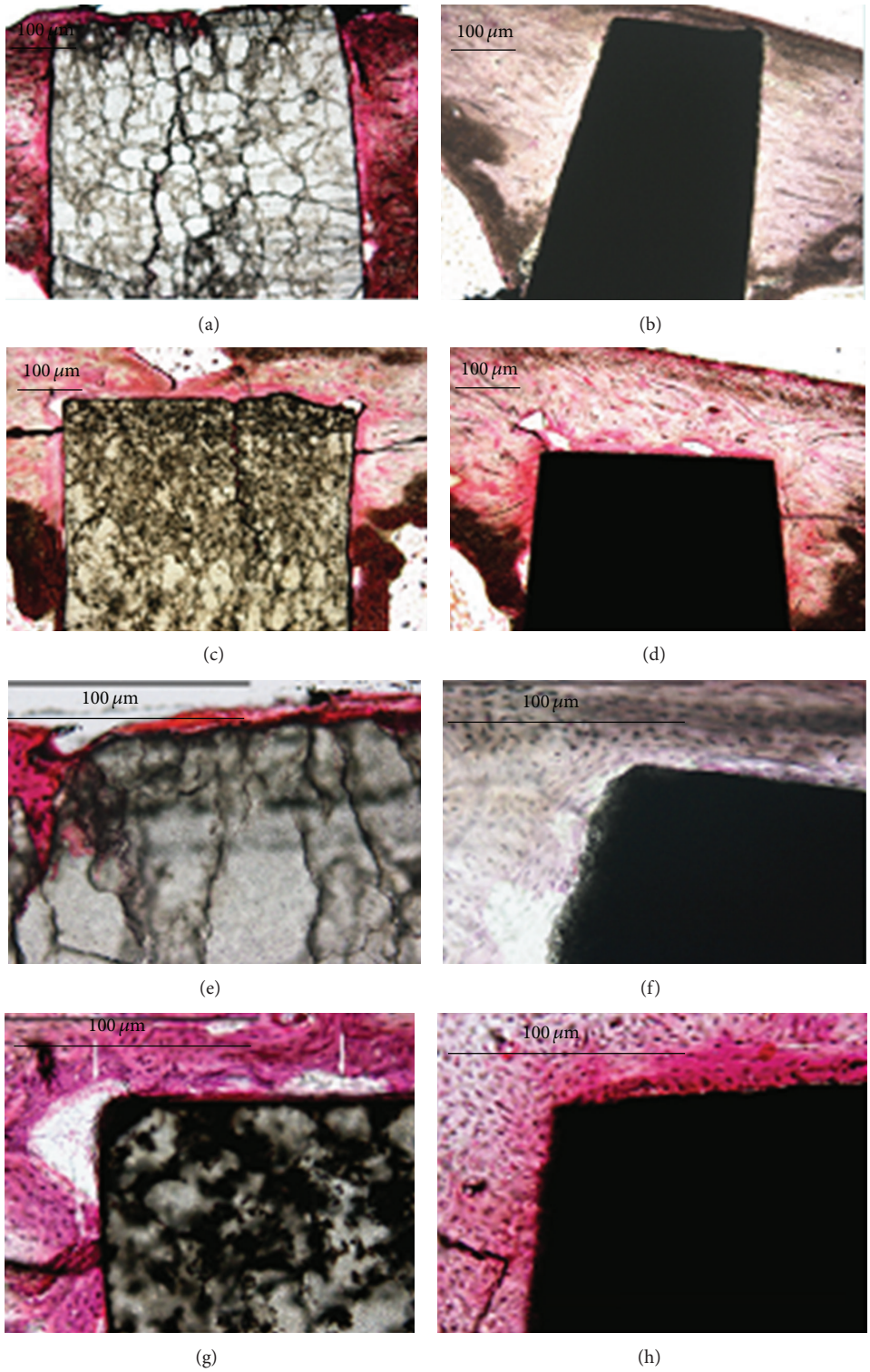

FIGURE 7: Enlarged image of the border between the specimen and the bone (200x). (a and e) Alumina ceramic was implanted after 12 weeks (40x, 220x); (b and f) CNTs/alumina composite was implanted after 12 weeks (40x, 220x); (c and g) alumina ceramic was implanted after 24 weeks (40x, 220x); (d and h) CNTs/alumina composite was implanted after 24 weeks (40x, 220x) [97].

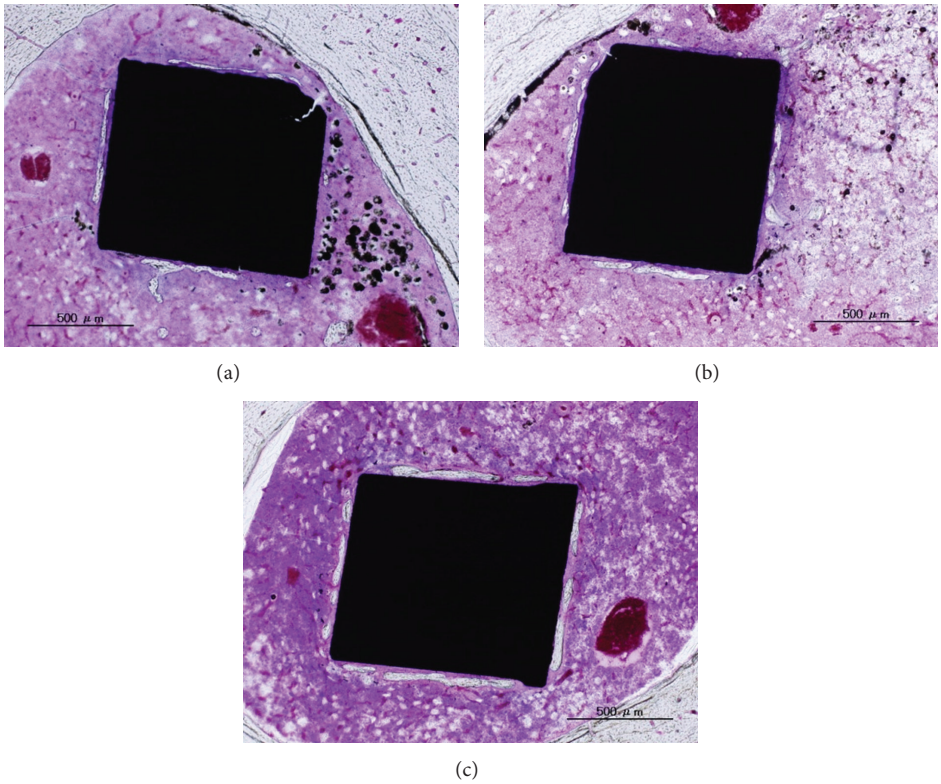

(a) (b)

(c)

Figure 8: Osteogenesis of (a) MWCNTs/20% PCS, (b) 100% MWCNTs monolith, and (c) MWCNTs/40%HA in the femur at 4 weeks [98, 111, 112].

improve their biocompatibility and effectively reinforce their mechanical properties. Above all, although there is still a lot of works to do, the CNTs-based reinforced composites will be not only applicable as artificial bone implant materials, but also for other biomedical applications potentially rewards opportunities to develop the next generation of engineered biomaterials in the future, such as tissue engineering, cell therapy, drug delivery, and diagnostic device.

Conflict of Interests

The authors declare that there is no conflict of interests regarding the publication of this paper.

Acknowledgments

The authors acknowledge the financial support from the Liaoning Provincial Department of Education Sciences Research Grant for Research on Advanced Medical Technology (L2011131). The authors acknowledge the graduate students in the Department of Prosthodontics, School of Stomatology, China Medical University for their kind help.

References

[1] J. Mortier and M. Engelhardt, "Foreign body reaction to a carbon fiber implant in the knee: case report and literature survey," *Zeitschrift für Orthopädie und ihre Grenzgebiete*, vol. 138, no. 5, pp. 390–394, 2000.

[2] S. Iijima, "Helical microtubules of graphitic carbon," *Nature*, vol. 354, no. 6348, pp. 56–58, 1991.

[3] X. Li, X. Liu, J. Huang, Y. Fan, and F.-Z. Cui, "Biomedical investigation of CNT based coatings," *Surface and Coatings Technology*, vol. 206, no. 4, pp. 759–766, 2011.

[4] I. Firkowska, M. Olek, N. Pazos-Peréz, J. Rojas-Chapana, and M. Giersig, "Highly ordered MWNT-based matrixes: topography at the nanoscale conceived for tissue engineering," *Langmuir*, vol. 22, no. 12, pp. 5427–5434, 2006.

[5] X. M. Li, Q. Feng, X. Liu, W. Dong, and F. Cui, "The use of nanoscaled fibers or tubes to improve biocompatibility and bioactivity of biomedical materials," *Journal of Nanomaterials*, vol. 3, pp. 1–16, 2013.

[6] N. W. S. Kam, T. C. Jessop, P. A. Wender, and H. Dai, "Nanotube molecular transporters: internalization of carbon nanotube-protein conjugates into mammalian cells," *Journal of the American Chemical Society*, vol. 126, no. 22, pp. 6850–6851, 2004.

[7] N. W. S. Kam, Z. Liu, and H. Dai, "Functionalization of carbon nanotubes via cleavable disulfide bonds for efficient intracellular delivery of siRNA and potent gene silencing," *Journal of the*

American Chemical Society, vol. 127, no. 36, pp. 12492–12493, 2005.

[8] T. W. Ebbesen, "Carbon nanotubes: prepartion and properties," in *From Carbon Fibers to Nanotubes*, M. Endo, R. Saito, M. S. Dresselhaus, and G. Dresselhaus, Eds., pp. 42–49, 1997.

[9] P. M. Ajayan, "Nanotubes from Carbon," *Chemical Reviews*, vol. 99, no. 7, pp. 1787–1799, 1999.

[10] K. P. De Jong and J. W. Geus, "Carbon nanofibers: catalytic synthesis and applications," *Catalysis Reviews*, vol. 42, no. 4, pp. 481–510, 2000.

[11] M. Ono-Ogasawara and T. Myojo, "Characteristics of multi-walled carbon nanotubes and background aerosols by carbon analysis, particle size and oxidation temperature," *Advanced Powder Technology*, vol. 24, no. 1, pp. 263–269, 2012.

[12] T. C. Lu and J. L. Tsai, "Characterizing load transfer efficiency in double-walled carbon nanotubes using multiscale finite element modeling," *Composites B*, vol. 44, no. 1, pp. 394–402, 2013.

[13] M. M. J. Treacy, T. W. Ebbesen, and J. M. Gibson, "Exceptionally high Young's modulus observed for individual carbon nanotubes," *Nature*, vol. 381, no. 6584, pp. 678–680, 1996.

[14] E. W. Wong, P. E. Sheehan, and C. M. Lieber, "Nanobeamme mechanics: elasticity, strength, and toughness of nanorods and nanotubes," *Science*, vol. 277, no. 5334, pp. 1971–1975, 1997.

[15] S. Iijima, C. Brabec, A. Maiti, and J. Bernholc, "Structural flexibility of carbon nanotubes," *Journal of Chemical Physics*, vol. 104, no. 5, pp. 2089–2092, 1996.

[16] N. Yu, Z. H. Zhang, and S. Y. He, "Fracture toughness and fatigue life of MWCNT/Epoxycomposites," *Science and Engineering A*, vol. 494, no. 1, pp. 380–384, 2008.

[17] S. G. Prolongo, M. Burón, M. R. Gude, R. Chaos-Morán, M. Campo, and A. Ureña, "Effects of dispersion techniques of carbon nanofibers on the thermo-physical properties of epoxy nanocomposites," *Composites Science and Technology*, vol. 68, no. 13, pp. 2722–2730, 2008.

[18] P. M. Ajayan, "Organics, polymers and biological materials," in *Handbook of Nanostructured Materials and Nanotechnology*, H. S. Nalwa, Ed., p. 375, Academic Press, San Diego, Calif, USA, 2000.

[19] M. Uo, K. Tamura, Y. Sato et al., "The cytotoxicity of metal-encapsulating carbon nanocapsules," *Small*, vol. 1, no. 8-9, pp. 816–819, 2005.

[20] T. Akasaka and F. Watari, "Nano-architecture on carbon nanotube surface by biomimetic coating," *Chemistry Letters*, vol. 34, no. 6, pp. 826–827, 2005.

[21] R. A. MacDonald, B. F. Laurenzi, G. Viswanathan, P. M. Ajayan, and J. P. Stegemann, "Collagen-carbon nanotube composite materials as scaffolds in tissue engineering," *Journal of Biomedical Materials Research A*, vol. 74, no. 3, pp. 489–496, 2005.

[22] K. Kiura, Y. Sato, M. Yasuda et al., "Activation of human monocytes and mouse splenocytes by single-walled carbon nanotubes," *Journal of Biomedical Nanotechnology*, vol. 1, no. 3, pp. 359–364, 2005.

[23] X. Li, H. Gao, M. Uo et al., "Maturation of osteoblast-like SaoS2 induced by carbon nanotubes," *Biomedical Materials*, vol. 4, no. 1, Article ID 015005, 2009.

[24] X. M. Li, X. H. Liu, G. P. Zhang et al., "Repairing 25 mm bone defect using fibres reinforced scaffolds as well as autograft bone," *Bone*, vol. 43, article S94, 2008.

[25] T. Akasaka, F. Watari, Y. Sato, and K. Tohji, "Apatite formation on carbon nanotubes," *Materials Science and Engineering C*, vol. 26, no. 4, pp. 675–678, 2006.

[26] Y. Sato, A. Yokoyama, K.-I. Shibata et al., "Influence of length on cytotoxicity of multi-walled carbon nanotubes against human acute monocytic leukemia cell line THP-1 in vitro and subcutaneous tissue of rats in vivo," *Molecular BioSystems*, vol. 1, no. 2, pp. 176–182, 2005.

[27] A. Yokoyama, Y. Sato, Y. Nodasaka et al., "Biological behavior of hat-stacked carbon nanofibers in the subcutaneous tissue in rats," *Nano Letters*, vol. 5, no. 1, pp. 157–161, 2005.

[28] A. Bianco, K. Kostarelos, and M. Prato, "Applications of carbon nanotubes in drug delivery," *Current Opinion in Chemical Biology*, vol. 9, no. 6, pp. 674–679, 2005.

[29] D. Cui, C. S. Ozkan, S. Ravindran, Y. Kong, and H. Gao, "Encapsulation of pt-labelled DNA molecules inside carbon nanotubes," *Mechanics & Chemistry of Biosystems*, vol. 1, no. 2, pp. 113–121, 2004.

[30] B. S. Harrison and A. Atala, "Carbon nanotube applications for tissue engineering," *Biomaterials*, vol. 28, no. 2, pp. 344–353, 2007.

[31] A. S. Ferlauto, D. Z. De Florio, F. C. Fonseca et al., "Chemical vapor deposition of multi-walled carbon nanotubes from nickel/yttria-stabilized zirconia catalysts," *Applied Physics A*, vol. 84, no. 3, pp. 271–276, 2006.

[32] M. Jagtoyen, J. Pardue, T. Rantell, and F. Derbyshire, "Porosity of carbon nanotubes," *Porosity of Carbon Nanotubes*, vol. 17, pp. 289–293, 2000.

[33] Y. Gao and I. Kyratzis, "Covalent immobilization of proteins on carbon nanotubes using the cross-linker 1-ethyl-3-(3-dimethylaminopropyl)carbodiimide: a critical assessment," *Bioconjugate Chemistry*, vol. 19, no. 10, pp. 1945–1950, 2008.

[34] P. Asuri, S. S. Karajanagi, E. Sellitto, D.-Y. Kim, R. S. Kane, and J. S. Dordick, "Water-soluble carbon nanotube-enzyme conjugates as functional biocatalytic formulations," *Biotechnology and Bioengineering*, vol. 95, no. 5, pp. 804–811, 2006.

[35] N. R. Palwai, D. E. Martyn, L. F. F. Neves, Y. Tan, D. E. Resasco, and R. G. Harrison, "Retention of biological activity and near-infrared absorbance upon adsorption of horseradish peroxidase on single-walled carbon nanotubes," *Nanotechnology*, vol. 18, no. 23, Article ID 235601, 2007.

[36] S. Shah, K. Solanki, and M. N. Gupta, "Enhancement of lipase activity in non-aqueous media upon immobilization on multi-walled carbon nanotubes," *Chemistry Central Journal*, vol. 1, no. 1, article 30, pp. 1–6, 2007.

[37] K. Jiang, L. S. Schadler, R. W. Siegel, X. Zhang, H. Zhang, and M. Terrones, "Protein immobilization on carbon nanotubes via a two-step process of diimide-activated amidation," *Journal of Materials Chemistry*, vol. 14, no. 30, pp. 37–39, 2004.

[38] W. Huang, S. Taylor, K. Fu et al., "Attaching proteins to carbon nanotubes via Diimide-Activated amidation," *Nano Letters*, vol. 2, no. 4, pp. 311–314, 2002.

[39] N. Z. Prlainovic, D. I. Bezbradica, Z. D. Knezevic-Jugovic et al., "Adsorption of lipase from Candida rugosa on multi walled carbon nanotubes," *Journal of Industrial and Engineering Chemistry*, vol. 19, pp. 279–285, 2013.

[40] G. V. Salmoria, R. A. Paggi, A. Lago, and V. E. Beal, "Microstructural and mechanical characterization of PA12/MWCNTs nanocomposite manufactured by selective laser sintering," *Polymer Testing*, vol. 30, no. 6, pp. 611–615, 2011.

[41] X. Li, X. Liu, W. Dong et al., "In vitro evaluation of porous poly(L-lactic acid) scaffold reinforced by chitin fibers," *Journal of Biomedical Materials Research B*, vol. 90, no. 2, pp. 503–509, 2009.

[42] W. X. Chen, J. P. Tu, L. Y. Wang, H. Y. Gan, Z. D. Xu, and X. B. Zhang, "Tribological application of carbon nanotubes in a metal-based composite coating and composites," *Carbon*, vol. 41, no. 2, pp. 215–222, 2003.

[43] J. P. Tu, Y. Z. Yang, L. Y. Wang, X. C. Ma, and X. B. Zhang, "Tribological properties of carbon-nanotube-reinforced copper composites," *Tribology Letters*, vol. 10, no. 4, pp. 225–228, 2001.

[44] S. R. Dong, J. P. Tu, and X. B. Zhang, "An investigation of the sliding wear behavior of Cu-matrix composite reinforced by carbon nanotubes," *Materials Science and Engineering A*, vol. 313, no. 1-2, pp. 83–87, 2001.

[45] L. Zhao and L. Gao, "Novel in situ synthesis of MWNTs-hydroxyapatite composites," *Carbon*, vol. 42, no. 2, pp. 423–426, 2004.

[46] Z. Xia, L. Riester, W. A. Curtin et al., "Direct observation of toughening mechanisms in carbon nanotube ceramic matrix composites," *Acta Materialia*, vol. 52, no. 4, pp. 931–944, 2004.

[47] A. B. Dalton, S. Collins, E. Muñoz et al., "Super-tough carbon-nanotube fibres," *Nature*, vol. 423, no. 6941 article 703, 2003.

[48] S. Kumar, H. Doshi, M. Srinivasarao, J. O. Park, and D. A. Schiraldi, "Fibers from polypropylene/nano carbon fiber composites," *Polymer*, vol. 43, no. 5, pp. 1701–1703, 2002.

[49] X. M. Li, L. Wang, Y. B. Fan, Q. L. Feng, and F. Z. Cui, "Biocompatibility and toxicity of nanoparticles and nanotubes," *Journal of Nanomaterials*, vol. 2012, Article ID 548389, 19 pages, 2012.

[50] L. Valentini, J. Biagiotti, J. M. Kenny, and S. Santucci, "Morphological characterization of single-walled carbon nanotubes-PP composites," *Composites Science and Technology*, vol. 63, no. 8, pp. 1149–1153, 2003.

[51] T. J. Webster, M. C. Waid, J. L. McKenzie, R. L. Price, and J. U. Ejiofor, "Nano-biotechnology: carbon nanofibres as improved neural and orthopaedic implants," *Nanotechnology*, vol. 15, no. 1, pp. 48–54, 2004.

[52] R. L. Price, K. M. Haberstroh, and T. J. Webster, "Improved osteoblast viability in the presence of smaller nanometre dimensioned carbon fibres," *Nanotechnology*, vol. 15, no. 8, pp. 892–900, 2004.

[53] P. Deng, Z. Xu, and J. Li, "Simultaneous determination of ascorbic acid and rutin in pharmaceutical preparations with electrochemical method based on multi-walled carbon nanotubes-chitosan composite film modified electrode," *Journal of Pharmaceutical and Biomedical Analysis*, vol. 76, pp. 234–242, 2013.

[54] H. Golnabi, "Carbon nanotube research developments in terms of published papers and patents, synthesis and production," *Scientia Iranica*, vol. 19, pp. 2012–2022, 2012.

[55] Y. Zhu, W. Wang, X. Jia, T. Akasaka, S. Liao, and F. Watari, "Deposition of TiC film on titanium for abrasion resistant implant material by ion-enhanced triode plasma CVD," *Applied Surface Science*, vol. 262, pp. 156–158, 2012.

[56] M. Kumar and Y. Ando, "Chemical vapor deposition of carbon nanotubes: a review on growth mechanism and mass production," *Journal of Nanoscience and Nanotechnology*, vol. 10, no. 6, pp. 3739–3758, 2010.

[57] M. N. Disfani and S. H. Jafari, "Assessment of intertube interactions in different functionalized multiwalled carbon nanotubes incorporated in a phenoxy resin," *Polymer Engineering and Science*, vol. 53, no. 1, pp. 168–175, 2013.

[58] H. Kwon, M. Estili, K. Takagi, T. Miyazaki, and A. Kawasaki, "Combination of hot extrusion and spark plasma sintering for producing carbon nanotube reinforced aluminum matrix composites," *Carbon*, vol. 47, no. 3, pp. 570–577, 2009.

[59] X. Zeng, G. Zhou, Q. Xu, Y. Xiong, C. Luo, and J. Wu, "A new technique for dispersion of carbon nanotube in a metal melt," *Materials Science and Engineering A*, vol. 527, no. 20, pp. 5335–5340, 2010.

[60] S. R. Bakshi, V. Singh, S. Seal, and A. Agarwal, "Aluminum composite reinforced with multiwalled carbon nanotubes from plasma spraying of spray dried powders," *Surface and Coatings Technology*, vol. 203, no. 10-11, pp. 1544–1554, 2009.

[61] G. Han, J. Yuan, G. Shi, and F. Wei, "Electrodeposition of polypyrrole/multiwalled carbon nanotube composite films," *Thin Solid Films*, vol. 474, no. 1-2, pp. 64–69, 2005.

[62] S. R. Bakshi and A. Agarwal, "An analysis of the factors affecting strengthening in carbon nanotube reinforced aluminum composites," *Carbon*, vol. 49, no. 2, pp. 533–544, 2011.

[63] T. Kuzumaki, K. Miyazawa, H. Ichinose, and K. Ito, "Processing of carbon nanotube reinforced aluminum composite," *Journal of Materials Research*, vol. 13, no. 9, pp. 2445–2449, 1998.

[64] A. Peigney, C. Laurent, O. Dumortier, and A. Rousset, "Carbon nanotubes-Fe-alumina nanocomposites. Part I: influence of the Fe content on the synthesis of powders," *Journal of the European Ceramic Society*, vol. 18, no. 14, pp. 1995–1104, 1998.

[65] C. Laurent, A. Peigney, O. Dumortier, and A. Rousset, "Carbon nanotubes-Fe-Alumina nanocomposites. Part II: microstructure and mechanical properties of the hot-Pressed composites," *Journal of the European Ceramic Society*, vol. 18, no. 14, pp. 2005–2013, 1998.

[66] S. B. Jagtap and D. Ratna, "Preparation and characterization of rubbery epoxy/multiwall carbon nanotubes composites using amino acid salt assisted dispersion technique," *Express Polymer Letter*, vol. 7, no. 4, pp. 329–339, 2013.

[67] J. Sandler, M. S. P. Shaffer, T. Prasse, W. Bauhofer, K. Schulte, and A. H. Windle, "Development of a dispersion process for carbon nanotubes in an epoxy matrix and the resulting electrical properties," *Polymer*, vol. 40, no. 21, pp. 5967–5971, 1999.

[68] L. S. Schadler, S. C. Giannaris, and P. M. Ajayan, "Load transfer in carbon nanotube epoxy composites," *Applied Physics Letters*, vol. 73, no. 26, pp. 3842–3844, 1998.

[69] F. H. Gojny, J. Nastalczyk, Z. Roslaniec, and K. Schulte, "Surface modified multi-walled carbon nanotubes in CNT/epoxy-composites," *Chemical Physics Letters*, vol. 370, no. 5-6, pp. 820–824, 2003.

[70] Z. Jia, Z. Wang, C. Xu et al., "Study on poly(methyl methacrylate)/carbon nanotube composites," *Materials Science and Engineering A*, vol. 271, no. 1-2, pp. 395–400, 1999.

[71] M. Lamy De La Chapelle, C. Stéphan, T. P. Nguyen et al., "Raman characterization of singlewalled carbon nanotubes and PMMA-nanotubes composites," *Synthetic Metals*, vol. 103, no. 1–3, pp. 2510–2512, 1999.

[72] X. M. Li, Y. Huang, L. S. Zheng et al., "Effect of substrate stiffness on the functions of rat bone marrow and adipose tissue derived mesenchymal stem cells in vitro," *Journal of Biomedical Materials Research A*, 2013.

[73] R. Haggenmueller, H. H. Gommans, A. G. Rinzler, J. E. Fischer, and K. I. Winey, "Aligned single-wall carbon nanotubes in composites by melt processing methods," *Chemical Physics Letters*, vol. 330, no. 3-4, pp. 219–225, 2000.

[74] M. S. P. Shaffer and A. H. Windle, "Fabrication and characterization of carbon nanotube/poly (vinyl alcohol) composites," *Advanced Materials*, vol. 11, no. 11, pp. 937–941, 1999.

[75] F. Li, H. M. Cheng, S. Bai, G. Su, and M. S. Dresselhaus, "Tensile strength of single-walled carbon nanotubes directly measured

from their macroscopic ropes," *Applied Physics Letters*, vol. 77, no. 20, pp. 3161–3163, 2000.

[76] G. G. Tibbetts and J. J. McHugh, "Mechanical properties of vapor-grown carbon fiber composites with thermoplastic matrices," *Journal of Materials Research*, vol. 14, no. 7, pp. 2871–2880, 1999.

[77] X. Tong, C. Liu, H.-M. Cheng, H. Zhao, F. Yang, and X. Zhang, "Surface modification of single-walled carbon nanotubes with polyethylene via in situ Ziegler-Natta polymerization," *Journal of Applied Polymer Science*, vol. 92, no. 6, pp. 3697–3700, 2004.

[78] K. Lozano, S. Yang, and R. E. Jones, "Nanofiber toughened polyethylene composites," *Carbon*, vol. 42, no. 11, pp. 2329–2331, 2004.

[79] J. K. W. Sandler, S. Pegel, M. Cadek et al., "A comparative study of melt spun polyamide-12 fibres reinforced with carbon nanotubes and nanofibres," *Polymer*, vol. 45, no. 6, pp. 2001–2015, 2004.

[80] D. E. Hill, Y. Lin, A. M. Rao, L. F. Allard, and Y.-P. Sun, "Functionalization of carbon nanotubes with polystyrene," *Macromolecules*, vol. 35, no. 25, pp. 9466–9471, 2002.

[81] K. Liao and S. Li, "Interfacial characteristics of a carbon nanotube-polystyrene composite system," *Applied Physics Letters*, vol. 79, no. 25, pp. 4225–4227, 2001.

[82] X. M. Li, L. Wang, Y. B. Fan, Q. L. Feng, F. Z. Cui, and F. Watari, "Nanostructured scaffolds for bone tissue engineering," *Journal of Biomedical Materials Research A*, vol. 101, no. 8, pp. 2424–2435, 2013.

[83] A. A. White, S. M. Best, and I. A. Kinloch, "Hydroxyapatite-carbon nanotube composites for biomedical applications: a review," *International Journal of Applied Ceramic Technology*, vol. 4, no. 1, pp. 1–13, 2007.

[84] X. Li, H. Liu, X. Niu et al., "Osteogenic differentiation of human adipose-derived stem cells induced by osteoinductive calcium phosphate ceramics," *Journal of Biomedical Materials Research A*, vol. 97, no. 1, pp. 10–19, 2011.

[85] Q. Wang, S. Ge, and D. Zhang, "Nano-mechanical properties and biotribological behaviors of nanosized HA/partially-stabilized zirconia composites," *Wear*, vol. 259, no. 7-12, pp. 952–957, 2005.

[86] J.-W. Choi, Y.-M. Kong, H.-E. Kim, and I.-S. Lee, "Reinforcement of hydroxyapatite bioceramic by addition of Ni3Al and Al_2O_3 ," *Journal of the American Ceramic Society*, vol. 81, no. 7, pp. 1743–1748, 1998.

[87] C. Chang, J. Shi, J. Huang, Z. Hu, and C. Ding, "Effects of power level on characteristics of vacuum plasma sprayed hydroxyapatite coating," *Journal of Thermal Spray Technology*, vol. 7, no. 4, pp. 484–488, 1998.

[88] H. Feng, Q. Meng, Y. Zhou, and D. Jia, "Spark plasma sintering of functionally graded material in the Ti-TiB2-B system," *Materials Science and Engineering A*, vol. 397, no. 1-2, pp. 92–97, 2005.

[89] T. Takeuchi, M. Tabuchi, H. Kageyama, and Y. Suyama, "Preparation of dense $BaTiO_3$ ceramics with submicrometer grains by spark plasma sintering," *Journal of the American Ceramic Society*, vol. 82, no. 4, pp. 939–943, 1999.

[90] Y. Zhou, K. Hirao, M. Toriyama, and H. Tanaka, "Very rapid densification of nanometer silicon carbide powder by pulse electric current sintering," *Journal of the American Ceramic Society*, vol. 83, no. 3, pp. 654–656, 2000.

[91] M. Nygren and Z. Shen, "On the preparation of bio-, nano- and structural ceramics and composites by spark plasma sintering," *Solid State Sciences*, vol. 5, no. 1, pp. 125–131, 2003.

[92] F. Watari, A. Yokoyama, M. Omori et al., "Biocompatibility of materials and development to functionally graded implant for bio-medical application," *Composites Science and Technology*, vol. 64, no. 6, pp. 893–908, 2004.

[93] H. Kondo, A. Yokoyama, M. Omori et al., "Fabrication of titanium nitride/apatite functionally graded implants by spark plasma sintering," *Materials Transactions*, vol. 45, no. 11, pp. 3156–3162, 2004.

[94] S. Hoshii, A. Kojima, and M. Goto, "Rapid baking of graphite powders by the spark plasma sintering method," *Carbon*, vol. 38, no. 13, pp. 1896–1899, 2000.

[95] H. Conrad, "Electroplasticity in metals and ceramics," *Materials Science and Engineering A*, vol. 287, no. 2, pp. 276–287, 2000.

[96] H. Yao, Y. Jin, M. H. Chen, H. Wu, N. Liu, and Q. W. Li, "Preparation and mechanical properties of carbon nanotubes reinfored Aluminum composite," *Materials Review*, vol. 26, no. 18, pp. 111–115, 2012.

[97] N. Ogihara, Y. Usui, K. Aoki et al., "Biocompatibility and bone tissue compatibility of alumina ceramics reinforced with carbon nanotubes," *Nanomedicine*, vol. 7, no. 7, pp. 981–993, 2012.

[98] W. Wang, A. Yokoyama, S. Liao et al., "Preparation and characteristics of a binderless carbon nanotube monolith and its biocompatibility," *Materials Science and Engineering C*, vol. 28, no. 7, pp. 1082–1086, 2008.

[99] W. A. Curtin and B. W. Sheldon, "CNT-reinforced ceramics and metals," *Materials Today*, vol. 7, no. 11, pp. 44–49, 2004.

[100] X. M. Li, Y. Yang, Y. Fan, Q. Feng, F. Cui, and F. Watari, "Biocomposites reinforced by fibers or tubes as scaffolds for tissue engineering or regenerative medicine," *Journal of Biomedical Materials Research A*, 2013.

[101] X. Li, H. Gao, M. Uo et al., "Effect of carbon nanotubes on cellular functions in vitro," *Journal of Biomedical Materials Research A*, vol. 91, no. 1, pp. 132–139, 2009.

[102] Q. Xu, X.-S. Zeng, and G.-H. Zhou, "Mechanical properties of CNTs/AZ31 composites prepared by adding CNTs block with plunger," *Chinese Journal of Nonferrous Metals*, vol. 20, no. 2, pp. 189–194, 2010.

[103] S. R. Bakshi, D. Lahiri, and A. Agarwal, "Carbon nanotube reinforced metal matrix composites: a review," *International Materials Reviews*, vol. 55, no. 1, pp. 41–64, 2010.

[104] L. Sun, J. T. Yang, Y. Q. Shi, and M. Q. Zhong, "Dynamic mechanical properties and analysis of toughening mechanism of PA6/CNTs nano-meter composite," *China Plastics Industry*, S1, 2007.

[105] F. Zomer Volpato, S. L. Fernandes Ramos, A. Motta, and C. Migliaresi, "Physical and in vitro biological evaluation of a PA 6/MWCNT electrospun composite for biomedical applications," *Journal of Bioactive and Compatible Polymers*, vol. 26, no. 1, pp. 35–47, 2011.

[106] I. T. Amr, A. Al-Amer, T. P. Selvin et al., "Effect of acid treated carbon nanotubes on mechanical, rheological and thermal properties of polystyrene nanocomposites," *Composites B*, vol. 42, no. 6, pp. 1554–1561, 2011.

[107] Y. C. Jung, H. H. Kim, Y. A. Kim et al., "Optically active multi-walled carbon nanotubes for transparent, conductive memory-shape polyurethane film," *Macromolecules*, vol. 43, no. 14, pp. 6106–6112, 2010.

[108] L. D. Tijing, C.-H. Park, W. L. Choi et al., "Characterization and mechanical performance comparison of multiwalled carbon nanotube/polyurethane composites fabricated by electrospinning and solution casting," *Composites B*, vol. 44, no. 1, pp. 613–619, 2013.

[109] N. Garmendia, I. Santacruz, R. Moreno, and I. Obieta, "Zirconia-MWCNT nanocomposites for biomedical applications obtained by colloidal processing," *Journal of Materials Science*, vol. 21, no. 5, pp. 1445–1451, 2010.

[110] W. Wang, M. Omori, F. Watari, and A. Yokoyama, "Novel bulk carbon nanotube materials for implant by spark plasma sintering," *Dental Materials Journal*, vol. 24, no. 4, pp. 478–486, 2005.

[111] W. Wang, F. Watari, M. Omori et al., "Mechanical properties and biological behavior of carbon nanotube/polycarbosilane composites for implant materials," *Journal of Biomedical Materials Research B*, vol. 82, no. 1, pp. 223–230, 2007.

[112] W. Wang, Y. Zhu, F. Watari et al., "Carbon nanotubes/hydroxyapatite nanocomposites fabricated by spark plasma sintering for bonegraft applications," *Applied Surface Science*, vol. 262, pp. 194–199, 2012.

[113] H. Aoki, *Marvelous Biomaterials: Apatite*, Ishiyaku Press, Tokyo, Japan, 1999.

[114] X. Li, Y. Fan, and F. Watari, "Current investigations into carbon nanotubes for biomedical application," *Biomedical Materials*, vol. 5, no. 2, Article ID 022001, 2010.

[115] Y. Usui, K. Aoki, N. Narita et al., "Carbon nanotubes with high bone-tissue compatibility and bone-formation acceleration effects," *Small*, vol. 4, no. 2, pp. 240–246, 2008.

[116] N. Aoki, A. Yokoyama, Y. Nodasaka et al., "Strikingly extended morphology of cells grown on carbon nanotubes," *Chemistry Letters*, vol. 35, no. 5, pp. 508–509, 2006.

[117] X. Li, H. Liu, X. Niu et al., "The use of carbon nanotubes to induce osteogenic differentiation of human adipose-derived MSCs in vitro and ectopic bone formation in vivo," *Biomaterials*, vol. 33, no. 19, pp. 4818–4827, 2012.

[118] K.-H. Im, S.-B. Lee, K.-M. Kim, and Y.-K. Lee, "Improvement of bonding strength to titanium surface by sol-gel derived hybrid coating of hydroxyapatite and titania by sol-gel process," *Surface and Coatings Technology*, vol. 202, no. 4–7, pp. 1135–1138, 2007.

[119] T. J. Webster, C. Ergun, R. H. Doremus, R. W. Siegel, and R. Bizios, "Specific proteins mediate enhanced osteoblast adhesion on nanophase ceramics," *Journal of Biomedical Materials Research*, vol. 51, no. 3, pp. 475–483, 2000.

[120] K. L. Elias, R. L. Price, and T. J. Webster, "Enhanced functions of osteoblasts on nanometer diameter carbon fibers," *Biomaterials*, vol. 23, no. 15, pp. 3279–3287, 2002.

[121] A. A. Bhirde, S. Patel, A. A. Sousa et al., "Distribution and clearance of PEG-single-walled carbon nanotube cancer drug delivery vehicles in mice," *Nanomedicine*, vol. 5, no. 10, pp. 1535–1546, 2010.

[122] C.-W. Lam, J. T. James, R. McCluskey, and R. L. Hunter, "Pulmonary toxicity of single-wall carbon nanotubes in mice 7 and 90 days after intractracheal instillation," *Toxicological Sciences*, vol. 77, no. 1, pp. 126–134, 2004.

[123] J. Miyawaki, M. Yudasaka, T. Azami, Y. Kubo, and S. Iijima, "Toxicity of single-walled carbon nanohorns," *ACS Nano*, vol. 2, no. 2, pp. 213–226, 2008.

[124] A. Abarrategi, M. C. Gutiérrez, C. Moreno-Vicente et al., "Multiwall carbon nanotube scaffolds for tissue engineering purposes," *Biomaterials*, vol. 29, no. 1, pp. 94–102, 2008.

[125] F. M. Tonelli, A. K. Santos, K. N. Gomes et al., "Carbon nanotube interaction with extracellular matrix proteins producing scaffolds for tissue engineering," *International Journal of Nanomedicine*, vol. 7, pp. 4511–4529, 2012.

[126] R. Verdejo, G. Jell, L. Safinia, A. Bismarck, M. M. Stevens, and M. S. P. Shaffer, "Reactive polyurethane carbon nanotube foams and their interactions with osteoblasts," *Journal of Biomedical Materials Research A*, vol. 88, no. 1, pp. 65–73, 2009.

[127] X. Li, C. A. van Blitterswijk, Q. Feng, F. Cui, and F. Watari, "The effect of calcium phosphate microstructure on bone-related cells in vitro," *Biomaterials*, vol. 29, no. 23, pp. 3306–3316, 2008.

[128] X. Liu, X. Li, Y. Fan et al., "Repairing goat tibia segmental bone defect using scaffold cultured with mesenchymal stem cells," *Journal of Biomedical Materials Research B*, vol. 94, no. 1, pp. 44–52, 2010.

[129] S. Garibaldi, C. Brunelli, V. Bavastrello, G. Ghigliotti, and C. Nicolini, "Carbon nanotube biocompatibility with cardiac muscle cells," *Nanotechnology*, vol. 17, no. 2, pp. 391–397, 2006.

[130] S. Tang, Y. Tang, L. Zhong et al., "Short- and long-term toxicities of multi-walled carbon nanotubes in vivo and in vitro," *Journal of Applied Toxicology*, vol. 32, no. 11, pp. 900–912, 2012.

[131] G. Ahn, D. W. Seol, S. G. Pyo, and D. Lee, "Calcium phosphate cement-multi-walled carbon nanotube hybrid material (CPC-MWCNT hybrid) enhances osteogenic differentiation," *Tissue Engineering and Regenerative Medicine*, vol. 8, no. 4, pp. 390–397, 2011.

[132] J. Muller, F. Huaux, and D. Lison, "Respiratory toxicity of carbon nanotubes: how worried should we be?" *Carbon*, vol. 44, no. 6, pp. 1048–1056, 2006.

[133] V. L. Colvin, "The potential environmental impact of engineered nanomaterials," *Nature Biotechnology*, vol. 21, no. 10, pp. 1166–1170, 2003.

[134] Z. Evis and R. H. Doremus, "Coatings of hydroxyapatite: nanosize alpha alumina composites on Ti-6Al-4V," *Materials Letters*, vol. 59, no. 29-30, pp. 3824–3827, 2005.

[135] D. B. Warheit, B. R. Laurence, K. L. Reed, D. H. Roach, G. A. M. Reynolds, and T. R. Webb, "Comparative pulmonary toxicity assessment of single-wall carbon nanotubes in rats," *Toxicological Sciences*, vol. 77, no. 1, pp. 117–125, 2004.

[136] Y. Zhang, T. Fu, Y. Han, Q. Wang, Y. Zhao, and K. Xu, "In vitro and in vivo tests of hydrothermally synthesised hydroxyapatite coating," *Biomolecular Engineering*, vol. 19, no. 2-6, pp. 57–61, 2002.

[137] X. Li, Q. Feng, X. Liu, W. Dong, and F. Cui, "Collagen-based implants reinforced by chitin fibres in a goat shank bone defect model," *Biomaterials*, vol. 27, no. 9, pp. 1917–1923, 2006.

[138] Z. Evis and R. H. Doremus, "Hot-pressed hydroxylapatite/monoclinic zirconia composites with improved mechanical properties," *Journal of Materials Science*, vol. 42, no. 7, pp. 2426–2431, 2007.

Hindawi Publishing Corporation
BioMed Research International
Volume 2013, Article ID 362918, 7 pages
http://dx.doi.org/10.1155/2013/362918

Research Article

The Use of Fiber-Reinforced Scaffolds Cocultured with Schwann Cells and Vascular Endothelial Cells to Repair Rabbit Sciatic Nerve Defect with Vascularization

Hongyang Gao,[1] Yang You,[2] Guoping Zhang,[1] Feng Zhao,[1] Ziyi Sha,[1] and Yong Shen[3]

[1] *Department of Orthopedics, The First Hospital of Hebei Medical University, Shijiazhuang 050031, China*
[2] *Department of Cardiovasology III, The First Hospital of Hebei Medical University, Shijiazhuang 050031, China*
[3] *Department of Spinal Surgery, The Third Affiliated Hospital of Hebei Medical University, Shijiazhuang 050051, China*

Correspondence should be addressed to Yong Shen; shenyongspinemd@163.com

Received 30 November 2013; Accepted 9 December 2013

Academic Editor: Xiaoming Li

Copyright © 2013 Hongyang Gao et al. This is an open access article distributed under the Creative Commons Attribution License, which permits unrestricted use, distribution, and reproduction in any medium, provided the original work is properly cited.

To explore the feasibility of biodegradable fiber-reinforced 3D scaffolds with satisfactory mechanical properties for the repair of long-distance sciatic nerve defect in rabbits and effects of vascularized graft in early stage on the recovery of neurological function, Schwann cells and vascular endothelial cells were cocultured in the fiber-reinforced 3D scaffolds. Experiment group which used prevascularized nerve complex for the repair of sciatic nerve defect and control group which only cultured with Schwann cells were set. The animals in both groups underwent electromyography to show the status of the neurological function recovery at 4, 8, and 16 weeks after the surgery. Sciatic nerve regeneration and myelination were observed under the light microscope and electron microscope. Myelin sheath thickness, axonal diameter, and number of myelinated nerve fiber were quantitatively analyzed using image analysis system. The recovery of foot ulcer, the velocity of nerve conduction, the number of regenerating nerve fiber, and the recovery of ultrastructure were increased in the experimental group than those in the control group. Prevascularized tissue engineered fiber-reinforced 3D scaffolds for the repair of sciatic nerve defects in rabbits can effectively promote the recovery of neurological function.

1. Introduction

Peripheral nerve injuries are common in clinical practice [1]. Peripheral nerve injuries can arise from trauma, cancer, or congenital defects [2, 3]. The regeneration of the injured nerve is slow and can result in complicated rehabilitation. Peripheral nerve injuries are challenging clinical issues to address. While short gaps less than 10 mm can be reconnected surgically with microsutures [4] or various nerve guidance channels [5–7], longer defects are more difficult to treat [8]. Autologous nerve graft is widely used in clinical surgery for nerve reconstructions and has been considered as the golden standard [9–11]. However, it still has several defectives including donor tissue availability limitation, extra incision, sacrifice of the donor nerve and danger of neuroma forming, multiple surgical sites, and possible size mismatch. Other options include allografts and xenografts, but those run the risk of disease transmission and immune rejection. Thus, there is a significant clinical need to address critical size nerve defects.

Nerve tissue engineering is a promising approach that has shown potential to address this need with synthetic nerve conduits. There has been a significant effort dedicated to developing synthetic nerve conduits that have resulted in encouraging regeneration and some degree of functional recovery of peripheral nerve defects without sacrificing other nerves [12]. However, simply bridging the transected nerve with an empty conduit would not satisfy the functional recovery. Numerous experiments indicated that, after nerve injury, oriented regrowth guidance and regeneration promoting factors played very important roles in nerve regeneration and functional recovery [13–15]. Schwann cells are closely associated with, and play key roles in, the development, maintenance, and regeneration of peripheral neurons [16–19].

The microenvironment of the conduit mimicking the biological situation is a vital issue in tissue regeneration. *In vivo*, nearly all tissues are supplied with nutrients and oxygen by a highly branched system of larger blood vessels, which are subdivided in the tissue into small capillaries, including the nerve system. The strategy based on the endothelial cells and their ability to form new vessels known as neoangiogenesis had been developed for the formation of the vessel system *in vivo*. Biomaterials with structural similarity to native extracellular matrix (ECM) have been shown to improve cell function.

In this paper, a new-typed fiber-reinforced 3D scaffold which had been demonstrated good biocompatibility *in vivo* [20, 21] was prepared to mimic ECM due to the critical role of the ECM in regulating cell function, acting as a nerve conduit, providing a permissive chamber for nerve regeneration in the rabbit sciatic nerve model. The 3D scaffold was cocultured with Schwann cells and vascular endothelial cells in order to support the vascularization and induce the nerve regeneration of the rabbit sciatic nerve. Two groups (nonvascularized and vascularized nerve tissue engineering scaffolds) were used to evaluate results of nerve regeneration.

2. Materials and Methods

2.1. Materials. M199 medium (Gibco), DMEM medium (Gibco), trypsin (Gibco), nerve growth factor (Xiamen Bioway Biotech Co., Ltd., China), fetal bovine serum (Hangzhou Sijiqing Biological Engineering Materials Co., Ltd., China), rabbit anti-S-100 protein antibody, TritonX-100 (Sigma, USA), vascular endothelial growth factor (Xiamen Bioway Biotech Co., Ltd.), and Chitosan fibres (80% deacetylated; diameter, 12.5 μm; tensile strength, 550 MPa) were obtained from Donghua University, China. PLLA was purchased from the Shandong Medical Appliance Factory, China, while Type I collagen (at a concentration of 1%), dioxane, and other chemicals were purchased from the Beijing Chemical Company Ltd, China. A total of 36 healthy adult New Zealand rabbits of both genders and one New Zealand rabbit (pregnancy on day 28) were provided by the Experimental Animal Center, Hebei Medical University, China.

2.2. Methods

2.2.1. Preparation of the Biodegradable Fiber-Reinforced 3D Scaffolds. The biodegradable fiber-reinforced 3D scaffolds were prepared in accordance with a previously published method by Li et al. [20]. The composites were cut into the appropriate size matching the nerve defect and sterilized by Co60.

2.2.2. Preparation of Nonvascularized and Vascularized Tissue Engineered Scaffolds. Sciatic nerve of fetal rabbits at 28 days of pregnancy was obtained. Schwann cells were cultured using two enzymatic digestions. Schwann cells of passage 2 at a concentration of 1×10^8/L were separately injected into both ends of the scaffolds with a 100 ul microsyringe. Thereby, nonvascularized tissue engineered scaffolds were obtained.

Thoracic aorta of fetal rabbit was obtained. Vascular endothelial cells were cultured using enzymatic digestion. Schwann cells and vascular endothelial cells of passage 2 at a ratio of 2 : 1 were cultured in DMEM containing 20% fetal bovine serum and M199 medium. By the same method, cell suspension was infused into the scaffolds (Schwann cell at a concentration of 1×10^8/L), forming vascularized tissue engineered scaffolds.

2.2.3. Establishment of Animal Models. Experimental animals were randomly assigned to control group (nonvascularized tissue engineered scaffolds) ($n = 18$) and experimental group (vascularized tissue engineered scaffolds) ($n = 18$).

All operations were done under aseptic conditions. Abdominal anesthesia and nerve suture were done by the same person. A 20 mm segment of sciatic nerve was transversely excised at about 5 mm from proximal end of knee joint of left hind limb of rabbits. Under the operating microscope, the fiber-reinforced scaffolds cocultured with vascular endothelial cells and Schwann cells were used for defect repair with nontraumatic suture as the experimental group while the fiber-reinforced scaffolds cultured with only Schwann cells were utilized as control.

2.3. Detection Methods and Indices

2.3.1. General Observation. Conditions of all over the body and wound were observed at various time points after surgery in both groups to compare foot ulceration and healing. During sampling, we paid great attention to whether there was a neuroma at the anastomotic site and to the adhesion condition between nerve graft and surrounding tissue.

2.3.2. Determination of Nerve Conduction Velocity. At 4, 8, and 16 weeks after nerve transplantation, sciatic nerve was exposed in the second operation in both groups. Stimulating electrodes were inserted on the proximal and distal ends of nerve graft. Recording electrodes were inserted in the tibialis anterior muscle belly. The same stimulus intensity and frequency were given. The latency and conduction velocity were measured with MEM-3210 electromyography.

2.3.3. Measurement of Wet Weight of Tibialis Anterior Muscle. At 4, 8, and 16 weeks after nerve transplantation, tibialis anterior muscle at operation side was incised, and blood on its surface was absorbed with blotting paper. Wet weight of tibialis anterior muscle was weighed with an electronic balance. Paired comparison was done.

2.3.4. Observation with the Light Microscope. At 4, 8, and 16 weeks after nerve transplantation, a 4 mm middle segment of nerve was obtained from both groups and equally divided into two parts (distal, proximal, each 2 mm). Proximal segment of the nerve was fixed in 10% formaldehyde, embedded in paraffin, and sliced into transverse sections. These sections were subjected to Masson staining. Morphology of myelin sheath, axonal number and distribution, and connective tissue structure was observed under the light microscope.

Images were analyzed using high-definition color image processing system (Institute of Beijing University of Aeronautics and Astronautics, China). Observation index was the number of nerve axon.

2.3.5. Observation with the Transmission Electron Microscope. Distal segment of the nerve obtained at various time points was fixed in 4% glutaral, dehydrated with gradient alcohol and acetone, embedded with epoxy resin, and then sliced with an ultramicrotome. These sections were stained with uranyl acetate and lead citrate. Transmission electron microscope (H/7500, Hitachi, Japan) was utilized to observe axon diameter, myelin sheath distribution, lamellar structure, microtubule, mitochondrion, and microfilament. Observational indexes were axon diameter and myelin sheath thickness.

2.3.6. Statistical Analysis. Data were analyzed with SAS software and expressed as mean ± SD. The difference between the two groups was compared with t-test. A value of $P < 0.05$ was considered statistically significant.

3. Results

3.1. General Observation of Animals. No apparent rejection was observed all over the body or in the operative field after allograft nerve complex transplantation in both groups. No noticeable infection appeared at the operative incision. At 2 weeks after operation, ulcer at different degrees was visible on the foot of the operation side. However, compared with the control group, at 5-6 weeks after operation, ulcer healing was better at the operation side in the experimental group. At 15-16 weeks after surgery, hindlimb braced in both groups and normal gait appeared in some animals.

Specimen collection during the secondary operation: tissue engineered scaffolds connected well to the host in both groups. No obvious neuroma was observed at the anastomotic site. There was no severe adhesion between the tissue engineered scaffolds and surrounding tissue and vascular network formed in the outer membrane.

3.2. Detection Results of Nerve Conduction Velocity. At 4 weeks after nerve transplantation, the animals of both groups did not respond to electrostimulation, with the absence of nerve conduction. Electromyogram showed a straight line. At 8 and 16 weeks after operation, nerve conduction velocity was restored to different degrees under the same stimulus intensity and frequency in both groups. Results revealed that the recovery of nerve conduction velocity was better in the experimental group than that in the control group ($P < 0.05$; Table 1).

3.3. Measurement of Wet Weight of Tibialis Anterior Muscle. The weight of animals in both groups was similar at various time points after nerve transplantation. Tibialis anterior muscle atrophy was obvious at the operation side in both groups at 4 weeks after operation. However, no significant difference in the wet weight of tibialis anterior muscle was detected between the two groups at 4 weeks ($P > 0.05$). The wet weight of tibialis anterior muscle increased at 8 and 16 weeks compared with that at 4 weeks in both groups to different degrees, indicating that the recovery was better in the experimental group than that in the control group ($P < 0.05$; Table 2).

3.4. Observational Results under the Light Microscope. The sections were observed under light microscope after Masson staining. The section dyed at week 16 can be seen in Figure 1. Masson staining revealed that the number of regenerating nerve per unit area was higher in the experimental group than that in the control group at 4, 8, and 16 weeks after operation. Compared with the control group, regenerating nerve arranged regularly uniformly, with a few connective tissues and a high proportion of thick fibers. There were significant differences in the number of regenerating nerve axons per unit area in both groups at 4, 8, and 16 weeks ($P < 0.05$; Table 3).

3.5. Observational Results under the Transmission Electron Microscope. The sections were observed under the transmission electron microscope after stained with uranyl acetate and lead citrate. The section stained at week 16 was showed in Figure 2. At 4 weeks, regular dense lamellar structure was detectable in the experimental group, with a majority of confluence, with the presence of obvious hyperplasia, abundant microfilaments and microtubules, and regular dense medullary cord. At 8 weeks, there were thick myelin sheath, regular dense lamellar structure, and abundant mitochondria, microfilaments, and microtubules in the experimental group. At 16 weeks, there were uniform myelin sheath, dense lamellar structure, and abundant regular mitochondria, microfilaments, and microtubules in the experimental group (Figure 2). At 4, 8, and 16 weeks, significant differences in the thickness of myelin sheath of new myelinated nerve fibers and the diameter of axons were detectable between both groups ($P < 0.05$; Tables 4 and 5).

4. Discussion

3D scaffold has been widely used in tissue engineering [22–24]. The microstructure of the 3D scaffold itself could mimic the ECM and induce the adhesion, differentiation, and proliferation of cell. After scaffold implantation, the growth of capillaries into the porous construct may be too slow to provide adequate nutrients to the cell within the scaffold, and this inhibits tissue formation in the scaffold core. Achieving successful vascularization remains one of the main problems in tissue engineering [25, 26].

Vascular endothelial cells are monolayer flat cells, an important component of blood capillary, and a selective permeability barrier between blood and vessel wall. Vascularization contains two mechanisms: angiogenesis and vasiformation. Vasiformation refers to enzymatic hydrolysis of vascular basement membrane, pullulation, proliferation, and then formation of new blood capillary. Moreover, vascular endothelial cells can synthesize and secrete vascular endothelial growth factor and basic fibroblast growth factor,

Table 1: Comparison of the nerve conduction velocity at different postoperative time in two groups ($n = 18$, $\overline{x} \pm s$, m/s).

Time (weeks)	Experimental group	Control group	t	P
4	—	—	—	—
8	23.35 ± 1.05	23.11 ± 0.80	2.13	0.04
16	39.52 ± 1.01	38.34 ± 0.15	2.15	0.04

Table 2: Comparison of the wet weight of tibialis anterior muscle at different postoperative time in two groups ($n = 18$, $\overline{x} \pm s$, g).

Time (weeks)	Experimental group	Control group	t	P
4	2.22 ± 0.13	2.20 ± 0.16	0.40	0.67
8	3.38 ± 0.11	3.28 ± 0.07	2.89	0.01
16	6.10 ± 0.22	5.97 ± 0.15	2.14	0.04

Table 3: Comparison of the quantity of nerve fibers at different postoperative time in two groups ($n = 18$, $\overline{x} \pm s$).

Time (weeks)	Experimental group	Control group	t	P
4	922.97 ± 25.06	901.48 ± 12.39	3.26	0.0025
8	1736.44 ± 36.28	1713.51 ± 25.00	2.20	0.03
16	2840.91 ± 20.93	2823.74 ± 14.42	2.86	0.04

Table 4: Comparison of the axon diameter of myelinated nerve fibers at different postoperative time in two groups ($n = 18$, $\overline{x} \pm s$, μm).

Time (weeks)	Experimental group	Control group	t	P
4	5.83 ± 0.16	5.58 ± 0.42	2.27	0.03
8	6.01 ± 0.09	5.87 ± 0.16	3.09	<0.01
16	6.11 ± 0.08	6.00 ± 0.07	4.62	<0.0001

Table 5: Comparison of myelin sheath thickness at different postoperative time in two groups ($n = 18$, $\overline{x} \pm s$, μm).

Time (weeks)	Experimental group	Control group	t	P
4	1.95 ± 0.14	1.70 ± 0.22	4.10	0.0002
8	1.99 ± 0.11	1.85 ± 0.16	3.10	0.0039
16	2.03 ± 0.05	1.90 ± 0.06	7.16	<0.0001

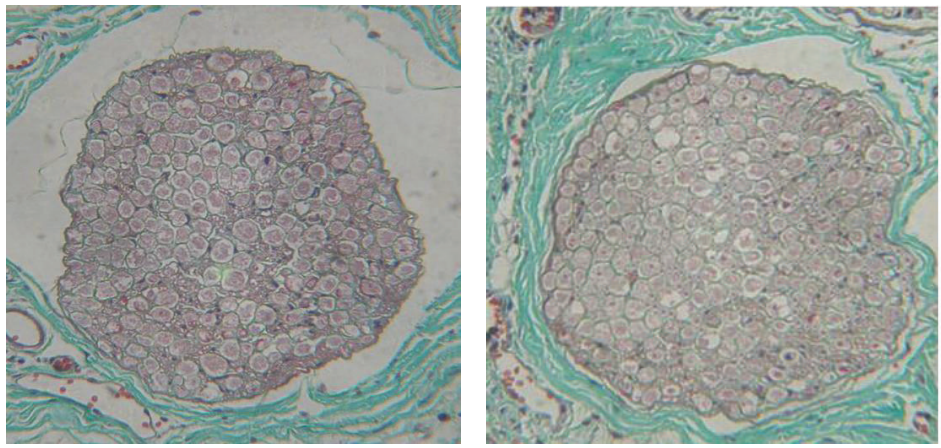

(a) (b)

Figure 1: The image of sections under light microscope after Masson staining at week 16 (Masson ×400) ((a) control group, (b) the experimental group).

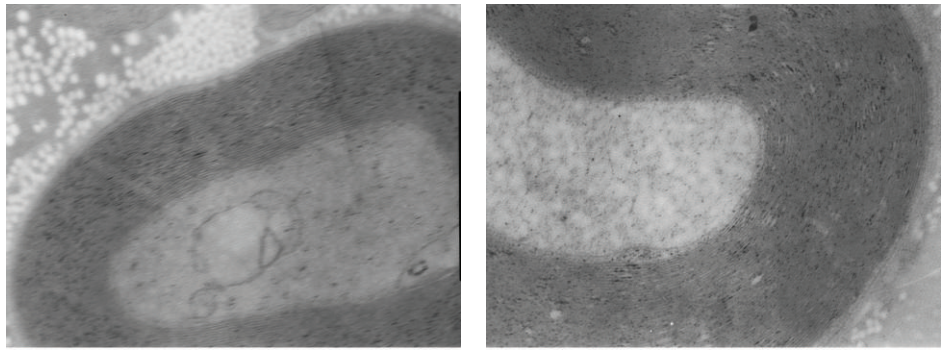

(a) (b)

Figure 2: The image of sections stained with uranyl aceate and lead citrate under transmission electron microscope after 16 weeks ECM ×25K ((a) the control group, (b) the experimental group).

which has effective promoting effects on vascular growth [25–27]. Sahota et al. found that at 1 day after the stent implanted with human microvascular endothelial cells was implanted in nude mouse, endothelial cells migrated in the stent. After 5 days, blood capillary-like conduit appeared. At week 1, microvessel appeared. At week 3, new microvessel was well connected to blood vessel of the host. These confirmed that vascular endothelial cells implanted in biomaterials could proliferate and differentiate into new vessels. Moreover, numerous studies also verified the important effect of vascular endothelial cells in vascularization of tissue engineered bone.

After peripheral nerve injury, local microenvironment suitable for nerve regeneration and nutrient substance needed by nerve regeneration are significant for nerve regeneration, and these are strongly associated with regional blood supply. Early vascularization of graft not only provides enough nutrient substance for Schwann cells and contributes to the growth of new axon but also reduces the production of collagen fiber *in vivo* and is convenient for new axon to traverse. In addition, early vascularization of nerve graft gathers macrophages derived from blood, is beneficial to rapidly clean the degenerated products of myelin sheath and axon after nerve injury, and provides a good channel for the growth of new proximal axon towards the distal end.

Recently, with the development of tissue engineering research, the studies concerning tissue engineered nerve for the repair of nerve defect have been paid great attention by more and more scholars [28–32]. Lots of studies addressed effects of chemically extracted acellular nerve-on-nerve regeneration and functional recovery, but revascularization strongly associated with this process has not been paid attention. Successful cell-based tissue engineering requires a rapid and thorough vascularization in order to ensure long-term implant survival and tissue integration [33, 34], while tissue engineered nerve cannot establish blood circulation in an early stage and restricts its further application in clinic [35, 36].

In the present study, Schwann cells of sciatic nerve of fetal rabbit and vascular endothelial cells of thoracic aorta of fetal rabbit were cocultured at a certain proportion in biodegradable fiber-reinforced 3D scaffolds with satisfactory mechanical properties *in vitro* to form prevascularized nerve complexes. Animal experiment results revealed that the recoveries of foot ulcer healing, nerve conduction velocity, nerve fiber number, and ultrastructure of myelin sheath and regenerating nerve were better in the experimental group than those in the control group. This study provides a new idea for finding a method to promote vascularization of tissue engineered nerve. Nevertheless, the growth of the two kinds of cells *in vivo* and the biocompatibility of vascular endothelial cells and the stent deserve further investigation. It remains poorly understood how to culture abundant Schwann cells and vascular endothelial cells and how the cells interact after implantation. New microvascular formation and precise structure in grafts require further studies.

5. Conclusion

The present study demonstrates that the fiber-reinforced 3D composites scaffolds cultured with Schwann cells and vascular endothelial cells can induce vascularized sciatic nerve formation. Prevascularized tissue engineered fiber-reinforced 3D scaffolds for the repair of sciatic nerve defects in rabbits can effectively promote the recovery of neurological function. The composites have satisfactory biocompatibility and are promising to be ideal nerve substitutes, which can promote the regeneration of vessel and nerve.

Conflict of Interests

The authors declare that they have no financial or personal relationship with any people or organization that may inappropriately influence their work; there is no professional or commercial interest of any kind in all the commercial identities mentioned in this paper.

Authors' Contribution

Hongyang Gao and Yang You contributed equally to this work.

Acknowledgment

The authors acknowledge the financial support from the Youth Science and Technology Project of Health Department of Hebei Province, no. 20100250.

References

[1] Y.-L. Lin, J.-C. Jen, S.-H. Hsu, and I.-M. Chiu, "Sciatic nerve repair by microgrooved nerve conduits made of chitosan-gold nanocomposites," *Surgical Neurology*, vol. 70, no. 1, pp. S9–S18, 2008.

[2] G. R. D. Evans, "Peripheral nerve injury: a review and approach to tissue engineered constructs," *Anatomical Record*, vol. 263, no. 4, pp. 396–404, 2001.

[3] M. G. Burnett and E. L. Zager, "Pathophysiology of peripheral nerve injury: a brief review," *Neurosurgical Focus*, vol. 16, no. 5, 2004.

[4] P. Scherman, M. Kanje, and L. B. Dahlin, "Bridging short nerve defects by direct repair under tension, nerve grafts or longitudinal sutures," *Restorative Neurology and Neuroscience*, vol. 22, no. 2, pp. 65–72, 2004.

[5] S. Zacchigna and M. Giacca, "Chapter 20 gene therapy perspectives for nerve repair," *International Review of Neurobiology*, vol. 87, pp. 381–392, 2009.

[6] S. R. Strasberg, S. E. Mackinnon, E. M. Genden et al., "Long-segment nerve allograft regeneration in the sheep model: experimental study and review of the literature," *Journal of Reconstructive Microsurgery*, vol. 12, no. 8, pp. 529–537, 1996.

[7] L. Dahlin, F. Johansson, C. Lindwall, and M. Kanje, "Chapter 28 future perspective in peripheral nerve reconstruction," *International Review of Neurobiology*, vol. 87, pp. 507–530, 2009.

[8] H. Xu, J. M. Holzwarth, Y. Yan et al., "Conductive PPY/PDLLA conduit for peripheral nerve regeneration," *Biomaterials*, vol. 35, no. 1, pp. 225–235, 2014.

[9] I. A. Ignatiadis, C. K. Yiannakopoulos, A. D. Barbitsioti et al., "Diverse types of epineural conduits for bridging short nerve defects. An experimental study in the rabbit," *Microsurgery*, vol. 27, no. 2, pp. 98–104, 2007.

[10] X. Wang, W. Hu, Y. Cao, J. Yao, J. Wu, and X. Gu, "Dog sciatic nerve regeneration across a 30-mm defect bridged by a chitosan/PGA artificial nerve graft," *Brain*, vol. 128, no. 8, pp. 1897–1910, 2005.

[11] K. Nakayama, K. Takakuda, Y. Koyama et al., "Enhancement of peripheral nerve regeneration using bioabsorbable polymer tubes packed with fibrin gel," *Artificial Organs*, vol. 31, no. 7, pp. 500–508, 2007.

[12] J. Cao, C. Sun, H. Zhao et al., "The use of laminin modified linear ordered collagen scaffolds loaded with laminin-binding ciliary neurotrophic factor for sciatic nerve regeneration in rats," *Biomaterials*, vol. 32, no. 16, pp. 3939–3948, 2011.

[13] H. S. Koh, T. Yong, W. E. Teo et al., "*In vivo* study of novel nanofibrous intra-luminal guidance channels to promote nerve regeneration," *Journal of Neural Engineering*, vol. 7, no. 4, Article ID 46003, 2010.

[14] X. Hu, J. Huang, Z. Ye et al., "A novel scaffold with longitudinally oriented microchannels promotes peripheral nerve regeneration," *Tissue Engineering A*, vol. 15, no. 11, pp. 3297–3308, 2009.

[15] E. O. Johnson, A. Charchanti, and P. N. Soucacos, "Nerve repair: experimental and clinical evaluation of neurotrophic factors in peripheral nerve regeneration," *Injury*, vol. 39, supplement 3, pp. S37–S42, 2008.

[16] X. M. Li, Y. B. Fan, and F. Watari, "Current investigations into carbon nanotubes for biomedical application," *Biomedical Materials*, vol. 5, no. 2, Article ID 022001, 2010.

[17] H. B. Zong, H. X. Zhao, Y. L. Zhao et al., "Nanoparticles carrying neurotrophin-3-modified Schwann cells promote repair of sciatic nerve defects," *Neural Regeneration Research*, vol. 8, no. 14, pp. 1262–1268, 2013.

[18] X. Li, H. Gao, M. Uo et al., "Maturation of osteoblast-like SaoS2 induced by carbon nanotubes," *Biomedical Materials*, vol. 4, no. 1, Article ID 015005, 2009.

[19] P. Xu, K. M. Rosen, K. Hedstrom et al., "Nerve injury induces glial cell line-derived neurotrophic factor (gdnf) expression in Schwann cells through purinergic signaling and the pkc-pkd pathway," *Glia*, vol. 61, no. 7, pp. 1029–1040, 2013.

[20] X. Li, Q. Feng, X. Liu, W. Dong, and F. Cui, "Collagen-based implants reinforced by chitin fibres in a goat shank bone defect model," *Biomaterials*, vol. 27, no. 9, pp. 1917–1923, 2006.

[21] X. M. Li, L. Wang, Y. B. Fan, Q. L. Feng, F.-Z. Cui, and F. Watari, "Nanostructured scaffolds for bone tissue engineering," *Journal of Biomedical Materials Research Part A*, vol. 101, no. 8, pp. 2424–2435, 2013.

[22] Z. Zhang, W. D. Ito, U. Hopfner et al., "The role of single cell derived vascular resident endothelial Progenitor cells in the enhancement of vascularization in scaffold-based skin regeneration," *Biomaterials*, vol. 32, no. 17, pp. 4109–4117, 2011.

[23] M. W. Laschke, A. Strohe, C. Scheuer et al., "*In vivo* biocompatibility and vascularization of biodegradable porous polyurethane scaffolds for tissue engineering," *Acta Biomaterialia*, vol. 5, no. 6, pp. 1991–2001, 2009.

[24] X. Li, H. Liu, X. Niu et al., "Osteogenic differentiation of human adipose-derived stem cells induced by osteoinductive calcium phosphate ceramics," *Journal of Biomedical Materials Research B*, vol. 97, no. 1, pp. 10–19, 2011.

[25] E. C. Novosel, C. Kleinhans, and P. J. Kluger, "Vascularization is the key challenge in tissue engineering," *Advanced Drug Delivery Reviews*, vol. 63, no. 4, pp. 300–311, 2011.

[26] L. Cao, J. Wang, J. Hou, W. Xing, and C. Liua, "Vascularization and bone regeneration in a critical sized defect using 2-*N*,6-*O*-sulfated chitosan nanoparticles incorporating BMP-2," *Biomaterials*, vol. 35, no. 2, pp. 684–698, 2014.

[27] X. Li, H. Gao, M. Uo et al., "Effect of carbon nanotubes on cellular functions *in vitro*," *Journal of Biomedical Materials Research A*, vol. 91, no. 1, pp. 132–139, 2009.

[28] L. Koepsell, T. Remund, J. Bao, D. Neufeld, H. Fong, and Y. Deng, "Tissue engineering of annulus fibrosus using electrospun fibrous scaffolds with aligned polycaprolactone fibers," *Journal of Biomedical Materials Research A*, vol. 99, no. 4, pp. 564–575, 2011.

[29] G. Wang, X. Hu, W. Lin, C. Dong, and H. Wu, "Electrospun PLGA–silk fibroin–collagen nanofibrous scaffolds for nerve tissue engineering," *In Vitro Cellular and Developmental Biology*, vol. 47, no. 3, pp. 234–240, 2011.

[30] X. Li, C. A. van Blitterswijk, Q. Feng, F. Cui, and F. Watari, "The effect of calcium phosphate microstructure on bone-related cells *in vitro*," *Biomaterials*, vol. 29, no. 23, pp. 3306–3316, 2008.

[31] Y. Wang, Z. Zhao, B. Zhao et al., "Biocompatibility evaluation of electrospun aligned poly (propylene carbonate) nanofibrous scaffolds with peripheral nerve tissues and cells *in vitro*," *Chinese Medical Journal*, vol. 124, no. 15, pp. 2361–2366, 2011.

[32] P. J. Johnson, P. Newton, D. A. Hunter, and S. E. MacKinnon, "Nerve endoneurial microstructure facilitates uniform distribution of regenerative fibers: a post hoc comparison of midgraft

nerve fiber densities," *Journal of Reconstructive Microsurgery*, vol. 27, no. 2, pp. 83–90, 2011.

[33] S. Ghanaati, R. E. Unger, M. J. Webber et al., "Scaffold vascularization *in vivo* driven by primary human osteoblasts in concert with host inflammatory cells," *Biomaterials*, vol. 32, no. 32, pp. 8150–8160, 2011.

[34] J. Rouwkema, N. C. Rivron, and C. A. van Blitterswijk, "Vascularization in tissue engineering," *Trends in Biotechnology*, vol. 26, no. 8, pp. 434–441, 2008.

[35] X. Li, H. Liu, X. Niu et al., "The use of carbon nanotubes to induce osteogenic differentiation of human adipose-derived MSCs *in vitro* and ectopic bone formation *in vivo*," *Biomaterials*, vol. 33, no. 19, pp. 4818–4827, 2012.

[36] Y.-G. Zhang, J.-H. Huang, X.-Y. Hu, Q.-S. Sheng, W. Zhao, and Z.-J. Luo, "Omentum-wrapped scaffold with longitudinally oriented micro-channels promotes axonal regeneration and motor functional recovery in rats," *PLoS ONE*, vol. 6, no. 12, Article ID e29184, 2011.

Hindawi Publishing Corporation
BioMed Research International
Volume 2013, Article ID 714103, 10 pages
http://dx.doi.org/10.1155/2013/714103

Review Article

The Application of Fiber-Reinforced Materials in Disc Repair

Bao-Qing Pei, Hui Li, Gang Zhu, De-Yu Li, Yu-Bo Fan, and Shu-Qin Wu

Key Laboratory for Biomechanics and Mechanobiology of Ministry of Education, School of Biological Science and Medical Engineering, Beihang University, Beijing 100191, China

Correspondence should be addressed to Bao-Qing Pei; pbq@buaa.edu.cn and Shu-Qin Wu; wushuqin@nuc.edu.cn

Received 16 October 2013; Accepted 18 November 2013

Academic Editor: Xiaoming Li

Copyright © 2013 Bao-Qing Pei et al. This is an open access article distributed under the Creative Commons Attribution License, which permits unrestricted use, distribution, and reproduction in any medium, provided the original work is properly cited.

The intervertebral disc degeneration and injury are the most common spinal diseases with tremendous financial and social implications. Regenerative therapies for disc repair are promising treatments. Fiber-reinforced materials (FRMs) are a kind of composites by embedding the fibers into the matrix materials. FRMs can maintain the original properties of the matrix and enhance the mechanical properties. By now, there are still some problems for disc repair such as the unsatisfied static strength and dynamic properties for disc implants. The application of FRMs may resolve these problems to some extent. In this review, six parts such as background of FRMs in tissue repair, the comparison of mechanical properties between natural disc and some typical FRMs, the repair standard and FRMs applications in disc repair, and the possible research directions for FRMs' in the future are stated.

1. Introduction

The intervertebral disc (IVD) is a heterogeneous, cartilaginous structure which contributes to the flexibility and load support in the spine. It consists of three parts: the nucleus pulposus (NP) in the center, the annulus fibrosus (AF) peripherally, and the cartilaginous endplates (CE) [1]. The fluid NP delivers loads to the AF in the form of swelling pressure while the multilayer and angle-ply AF wraps NP like a net bag guarded against the excessive expansion of NP (Figure 1). The direction of the fibers was angled varying from 40° to 70° to the vertical axis [1]. The intervertebral disc is in contact with the vertebral bodies through CE which is responsible for the exchange of substance through the microporous structure [2]. Anyone off normal of these three parts may cause the disc degeneration.

The spine disease which is related to the disc degeneration affects human health and normal life. The treatment and regeneration of the degenerated disc is one of the most urgent current clinical problems. There are complex mechanical and structures requirements for the disc repair. The fluid nature of the NP ensures the compressive loading applied to a disc to generate a tensile hoop stress (T) in the annulus (Figure 1) [3, 4]. Meanwhile, since the IVD joint possess 6-degree freedom of motion, AF needs to bear axial and radial compression and stretch as well [5]. According to the *in vivo* and *vitro* results, the interdiscal pressure under 300 N loading is approximately 1.3 MPa, the circumference stretch stress of the AF is 12.7 MPa [6], and the shear modulus is 25~110 KPa [7]. In this view, high mechanical properties and complex load bearing capacity are necessary for IVD repair materials.

Many methods for disc restoration are aimed at the reinforcement of disc mechanical properties, such as injection of the polymethylmethacrylate for the traditional intervertebral injury and fracture [8], the usage of biocompatible cage and metal internal fixations for bone fusion, and preventing the intervertebral collapse and failure restoration [9]. Some chemistry technologies such as doubly cross-linked microgels can make the strength enhanced by 3 to 5 times compared to original materials and dynamic properties similar to the health disc [10]. The fiber-reinforced technology is commonly used for increasing the mechanical properties of materials and some researchers are trying to use FRMs into the field of disc repair.

Many biocompatible and biodegradable fiber-reinforced polymers combined with matrix form new mechanical enhanced FRMs and have mature application in bone repair field. The calcium phosphate cement (CPC) reinforced with

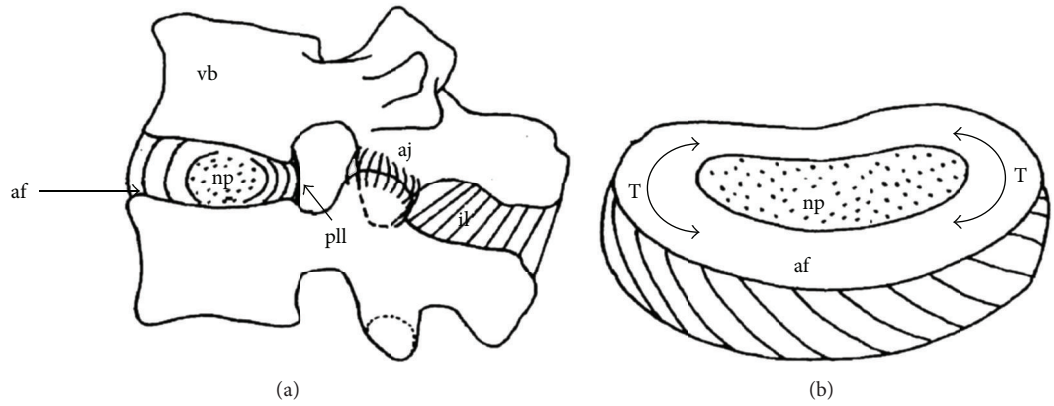

Figure 1: Schematic structure of the IVD and NP-AF interaction under compression [4]. vb: verterbral body; af: annulus fibrosus; np: nucleus pulposus; aj: apophyseal joint; pll: posterior longitudinal ligament; il: interspinous ligaments; T: tensile stress.

polycaprolactone polymer (PCL) fibers in different weight increased the modulus nearly twofold from 85 to 155 Mpa [16]. CPC power matrix addition to poly(coglycolide) (PLGA) fibers makes the compressive and bending strength close to the bone [17]. 15 wt% self-reinforced poly-L-lactide (PLLA) fiber coated with hydroxyapatite (HA) composite makes the original bending modulus increase from 8.3 Gpa to 9.7 Gpa [18]. Multi-fiber-reinforced CPC compound with the compressive strength from 0.9 to 69 Mpa [19] and the energy to fracture increase by 390X compared to pure CPC, with bending strength range from 1.2 to 60 Mpa. Chitosan fiber-reinforced composite which possesses well-rheological behavior [20] and biodegradability [21] repairs 40 mm goat shank bone defect successfully after 15 weeks, with the chitosan FRM group recovering to the same level BMD and bone mechanical strength to the intact group [22–26]. The porous three-dimensional poly(L-lactic acid) scaffold reinforced by the chitin fibers with link is an appropriate scaffold for tissue engineering [27]. As for the cell level, the material microstructure after fiber being reinforced is more suitable for cell adhesion and reproduction. Poly(3-caprolactone) (PCL)/b-tricalcium phosphate (TCP) nanofibre-reinforced hierarchical collagen scaffolds cell seeding efficiency increased from 55% for pure collagen scaffolds to 78% after fiber reinforced with tensile modulus increased by 7 times as well [28]. The carbon nanotube reinforced materials have a better ability to adsorb proteins and better cell attachment, proliferation, and differentiation than graphite [29], so they could also induced more bone formation [30]. Hydrogel is widely used for many soft tissues and is supposed to be the most promising disc repair materials [31]. However, pure hydrogel is proved to be insufficient for disc mechanical restoration [32]. Elastin fiber-reinforced hydrogel makes a better performance and can achieve cartilage-like properties [33]. The hyaluronic acid matrix reinforced by cellulose and elastin-like polypeptide fibers with adding collagen, hyaluronic acid, and chondroitin sulfate can obtain a better collision property [34–36]. Although these researches have not reached the stage of tissue fabrication or the *in vivo* and *vitro* experiments, the composites' properties got enhancement through the fiber-reinforced technology.

Scaffolds play fatal roles in both disc arthroplasty and whole disc replacement tissue regeneration [37–40]. The FRMs are becoming the ideal material for kinds of hard and soft tissue regeneration. A combination of matrix materials and different fibers arrays may help address the weakness of each component as a scaffold and supply easy grown mechanical and structure environments. So far, FRMs have been widely used in bone repair and bone tissue engineering [41]. A great many of fibers may be used for fiber-reinforced material fabrication such as polymer fibers such as polyethylene (PE), polylactic acid (PLA), and chitosan [42], biological ceramic fibers like bioglass, HA and calcium polyphosphate [43], and metallic fibers such as stainless steel and titanium [44].

This review addresses the mechanical requirement for disc tissue repair, compares the mechanical properties of FRM and disc tissue, and summarizes typical FRMs applications in disc tissue engineering. The adjustable mechanical properties by different spatial configuration of the fibers and their impacts on the cell growth have also been discussed preliminarily. Currently, the definition and summary about the FRMs for disc repair are not that much. The developments of FRMs in the field of disc tissue repair have very important practical applications and biomimetic meanings for the clinical spinal surgery.

2. Comparison of Mechanical Properties between Nature Disc and FRMs

2.1. The Mechanical Properties of Healthy Human Disc. The properties of the disc as a whole are determined by the mechanical behavior of the NP. NP is the most active element of the physiological hydrodynamical system of the intervertebral disc extradiscal space [56]. The most important characteristic of this system is the intradiscal pressure (IP) which depends on the external loads and the degree of hydration of the nucleus. The IP when being in latericumbent position is 0.3234 Mpa and 0.8428 Mpa when sitting. The standing IP is 60~80% sitting pressure. In young people aged from 20 to 30, the vertical stretch strength is about

Table 1: Compressive stiffness and modulus of healthy human discs.

Load (N)	Stiffness (N/mm)	Modulus (Mpa) [45]
490	392–490	16.366
490–1470	666.4–3479	8.624~26.166
1470–9800	1400–7791	9.604~21.364

0.196 Mpa, and the horizontal one is 0.294 Mpa. The vertical tensile strength of the outer layer AF is 15.68 Mpa and that of the inner layer is 6.664 Mpa. The horizontal outer layer is 7.84 Mpa and inner layer is 4.4 Mpa [45, 57]. The compressive stiffness is increased with loading while the modulus is not increased as significantly as the stiffness. The compressive stiffness and modulus are shown in Table 1. The *in vitro* human lumbar torsional stiffness is 2.0 Nm/deg [58], and the compressive stiffness is 2~14 KN [59]. The unconfined compressive elastic modulus of human disc is 5 kpa, and the Poisson ratio is 0.62, and relaxation rate is 65% [60]. The confined compressive elastic modulus is 0.14 Mpa, effective modulus is 1 Mpa, and permeability is $0.9E - 15$ m4/Ns [61]. The torsional shear modulus is from 7.4 to 19.8 Kpa; phase angle is between 23° and 30° [60]. The disc system is a typical MKC oscillatory system, with inherent frequency about 4~5 Hz [62].

The NP mechanical properties are related to the content of glycosaminoglycan (GAG) and water. The normal NP swelling pressure is about 0.138 ± 0.029 MPa; effective aggregate modulus is 1.01 ± 0.43 MPa [63]. The average vertical strain is 2~8% and radial strain is 1~4% of human lumbar AF under neutral compression [64]. Healthy NP compressive strain is −10%~+10% [65]. The elastic modulus is 3~6 Kpa [66]. The single axial compression of the AF has obvious compliance, but after the strain increased to 20%~40%, the stiffness grows spurt. The horizontal shear compliance is smaller than the vertical ones. When the strain loads over 60%, the AF fracture not happened, but irreversible deformation happened [67].

2.2. Mechanical Properties of FRMs. The mechanical properties of FRMs increase with the content of fibers mostly, but the low density indicates a desired reinforcing storage and loss modulus of nanofibers [49]. It is possible to control the porosity and porous size through fiber-reinforced method, and the critical length of the fibers could be calculated using empirical formula, and so does the compressive strength of the scaffold using the fiber length [68]. Higher density fibers may result in a morphological change of the gel structure where the occurrence of nanofibers disrupts the continuity of the gel network and overall weakening of the construct. Meanwhile, the fiber processing technique may bring in bubble; the more the fibers added, the more the bubbles taken in, and this may be an important factor of modulus weaken ing. Table 2 shows some FRMs for disc and disc-like joint and cartilage tissue engineering. The average compressive stiffness of the human lumbar when loaded by 577 ~ 2058 N was 1400 N/mm [69], while the biomimetic artificial IVD with fiber-reinforced annulus structure got a 2-fold stiffness of the normal disc [70]. Using 3D printed technique for the rat tissue engineered-total disc replacement (TE-TDR) with cell-seeded alginate and cell-seeded collage fibers was found a similar dynamic modulus (235±51 kPa) with the native disc (238 ± 68 kPa) [71].

These FRMs are characterized by the following features. (1) Properties tunableness: a wide range of properties could be obtained through adjustment of fiber scales, processing technology, and geometry space configuration. (2) Good viscoelastic properties: body tissues are viscoelastic materials to some extent. The IVD restoration needs more significant viscosity properties than other tissues and load bearing strength as well. (3) Different fibers and matrix mix and match increase material diversity: as for this point, some researchers suggested that the focus should be on the deep boost of several certain mature compounds instead of keep searching for different materials with a smattering of knowledge of each one such as only culture cells for only days.

The main structure of the FRMs is the fiber. A study reported the diameters of the individual collage fibrils which are the main structural components of the NP and found that the nanoscale (with a mean diameter of 92.1 ± 26.54 nm) of the collage fibrils had a mild linear correlation with the compressive modulus of the NP [72]. The human fibrous tissue (FT) was compared with annulus and nucleus in relaxation and dynamic properties [60]. The percent relaxation of the FT was 90% included both AF and NP (70%~80%). The storage modulus of the fibrous tissue was also larger than that of the AF and NP. The FT is not proved to be a substitute for native tissue within the disc space.

Many researches regarded the constitutive equation of FRMs under different loading as very important research fields for FRMs tissue engineering. The models included anisotropic viscoelastic behavior under finite deformation [73, 74] and large-strain deformation [75] of soft composites. The stress transfer in collagen fibrils reinforcing tissues was infected by the fibril slenderness significantly. A large slenderness value led to high stress in a fibril and it is beneficially provided since they do not exceed the fracture stress of collagen. Fibers with taper-type shape are better than fibers with uniform cylindrical shape in against fiber fracture [76].

2.3. FRMs and Cell Culture. The small porosity of some high densely arranged nanofiber-reinforced materials makes it difficult for cell permeating into the fiber bundles and leads to abnormal ECM environment, so the material restoration fails to recover a normal tissue mechanical and physical standard finally. In response to this issue, a new method called dynamic cell culture technique can enhance the permeability of the stem cell and the quality of the ECMs [77]. NP cell bears the hydrostatic pressure while the cells between AF and NP enduring the deformation stimulate mostly. The cell geometry is impacted by the micromechanical environment which is affected by the fiber-reinforced technique, and the adapt law of the cell development direction is the reduction of the strain load [78].

The cell growth situation is affected by the material scale. Nanoscaled fibers which can stimulated a variety of

Table 2: Typical FRM use in disc implants and some similar tissues.

Fibers	Matrix	Mechanical properties			Fiber scale	Processing	Repaired tissue	literature
		Breaking stress (Mpa)	Breaking strain (%)	Elastic modulus (Mpa)				
Elastin	Hydrogel	0.08~2.08	10.6~247	0.8~3.68	Mircon	3D syringe drops crossed "log-piles"	Cartilage	Agrawal et al., 2013 [33]
PCL	Gelatin Dry	5~25		20~120	Nano	Electrospun	AF	Beachley and Wen, 2009 [46]
	Wet	0.1~0.9		1~10				
Collagen	Elastin-like	1.85~4.08	23~314	5.3~33.1	Mircon	Winding	Abdominal wall	Caves et al., 2011 [47]
Polydioxanone (PDO)	PLA					Electrospun	AF	Cont et al., 2013 [48]
PCL	Hydrogel	Storage modulus 0.03 Mpa	Loss modulus 0.006 Mpa		Nano	Electrospun	NP	Thorvaldsson et al., 2012 [49]
N-vinyl-2-pyrrol-idone (NFC)	Hydrogel	Storage modulus 0.14 Mpa	Loss modulus 0.019 Mpa	0.02~8		Curing	NP	Borges et al., 2010 [50]

interactions at the cellular level may promote greater amounts of specific protein interactions and more efficiently new bone formation [79]. The microstructured calcium phosphate materials concentrate more proteins and also are proved to induce more bone formation. The biocompatibility and bioactivity are also promoted by the nanoscaled materials [80]. The carbon nanotubes can induce cells in soft tissues to form inductive bone by concentrating more proteins including bone-inducing proteins [81, 82], which is also the contribution of the nanoscale structure. Though the nanoscale materials have stimulative effects on cell growth and induced differentiation, the biocompatibility and toxicity still need cautious experiments before *in vivo* attempt [83].

3. The Disc Restoration Objects

The intervertebral disc (IVD) is the mechanical and structural unit of the spine, so the functional restoration is very important and needs some standard indicators for evaluation. There are many mechanical characters of the IVD including nonlinearity, viscoelasticity, anisotropy, heterogeneity, and permeability. Finding limited crucial and reasonable properties is more meaningful. One of the clinical golden standards for IVD examination is the IVD height from MRI and X-ray plain film [84]. As for the experimental purpose, the neutral zone stiffness and the relative length during axial low load can estimate the recovery condition from needle damage and the endplate injury. As for large and severe AF defects and IVD degeneration, the torsion strength and ROM can test the restoration effects [84]. The dynamic modulus and stress relaxation and creep test make a judgment of the viscoelasticity behavior of the repaired disc [53]. For the implantable tissue replacement methods, shear strength of the interface is very crucial indicator of tissue fusion [85].

The synthesis and maintenance of extracellular matrix (ECM) are necessary for tissue activity and cell reproduction. The collage and GAGs are main substances for disc ECM [86]. Immunohistochemical methods can make qualitative and quantitative measurement for these two ingredients. The DNA transfer and mRNA expression can reflect the activity and propagation of newborn cells [87]. Though the cell-based therapy methods are more mature than whole IVD transplantation, the inadequacy for severe degeneration and disc prolapse stage limited its development and more and more focuses are on the latter. By now, whole IVD tissue engineering method remains under the exploration and experimentation step. Generally, it needs stages from a material to an artificial tissue use *in vivo*. The duration selections for the stages are shown in Table 3. At present, the time span for each period has not obtained a unified time yet.

4. The Application of FRM in Disc Arthroplasty

As was mentioned in the front part, some materials such as coralline and hydroxyapatite could induce osteogenesis. Spinal fusion is widely used in clinical for intervertebral decompression which aims at complete bony fusion. So, these materials have good performance for intervertebral fusion, especially after being reinforced by fibers such as PLA, PEG, or carbon fibers [88–90]. Though fusion is not the ideal choice for disc repair, FRMs used for fusion materials are also a research hotspot at present.

Table 3: Time span for experimental validation.

Experimental objects	Plant mode	Culture *ex vivo* (week)	Culture *in vivo* (month)
Canine model [51]	Cell-based		3, 6, 9, 12
Polymer scaffolds [52]	Explant	4, 8, 12	
Rodent model [53]	Implant		6
Collagen-gel compound [54]	Explant	3 days	
Alginate composite [55]	Explant	4	

(a) (b) (c)

Figure 2: The parts and the whole of the disc prosthesis. (a) Two sides of HAPEX endplates, (b) composite hydrogel for IVD substitute, and (c) total IVD substitute prototype [11].

The materials for disc replacement prosthesis need to possess different mechanical properties and composite structures. Flexibility, toughness, and high strength are basic characteristics of the soft biological tissues. For this reason, by employing materials with a single structural arrangement, it is not possible to combine all of these features. So, the structure of natural disc has been reproduced by adopting a biomimetic approach. This led to the development of a fiber-reinforced hydrogel able to match the performances of the natural disc and those of the surrounding tissues [91].

Disc arthroplasty is a kind of disc therapy which uses disc prosthesis (DP) with no biological activities for disc replacement and functional disc repair. The metallic and high polymer-core DP incurs DP sinking and wear and also ADD (adjacent disc degeneration) because of the high stiffness of the DP materials. The ideal artificial disc should be biomimetic which means that the mechanical properties, structure constitution and the motion function are similar with the nature disc tissue. Since, 1990s researchers have begun to use polyethylene and polyurethane fiber-reinforced silicon elastomers to make disc spacers. The artificial disc obtained the same compressive and torsional properties through adjusting the fiber direction, numbers of fiber layers, and the sequence of reinforcement [92]. The compressive modulus increased with the fiber angle and fiber content positively [93].

Hydrogel is always used for disc tissue engineering materials for its close properties to IVD tissue. Using fibers to reinforce hydrogel makes the composite with better stiffness and strength and maintenance of original properties. After fiber have added, the water absorption rate decreased for the new FRMs, is 30 wt% fibers addition with only 25% water absorption [93]. This rate is the same as the collage in disc, and the FRM with 30 wt% fibers could achieve suitable mechanical properties demanded by the normal IVD.

Gloria et al. [11] developed a new disc prosthesis using poly(2-hydroxyethyl methacrylate)/poly(methyl methacrylate) (PHEMA/PMMA) (80/20 w/w) semi-interpenetrating polymer network (s-IPN) composite hydrogel reinforced with poly(ethylene terephthalate) (PET) fibers as annulus/nucleus substitute and two hydroxyapatite-reinforced polyethylene composites (HAPEXTM) as endplates as was shown in Figure 2. This FRMs' disc performed enough static properties compared to normal disc, with maximum static compressive stiffness 4030 ± 612 N/mm, torsional rigidity 2.8 ± 0.3 Nm/deg, and shear stiffness 205 ± 22.1 N/mm. The ten million times fatigue test indicated that no damage or wear happened during the test, which is much better than some products in the markets. Meanwhile, the hydrogel matrix FRMs' disc has the similar dynamic and viscoelastic properties for the healthy disc to the other prosthesis.

5. The Application of FRM in Disc Tissue Engineering

It is more and more prevalent for disc restoration using tissue engineering method. The cell-based method includes two main directions which are the cell transplantation and the bioactive tissue transplantation. The bioactive tissue material used for disc repair is a research focus at present. The microstructure of the FRMs [94] is proved to promote cell adhesion and growth by supporting a 3D growing space [95]. Some studies have used FRMs for disc repair and various fiber features may lead to different repair effects.

The main cells used for disc regeneration are NP cell, AF cell, and stem cells. The NP cells and AF cells are like the chondrocyte and fibroblast, respectively, in both structure and function. These two kinds of cells are always used for testing materials bioactivity. Some biocompatibility (BC) matrixes after reinforced by the biodegradable nanofibers may improve the brittleness of single fibers and the fiber density become less dense after reinforcing the matrix, making cells easier grow into the fibers. The fibroblasts were cultured in single array and square crossing fibers in FRMs, respectively, and were found to grow along the fibers as a line

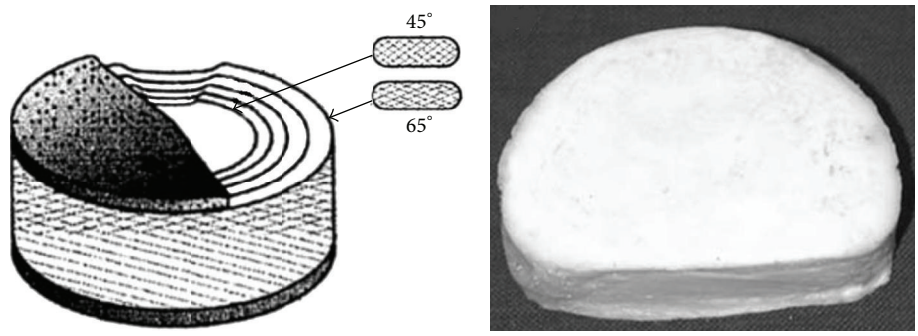

(a) (b)

Figure 3: (a) A schematic representation of the fiber-reinforced disc substitute with hydroxyapatite reinforcing hydrogel endplates, (b) The total intervertebral disc substitute prototype [12].

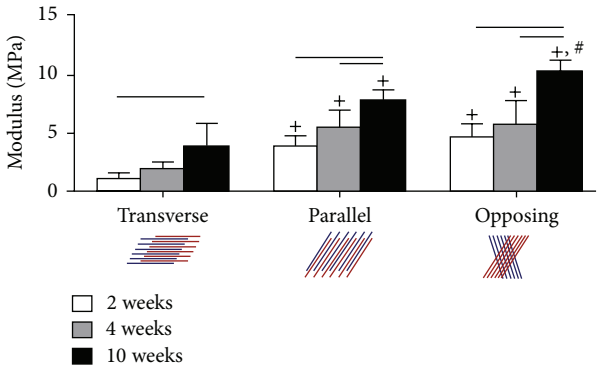

Figure 4: Three type of fiber organization between layers and the shear modulus when loaded tensile [13].

in the single array group and distribute in the meshes in the crossing one. The nanoscale FRMs process abilities to induce cell grow directions [96].

The mechanical strength of the composite may be enhanced after fiber being reinforced. We could obtain certain properties through increasing fiber content and changing fiber angles. PET fibers' angle changeing from 45° to 60° (shown in Figure 3) (angle to the load) which were added into hydrogel makes compressive modulus (CM) increased by 2~3 times. After changing volume fraction of PCL fibers from 0% to 30%, CM increases by 15 times [12]. PGA (polyglycolic acid) is reinforced by PLA fibers; CM increased with volume of PLA fibers linearly, which change by 0%~68% CM increased by 20 times [97]. 3%~17% volume change of elastic fibers was reinforced by collage fibers; the stretch modulus increased by 1 time with the same fiber angles while the angle change for 15 not significant changed the stretch modulus.

Researchers used PCL (polycaprolactone) nanofiber-reinforced hydrogel for NP tissue engineering. The dynamic properties of the materials are not increased with fiber density; on the contrary lower density obtained a closer storage and loss modulus to the real disc. We may draw a conclusion that fiber content got a bigger weighting factor than the fiber angles on the impact of mechanical properties. Change angles may adjust FRMs in a small range.

The annulus fibrosus is a natural fiber-reinforced structured tissue. Some researches focus on the organization of collagen fibers into planes of alternating alignment and found that it played an important role in annulus fibrosus tissue function. By using MSC-seeded nanofibrous scaffolds and applying the constitutive model to uniaxial tensile stress-strain data for bilayers with three different fiber orientations, they found that fiber orientation of adjacent layers with an opposing style got the biggest strength against the shear between layers under tensile load as shown in Figure 4 [13].

6. Conclusion and Perspectives

Current therapies for disc degeneration and spinal disease mainly focus on the relieving pains instantly instead of functional and physiological repair on the long run. Tissue engineering provides new treatment strategy for disc repair. The application of fiber-reinforced materials in tissue repair has a wide range of use and mature background, considering the excellent mechanical properties, and will make a new direction for disc restoration.

FRMs are on the developing stage for disc repair; some problems and research fields such as the choice of fibers, the interaction of fibers-matrix, and also the processing technology effects for properties coordination deserve more deeply discussion. Meanwhile, the mechanisms of FRMs for cell growth and propagation are still not known yet.

MSC differentiation *in vivo* technique is widely studied for tissue regeneration. Recent research shows that the MSCs' function is related to the substrate stiffness which could be adjusted by fiber-reinforced methods [98, 99]. As the disc cell lives in hypoxia, it has been proved that MSC differentiation shows better cell survival rate and activity under low oxygen environment [100]. By controlling technology and fiber density, FRMs could obtain nanoscale 3D cell growth space and fulfill the oxygen concentration control.

The cartilage endplates of the disc have very important structure and many disc diseases originate form endplate degeneration. As for the special position, the junction of

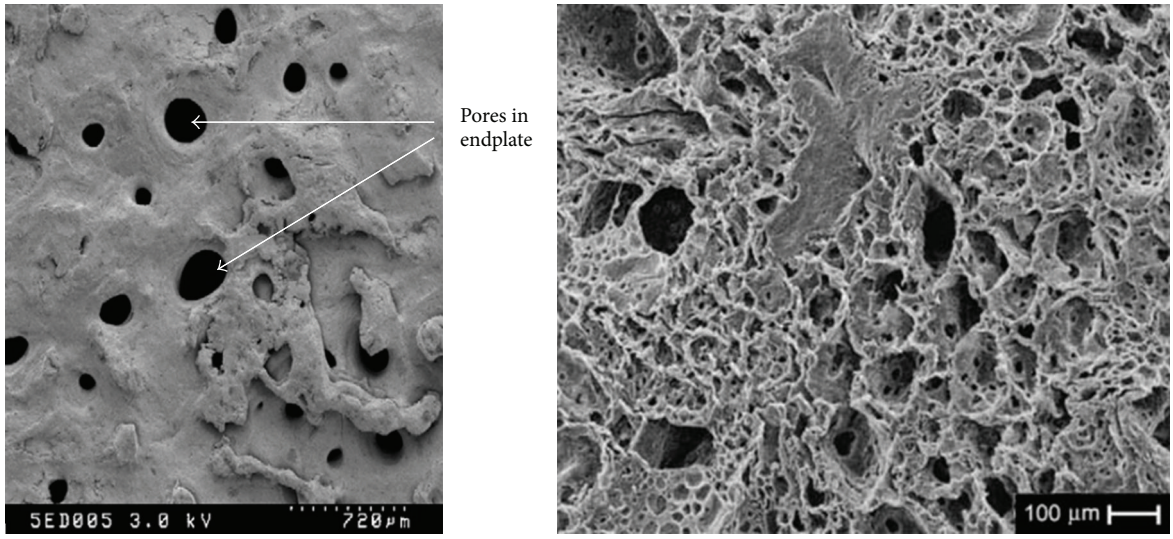

(a) (b)

Figure 5: The similar scale of the pores in endplate and pores in FRM composite. (a) REM image of a vertebral endplate with 720 μm scale plate [14] and (b) SEM analysis of FRM scaffolds with a 100 μm scale plate [15].

the vertebra, and disc tissue, the endplates are responsible for material exchange. The pores in the endplate (shown in Figure 5(a)) make it possible for mass metabolism between the inside and outside [14]. So the repair of this structure needs not only mechanical function but also diffusion and interface fusion properties. FRMs have a better bone fusion ability and can show better interface strength. At the same time, the microporous (shown in Figure 5(b)) formed by the embedded fibers may ensure the diffusion function [15]. Also, the endplates' tissue replacement needs two different properties in one piece of materials. FRMs' coordinability properties make this possible for a functional endplate.

Acknowledgment

This work was supported by the National Natural Science Foundation of China (11372029).

References

[1] A. I. Kapandji, *The Physiology of the Joints: The Spinal Column Pelvic Girdle and Head*, 6 edition, 2011.

[2] M. A. Adams, P. Dolan, and D. S. McNally, "The internal mechanical functioning of intervertebral discs and articular cartilage, and its relevance to matrix biology," *Matrix Biology*, vol. 28, no. 7, pp. 384–389, 2009.

[3] C. C. Guterl, E. Y. See, S. B. Blanquer et al., "Challenges and strategies in the repair of ruptured annulus fibrosus," *European Cells and Materials*, vol. 25, pp. 1–21, 2013.

[4] M. A. Adams and P. Dolan, "Spine biomechanics," *Journal of Biomechanics*, vol. 38, no. 10, pp. 1972–1983, 2005.

[5] M. A. Adams, D. S. McNally, and P. Dolan, "'Stress' distributions inside intervertebral discs: the effects of age and degeneration," *Journal of Bone and Joint Surgery B*, vol. 78, no. 6, pp. 965–972, 1996.

[6] E. R. Acaroglu, J. C. Iatridis, L. A. Setton, R. J. Foster, V. C. Mow, and M. Weidenbaum, "Degeneration and aging affect the tensile behavior of human lumbar anulus fibrosus," *Spine*, vol. 20, no. 24, pp. 2690–2701, 1995.

[7] J. C. Iatridis, S. Kumar, R. J. Foster, M. Weidenbaum, and V. C. Mow, "Shear mechanical properties of human lumbar annulus fibrosus," *Journal of Orthopaedic Research*, vol. 17, no. 5, pp. 732–737, 1999.

[8] D. C. Wilson, R. J. Connolly, Q. Zhu et al., "An ex vivo biomechanical comparison of a novel vertebral compression fracture treatment system to kyphoplasty," *Clinical Biomechanics*, vol. 27, no. 4, pp. 346–353, 2012.

[9] R. Lindsay, S. L. Silverman, C. Cooper et al., "Risk of new vertebral fracture in the year following a fracture," *Journal of the American Medical Association*, vol. 285, no. 3, pp. 320–323, 2001.

[10] A. H. Milani, A. J. Freemont, J. A. Hoyland, D. J. Adlam, and B. R. Saunders, "Injectable doubly cross-linked microgels for improving the mechanical properties of degenerated intervertebral discs," *Biomacromolecules*, vol. 13, no. 9, pp. 2793–2801, 2012.

[11] A. Gloria, R. De Santis, L. Ambrosio, F. Causa, and K. E. Tanner, "A multi-component fiber-reinforced PHEMA-based hydrogel/HAPEXTM device for customized intervertebral disc prosthesis," *Journal of Biomaterials Applications*, vol. 25, no. 8, pp. 795–810, 2011.

[12] A. Gloria, F. Causa, R. de Santis, P. A. Netti, and L. Ambrosio, "Dynamic-mechanical properties of a novel composite intervertebral disc prosthesis," *Journal of Materials Science*, vol. 18, no. 11, pp. 2159–2165, 2007.

[13] N. L. Nerurkar, R. L. S. Mauck, and D. M. Elliott, "Modeling interlamellar interactions in angle-ply biologic laminates for annulus fibrosus tissue engineering," *Biomechanics and Modeling in Mechanobiology*, vol. 10, no. 6, pp. 973–984, 2011.

[14] G. Huber, M. M. Morlock, and K. Ito, "Consistent hydration of intervertebral discs during in vitro testing," *Medical Engineering and Physics*, vol. 29, no. 7, pp. 808–813, 2007.

[15] V. Guarino, F. Causa, P. Taddei et al., "Polylactic acid fibre-reinforced polycaprolactone scaffolds for bone tissue engineering," *Biomaterials*, vol. 29, no. 27, pp. 3662–3670, 2008.

[16] L. H. Leung, A. DiRosa, and H. E. Naguib, "Physical and mechanical properties of poly(e-caprolactone) hydroxyapatite composites for bone tissue engineering applications," in *Proceedings of the ASME International Mechanical Engineering Congress and Exposition (IMECE '09)*, pp. 17–23, New York, NY, USA, November 2009.

[17] L. A. Vasconcellos and L. A. dos Santos, "Calcium phosphate cement scaffolds with PLGA fibers," *Materials Science and Engineering C*, vol. 33, no. 3, pp. 1032–1040, 2013.

[18] L. F. Charles, E. R. Kramer, M. T. Shaw, J. R. Olson, and M. Wei, "Self-reinforced composites of hydroxyapatite-coated PLLA fibers: fabrication and mechanical characterization," *Journal of the Mechanical Behavior of Biomedical Materials*, vol. 17, pp. 269–277, 2013.

[19] R. Kruger and J. Groll, "Fiber reinforced calcium phosphate cements: on the way to degradable load bearing bone substitutes?" *Biomaterials*, vol. 33, no. 25, pp. 5887–5900, 2012.

[20] X. M. Li and Q. L. Feng, "Dynamic rheological behaviors of the bone scaffold reinforced by chitin fibres," *Materials Science Forum*, vol. 475-479, pp. 2387–2390, 2005.

[21] X. Li, Q. Feng, and F. Cui, "In vitro degradation of porous nano-hydroxyapatite/collagen/PLLA scaffold reinforced by chitin fibres," *Materials Science and Engineering C*, vol. 26, no. 4, pp. 716–720, 2006.

[22] X. Li, Y. Yang, Y. Fan, Q. Feng, F. Z. Cui, and F. Watari, "Biocomposites reinforced by fibers or tubes as scaffolds for tissue engineering or regenerative medicine," *Journal of Biomedical Materials Research A*, 2013.

[23] X. Li, Q. Feng, X. Liu, W. Dong, and F. Cui, "Collagen-based implants reinforced by chitin fibres in a goat shank bone defect model," *Biomaterials*, vol. 27, no. 9, pp. 1917–1923, 2006.

[24] X. Liu, X. Li, Y. Fan et al., "Repairing goat tibia segmental bone defect using scaffold cultured with mesenchymal stem cells," *Journal of Biomedical Materials Research B*, vol. 94, no. 1, pp. 44–52, 2010.

[25] X. Li, X. Liu, G. Zhang et al., "Repairing 25 mm bone defect using fibres reinforced scaffolds as well as autograft bone," *Bone*, vol. 43, Supplement 1, S94 pages, 2008.

[26] X. Niu, Y. Fan, X. Liu et al., "Repair of bone defect in femoral condyle using microencapsulated chitosan, nanohydroxyapatite/collagen and poly(l-lactide)-based microsphere-scaffold delivery system," *Artificial Organs*, vol. 35, no. 7, pp. E119–E128, 2011.

[27] X. Li, X. Liu, W. Dong et al., "In vitro evaluation of porous poly(L-lactic acid) scaffold reinforced by chitin fibers," *Journal of Biomedical Materials Research B*, vol. 90, no. 2, pp. 503–509, 2009.

[28] Y. B. Kim and G. Kim, "Rapid-prototyped collagen scaffolds reinforced with PCL/beta-TCP nanofibres to obtain high cell seeding efficiency and enhanced mechanical properties for bone tissue regeneration," *Journal of Materials Chemistry*, vol. 22, no. 33, pp. 16880–16889, 2012.

[29] X. Li, H. Gao, M. Uo et al., "Effect of carbon nanotubes on cellular functions in vitro," *Journal of Biomedical Materials Research A*, vol. 91, no. 1, pp. 132–139, 2009.

[30] X. Li, H. Gao, M. Uo et al., "Maturation of osteoblast-like $SaoS_2$ induced by carbon nanotubes," *Biomedical Materials*, vol. 4, no. 1, Article ID 015005, 2009.

[31] S. C. W. Chan and B. Gantenbein-Ritter, "Intervertebral disc regeneration or repair with biomaterials and stem cell therapy: feasible or fiction?" *Swiss Medical Weekly*, vol. 142, Article ID w13598, 2012.

[32] S. Reitmaier, U. Wolfram, A. Ignatius et al., "Hydrogels for nucleus replacement: facing the biomechanical challenge," *Journal of the Mechanical Behavior of Biomedical Materials*, vol. 14, pp. 67–77, 2012.

[33] A. Agrawal, N. Rahbar, and P. D. Calvert, "Strong fiber-reinforced hydrogel," *Acta Biomaterialia*, vol. 9, no. 2, pp. 5313–5318, 2013.

[34] A. T. Reza and S. B. Nicoll, "Characterization of novel photocrosslinked carboxymethylcellulose hydrogels for encapsulation of nucleus pulposus cells," *Acta Biomaterialia*, vol. 6, no. 1, pp. 179–186, 2010.

[35] E. C. Collin, S. Grad, D. I. Zeugolis et al., "An injectable vehicle for nucleus pulposus cell-based therapy," *Biomaterials*, vol. 32, no. 11, pp. 2862–2870, 2011.

[36] B. Huang, C.-Q. Li, Y. Zhou, G. Luo, and C.-Z. Zhang, "Collagen II/hyaluronan/chondroitin-6-sulfate tri-copolymer scaffold for nucleus pulposus tissue engineering," *Journal of Biomedical Materials Research B*, vol. 92, no. 2, pp. 322–331, 2010.

[37] A. D. Diwan, H. K. Parvataneni, S. N. Khan, H. S. Sandhu, F. P. Girardi, and F. P. Cammisa Jr., "Current concepts in intervertebral disk restoration," *Orthopedic Clinics of North America*, vol. 31, no. 3, pp. 453–464, 2000.

[38] G. Lewis, "Nucleus pulposus replacement and regeneration/repair technologies: present status and future prospects," *Journal of Biomedical Materials Research B*, vol. 100, no. 6, pp. 1702–1720, 2012.

[39] B. R. Whatley and X. Wen, "Intervertebral disc (IVD): structure, degeneration, repair and regeneration," *Materials Science and Engineering C*, vol. 32, no. 2, pp. 61–77, 2012.

[40] W. Fu and Z. Xiang, "Regeneration strategies of intervertebral disc," *Chinese Journal of Reparative and Reconstructive Surgery*, vol. 27, no. 2, pp. 227–232, 2013.

[41] R. Kruger and J. Groll, "Fiber reinforced calcium phosphate-cements: on the way to degradable load bearing bone substitutes?" *Biomaterials*, vol. 33, no. 25, pp. 5887–5900, 2012.

[42] D. T.-J. Barone, J.-M. Raquez, and P. Dubois, "Bone-guided regeneration: from inert biomaterials to bioactive polymer (nano)composites," *Polymers for Advanced Technologies*, vol. 22, no. 5, pp. 463–475, 2011.

[43] T. Eliades, "Orthodontic materials research and applications. Part 2: current status and projected future developments in materials and biocompatibility," *The American Journal of Orthodontics and Dentofacial Orthopedics*, vol. 131, no. 2, pp. 253–262, 2007.

[44] A. Parashar and P. Mertiny, "Adhesively bonded composite tubular joints: review," *International Journal of Adhesion and Adhesives*, vol. 38, pp. 58–68, 2012.

[45] K. G. Bomshtein, V. I. Danilov, and V. N. Pravetskii, "Statics and dynamics of intervertebral discs," *Mechanics of Composite Materials*, vol. 15, no. 4, pp. 419–423, 1980.

[46] V. Beachley and X. Wen, "Fabrication of nanofiber reinforced protein structures for tissue engineering," *Materials Science and Engineering C*, vol. 29, no. 8, pp. 2448–2453, 2009.

[47] J. M. Caves, W. Cui, J. Wen, V. A. Kumar, C. A. Haller, and E. L. Chaikof, "Elastin-like protein matrix reinforced with collagen microfibers for soft tissue repair," *Biomaterials*, vol. 32, no. 23, pp. 5371–5379, 2011.

[48] L. Cont, D. Grant, C. Scotchford, M. Todea, and C. Popa, "Composite PLA scaffolds reinforced with PDO fibers for tissue engineering," *Journal of Biomaterials Applications*, vol. 27, no. 6, pp. 707–716, 2013.

[49] A. Thorvaldsson, J. Silva-Correia, J. M. Oliveira et al., "Development of nanofiber-reinforced hydrogel scaffolds for nucleus pulposus regeneration by a combination of electrospinning and spraying technique," *Journal of Applied Polymer Science*, vol. 128, no. 2, pp. 1158–1163, 2013.

[50] A. C. Borges, P.-E. Bourban, D. P. Pioletti, and J.-A. E. Månson, "Curing kinetics and mechanical properties of a composite hydrogel for the replacement of the nucleus pulposus," *Composites Science and Technology*, vol. 70, no. 13, pp. 1847–1853, 2010.

[51] T. Ganey, J. Libera, V. Moos et al., "Disc chondrocyte transplantation in a Canine model: a treatment for degenerated or damaged intervertebral disc," *Spine*, vol. 28, no. 23, pp. 2609–2620, 2003.

[52] J. M. Moran, D. Pazzano, and L. J. Bonassar, "Characterization of polylactic acid-polyglycolic acid composites for cartilage tissue engineering," *Tissue Engineering*, vol. 9, no. 1, pp. 63–70, 2003.

[53] R. D. Bowles, H. H. Gebhard, R. Härtl, and L. J. Bonassar, "Tissue-engineered intervertebral discs produce new matrix, maintain disc height, and restore biomechanical function to the rodent spine," *Proceedings of the National Academy of Sciences of the United States of America*, vol. 108, no. 32, pp. 13106–13111, 2011.

[54] R. D. Bowles, R. M. Williams, W. R. Zipfel, and L. J. Bonassar, "Self-assembly of aligned tissue-engineered annulus fibrosus and intervertebral disc composite via collagen gel contraction," *Tissue Engineering A*, vol. 16, no. 4, pp. 1339–1348, 2010.

[55] J. L. Bron, L. A. Vonk, T. H. Smit, and G. H. Koenderink, "Engineering alginate for intervertebral disc repair," *Journal of the Mechanical Behavior of Biomedical Materials*, vol. 4, no. 7, pp. 1196–1205, 2011.

[56] I. Kramer, "Biomechanical changes in the lumbar section of movements," *Die Wirbelsaule in Forschung und Praxis*, vol. 58, p. 109, 1973.

[57] T. Steffen, H. G. Baramki, R. Rubin, J. Antoniou, and M. Aebi, "Lumbar intradiscal pressure measured in the anterior and posterolateral annular regions during asymmetrical loading," *Clinical Biomechanics*, vol. 13, no. 7, pp. 495–505, 1998.

[58] A. Bisschop, J. H. van Dieën, I. Kingma et al., "Torsion biomechanics of the spine following lumbar laminectomy: a human cadaver study," *European Spine Journal*, vol. 22, no. 8, pp. 1785–1793, 2013.

[59] E. Karadogan and R. L. Williams, "Three-dimensional static modeling of the Lumbar spine," *Transactions of the ASME-K-Journal of Biomechanical Engineering*, vol. 134, no. 8, Article ID 084504, 2012.

[60] A. L. Freeman, G. R. Buttermann, B. P. Beaubien, and W. E. Rochefort, "Compressive properties of fibrous repair tissue compared to nucleus and annulus," *Journal of Biomechanics*, vol. 46, no. 10, pp. 1714–1721, 2013.

[61] Y. Schroeder, D. M. Elliott, W. Wilson, F. P. T. Baaijens, and J. M. Huyghe, "Experimental and model determination of human intervertebral disc osmoviscoelasticity," *Journal of Orthopaedic Research*, vol. 26, no. 8, pp. 1141–1146, 2008.

[62] W. D. Merryman, K. Loveless, and M. Kasra, "Disc nucleus cellular response to dynamic pressures at critical frequencies: a pig model," in *Proceedings of the ASME International Mechanical Engineering Congress*, pp. 261–262, New York, NY, USA, November 2003.

[63] W. Johannessen and D. M. Elliott, "Effects of degeneration on the biphasic material properties of human nucleus pulposus in confined compression," *Spine*, vol. 30, no. 24, pp. E724–E729, 2005.

[64] G. D. O'Connell, E. J. Vresilovic, and D. M. Elliott, "Human intervertebral disc internal strain in compression: the effect of disc region, loading position, and degeneration," *Journal of Orthopaedic Research*, vol. 29, no. 4, pp. 547–555, 2011.

[65] A. Tsantrizos, K. Ito, M. Aebi, and T. Steffen, "Internal strains in healthy and degenerated lumbar intervertebral discs," *Spine*, vol. 30, no. 19, pp. 2129–2137, 2005.

[66] J. M. Cloyd, N. R. Malhotra, L. Weng, W. Chen, R. L. Mauck, and D. M. Elliott, "Material properties in unconfined compression of human nucleus pulposus, injectable hyaluronic acid-based hydrogels and tissue engineering scaffolds," *European Spine Journal*, vol. 16, no. 11, pp. 1892–1898, 2007.

[67] T. P. Driscoll, R. H. Nakasone, S. E. Szczesny, D. M. Elliott, and R. L. Mauck, "Biaxial mechanics and inter-lamellar shearing of stem-cell seeded electrospun angle-ply laminates for annulus fibrosus tissue engineering," *Journal of Orthopaedic Research*, vol. 31, no. 6, pp. 864–870, 2013.

[68] X. Li, Q. Feng, Y. Jiao, and F. Cui, "Collagen-based scaffolds reinforced by chitosan fibres for bone tissue engineering," *Polymer International*, vol. 54, no. 7, pp. 1034–1040, 2005.

[69] A. Joshi, S. Mehta, E. Vresilovic, A. Karduna, and M. Marcolongo, "Nucleus implant parameters significantly change the compressive stiffness of the human lumbar intervertebral disc," *Journal of Biomechanical Engineering*, vol. 127, no. 3, pp. 536–540, 2005.

[70] P. R. van den Broek, J. M. Huyghe, and K. Ito, "Biomechanical behavior of a biomimetic artificial intervertebral disc," *Spine*, vol. 37, no. 6, pp. E367–E373, 2012.

[71] R. D. Bowles, H. H. Gebhard, R. Härtl, and L. J. Bonassar, "Tissue-engineered intervertebral discs produce new matrix, maintain disc height, and restore biomechanical function to the rodent spine," *Proceedings of the National Academy of Sciences of the United States of America*, vol. 108, no. 32, pp. 13106–13111, 2011.

[72] D. M. K. Aladin, K. M. C. Cheung, A. H. W. Ngan et al., "Nanostructure of collagen fibrils in human nucleus pulposus and its correlation with macroscale tissue mechanics," *Journal of Orthopaedic Research*, vol. 28, no. 4, pp. 497–502, 2010.

[73] T. D. Nguyen, R. E. Jones, and B. L. Boyce, "Modeling the anisotropic finite-deformation viscoelastic behavior of soft fiber-reinforced composites," *International Journal of Solids and Structures*, vol. 44, no. 25-26, pp. 8366–8389, 2007.

[74] G. Limbert and M. Taylor, "On the constitutive modeling of biological soft connective tissues. A general theoretical framework and explicit forms of the tensors of elasticity for strongly anisotropic continuum fiber-reinforced composites at finite strain," *International Journal of Solids and Structures*, vol. 39, no. 8, pp. 2343–2358, 2002.

[75] A. E. Ehret, M. Itskov, and G. W. Weinhold, "A micromechanically motivated model for the viscoelastic behaviour of soft biological tissues at large strains," *Nuovo Cimento della Societa Italiana di Fisica C*, vol. 32, no. 1, pp. 73–80, 2009.

[76] K. L. Goh, J. R. Meakin, R. M. Aspden, and D. W. L. Hukins, "Stress transfer in collagen fibrils reinforcing connective tissues: effects of collagen fibril slenderness and relative stiffness," *Journal of Theoretical Biology*, vol. 245, no. 2, pp. 305–311, 2007.

[77] N. L. Nerurkar, S. Sen, B. M. Baker, D. M. Elliott, and R. L. Mauck, "Dynamic culture enhances stem cell infiltration and modulates extracellular matrix production on aligned electrospun nanofibrous scaffolds," *Acta Biomaterialia*, vol. 7, no. 2, pp. 485–491, 2011.

[78] A. E. Baer, T. A. Laursen, F. Guilak, and L. A. Setton, "The micromechanical environment of intervertebral disc cells determined by a finite deformation, anisotropic, and biphasic finite element model," *Journal of Biomechanical Engineering*, vol. 125, no. 1, pp. 1–11, 2003.

[79] X. Li, L. Wang, Y. Fan, Q. Feng, F. Z. Cui, and F. Watari, "Nanostructured scaffolds for bone tissue engineering," *Journal of Biomedical Materials Research A*, vol. 101, no. 8, pp. 2424–2435, 2013.

[80] X. Li, R. Cui, W. Liu et al., "The use of nano-scaled fibers or tubes to improve biocompatibility and bioactivity of biomedical materials," *Journal of Nanomaterials*, vol. 2013, Article ID 728130, 16 pages, 2013.

[81] X. Li, Y. Fan, and F. Watari, "Current investigations into carbon nanotubes for biomedical application," *Biomedical Materials*, vol. 5, no. 2, Article ID 022001, 2010.

[82] X. Li, H. Liu, X. Niu et al., "The use of carbon nanotubes to induce osteogenic differentiation of human adipose-derived MSCs in vitro and ectopic bone formation in vivo," *Biomaterials*, vol. 33, no. 19, pp. 4818–4827, 2012.

[83] X. Li, L. Wang, Y. Fan, Q. Feng, and F. Z. Cui, "Biocompatibility and toxicity of nanoparticles and nanotubes," *Journal of Nanomaterials*, vol. 2012, Article ID 548389, 19 pages, 2012.

[84] J. C. Iatridis, S. B. Nicoll, A. J. Michalek, B. A. Walter, and M. S. Gupta, "Role of biomechanics in intervertebral disc degeneration and regenerative therapies: what needs repairing in the disc and what are promising biomaterials for its repair?" *Spine Journal*, vol. 13, no. 3, pp. 243–262, 2013.

[85] D. J. Hamilton, C. A. Séguin, J. Wang, R. M. Pilliar, and R. A. Kandel, "Formation of a nucleus pulposus-cartilage endplate construct in vitro," *Biomaterials*, vol. 27, no. 3, pp. 397–405, 2006.

[86] A. D. Diwan, H. K. Parvataneni, S. N. Khan, H. S. Sandhu, F. P. Girardi, and F. P. Cammisa Jr., "Current concepts in intervertebral disk restoration," *Orthopedic Clinics of North America*, vol. 31, no. 3, pp. 453–464, 2000.

[87] B. M. Holzapfel, J. C. Reichert, J. T. Schantz et al., "How smart do biomaterials need to be? A translational science and clinical point of view," *Advanced Drug Delivery Reviews*, vol. 65, no. 4, pp. 581–603, 2013.

[88] I. Ahmed, I. A. Jones, A. J. Parsons et al., "Composites for bone repair: phosphate glass fibre reinforced PLA with varying fibre architecture," *Journal of Materials Science*, vol. 22, no. 8, pp. 1825–1834, 2011.

[89] C. V. Rahman, G. Kuhn, L. J. White et al., "PLGA/PEG-hydrogel composite scaffolds with controllable mechanical properties," *Journal of Biomedical Materials Research B*, vol. 101, no. 4, pp. 648–655, 2013.

[90] D. Mikociak, S. Blazewicz, and J. Michalowski, "Biological and mechanical properties of nanohydroxyapatite-containing carbon/carbon composites," *International Journal of Applied Ceramic Technology*, vol. 9, no. 3, pp. 468–478, 2012.

[91] A. Gloria, D. Ronca, T. Russo et al., "Technical features and criteria in designing fiber-reinforced composite materials: from the aerospace and aeronautical field to biomedical applications," *Journal of Applied Biomaterials and Biomechanics*, vol. 9, no. 2, pp. 151–163, 2011.

[92] N. A. Langrana, J. R. Parsons, C. K. Lee, M. Vuono-Hawkins, S. W. Yang, and H. Alexander, "Materials and design concepts for an intervertebral disc spacer. I: fiber-reinforced composite design," *Journal of Applied Biomaterials*, vol. 5, no. 2, pp. 125–132, 1994.

[93] L. Ambrosio, P. A. Netti, S. Iannace, S. J. Huang, and L. Nicolais, "Composite hydrogels for intervertebral disc prostheses," *Journal of Materials Science*, vol. 7, no. 5, pp. 251–254, 1996.

[94] X. Li, C. A. van Blitterswijk, Q. Feng, F. Cui, and F. Watari, "The effect of calcium phosphate microstructure on bone-related cells in vitro," *Biomaterials*, vol. 29, no. 23, pp. 3306–3316, 2008.

[95] K. D. Hudson, M. Alimi, P. Grunert, R. Hartl, and L. J. Bonassar, "Recent advances in biological therapies for disc degeneration: tissue engineering of the annulus fibrosus, nucleus pulposus and whole intervertebral discs," *Current Opinion in Biotechnology*, vol. 24, no. 5, pp. 872–879, 2013.

[96] V. Beachley and X. Wen, "Fabrication of nanofiber reinforced protein structures for tissue engineering," *Materials Science and Engineering C*, vol. 29, no. 8, pp. 2448–2453, 2009.

[97] J. M. Moran, D. Pazzano, and L. J. Bonassar, "Characterization of polylactic acid-polyglycolic acid composites for cartilage tissue engineering," *Tissue Engineering*, vol. 9, no. 1, pp. 63–70, 2003.

[98] X. M. Li, Y. Huang, L. S. Zheng et al., "Effect of substrate stiffness on the functions of rat bone marrow and adipose tissue derived mesenchymal stem cells in vitro," *Journal of Biomedical Materials Research A*, 2013.

[99] X. Li, H. Liu, X. Niu et al., "Osteogenic differentiation of human adipose-derived stem cells induced by osteoinductive calcium phosphate ceramics," *Journal of Biomedical Materials Research B*, vol. 97, no. 1, pp. 10–19, 2011.

[100] P. Malladi, Y. Xu, M. Chiou, A. J. Giaccia, and M. T. Longaker, "Effect of reduced oxygen tension on chondrogenesis and osteogenesis in adipose-derived mesenchymal cells," *The American Journal of Physiology*, vol. 290, no. 4, pp. C1139–C1146, 2006.

Hindawi Publishing Corporation
BioMed Research International
Volume 2013, Article ID 854917, 7 pages
http://dx.doi.org/10.1155/2013/854917

Research Article

Vascularized Bone Tissue Formation Induced by Fiber-Reinforced Scaffolds Cultured with Osteoblasts and Endothelial Cells

Xinhui Liu,[1] Guoping Zhang,[2] Chuanyong Hou,[1] Hua Wang,[1] Yelin Yang,[1] Guoping Guan,[1] Wei Dong,[2] Hongyang Gao,[2] and Qingling Feng[3]

[1] *Department of Orthopaedics, The Affiliated Jiangning Hospital of Nanjing Medical University, Nanjing 211100, China*
[2] *Department of Orthopaedics, The First Hospital of Hebei Medical University, Shijiazhuang 050031, China*
[3] *Department of Materials Science and Engineering, Tsinghua University, Beijing 100084, China*

Correspondence should be addressed to Xinhui Liu; professorlxh2008@163.com

Received 31 October 2013; Accepted 13 November 2013

Academic Editor: Xiaoming Li

Copyright © 2013 Xinhui Liu et al. This is an open access article distributed under the Creative Commons Attribution License, which permits unrestricted use, distribution, and reproduction in any medium, provided the original work is properly cited.

The repair of the damaged bone tissue caused by damage or bone disease was still a problem. Current strategies including the use of autografts and allografts have the disadvantages, namely, diseases transmission, tissue availability and donor morbidity. Bone tissue engineering has been developed and regarded as a new way of regenerating bone tissues to repair or substitute damaged or diseased ones. The main limitation in engineering in vitro tissues is the lack of a sufficient blood vessel system, the vascularization. In this paper, a new-typed hydroxyapatite/collagen composite scaffold which was reinforced by chitosan fibers and cultured with osteoblasts and endothelial cells was fabricated. General observation, histological observation, detection of the degree of vascularization, and X-ray examination had been done to learn the effect of vascularized bone repair materials on the regeneration of bone. The results show that new vessel and bone formed using implant cultured with osteoblasts and endothelial cells. Nanofiber-reinforced scaffold cultured with osteoblasts and endothelial cells can induce vascularized bone tissue formation.

1. Introduction

It is a problem to repair the damaged bone tissue caused by damage or bone disease. Some current strategies including the use of autografts and allografts have the disadvantages, namely, diseases transmission, tissue availability and donor morbidity. Thus, there is a need to develop the artificial bone substitutes to repair the damaged bone tissue. Bone tissue engineering has been regarded as a new way of regenerating bone tissues to repair or substitute damaged or diseased ones [1].

The main limitation in engineering in vitro tissues is the lack of a sufficient blood vessel system, the vascularization. In vivo, nearly all tissues are supplied with nutrients and oxygen by a highly branched system of larger blood vessels, which are subdivided in the tissue into small capillaries. Some strategies have been developed for the formation of the vessel system in vivo. The first one is based on the endothelial cells and their ability to form new vessels known as neoangiogenesis. Herein prevascularization techniques are compared to approaches in which biomolecules, such as growth factors, cytokines, peptides, and proteins, as well as cells, are applied to generate new vessels. The second strategy is focused on scaffold-based techniques. Naturally derived scaffolds, which contain vessels, are distinguished from synthetically manufactured matrices [2].

Biomaterials are often designed to mimic extracellular matrices (ECM) due to the critical role of the ECM in regulating cell function. Biomaterials with chemical and/or structural similarity to native ECM have been shown to improve cell function [3–5]. An ideal bone tissue engineering graft should have both excellent proosteogenesis and proangiogenesis to rapidly realize the bone regeneration in vivo [6]. The reconstruction of bone defects based on cell-seeded constructs requires a functional microvasculature that meets the metabolic demands of the engineered tissue. Combining

the use of cells and materials may open new options for tissue/organ repair and regeneration [7].

In this paper, a new-typed hydroxyapatite/collagen composite scaffold reinforced by chitosan fibers and cultured with osteoblasts and endothelial cells which could support the vascularization of a complex tissue engineered construct for bone [8] has been discussed. Hydroxyapatite and collagen are the main components in natural bone. It has also been proved that nHAC is a very biodegradable and biocompatible material,which can enhance the formation of new bone tissue by increasing osteoblast adhesion, osseointegration, and deposition of calcium-containing minerals on its surface [9–11]. Besides, it has been reported that chitosan can promote adhesion and functional expression of osteoblasts because of its similarity to glycosaminoglycan in structure [12–14]. The biodegradable and biocompatible nanostructured chitosan fibres were added to the scaffold and a porous collagen-based bone scaffold, strengthened with chitosan fibers, with satisfactory porosity properties was prepared. Osteoblasts and endothelial cells have been cultured with the fiber-reinforced scaffolds for the formation of vessels system in vivo.

2. Materials and Methods

2.1. Reagents and Instruments. They include lymphocyte separation medium (percoll, 1.073 g/mL, Shanghai Huamei Company); DMEM medium (Gibco, USA); heparin, ascorbic acid, dexamethasone, and glycerophosphate (Gibco, USA); trypsin (Sigma Inc., USA); fetal calf serum (Hangzhou Evergreen Company); multilabel immunoassay system (1420, WALLAC, BLCTOR2); Leica Microsystems Heidelberg (GmbH); IVcollagenase (Sigma, USA); 4% paraformaldehyde and 2% glutaraldehyde ECGF (Sigma USA); mouse antihuman factor VIII monoclonal antibody (anti-F VIII-RAg, Boster); multilabel immunoassay system (1420, WALLAC BLCTOR); centrifuge (Heraeus, Germany); inverted microscope (Chongguang Chongqing); immunofluorescence microscopy (Leica, Germany).

2.2. Materials. Chitosan fibres (80% deacetylated; diameter, 12.5 μm; tensile strength, 550 MPa) were obtained from Donghua University, China; PLLA was purchased from the Shandong Medical Appliance Factory, China, while type I collagen (at a concentration of 1%), dioxane and other chemicals were purchased from the Beijing Chemical Company Ltd, China; osteoblasts and endothelial cells of rabbit. New Zealand rabbits (8–10 weeks old, about 2 kg, without distinguishing gender). All animals were from a closed colony.

2.3. Methods

2.3.1. Preparation of Composite Scaffold Reinforced by Chitosan Fibers. The scaffold was prepared based on the study of Li et al. [5, 6]. First, type I collagen was dissolved in acetic acid to give a solution with a concentration of 0.0015 g mL^{-1}. Then, a solution containing PO_4^{3-} was added to the collagen solution until the content ratio of PO_4^{3-}/collagen reached 0.05 mol g^{-1}. Next, a solution containing Ca^{2+} was added to the previous solution until the molar ratio of Ca^{2+}/PO_4^{3-} reached 1.66, followed by the addition of NaOH solution until the pH of the system (determined with a pH meter) was about 7. Finally, after standing for 2 d, the resulting solution was centrifuged and the deposit was lyophilized after rinsing (three times) with distilled water. Subsequently, the lyophilized deposit was ground into a fine powder.

PLLA, with a weight-average molecular weight of 105 g mol^{-1}, was dissolved in dioxane (pore-forming agent) at a concentration of 0.08 g mL^{-1}. Then, nHAC powder was added to the solution until the weights of nHAC and PLLA were equal. Finally, the prepared liquid was dispersed ultrasonically for 30 min and the system lyophilized for 12 h.

The chitosan fibres were gradually added to the nHAC/PLLA solution, while being stirred with a magnetic stirrer. Then, the liquid was dispersed ultrasonically for 45 min and finally the system was lyophilized for 12 h.

The composites were cut into the size of 15 mm × 15 mm × 5 mm, sterilized by Co_{60}.

2.3.2. Vascularization of Tissue Engineering Bone In Vitro. The osteoblasts and endothelial cells were planted in the four surfaces of the prepared nanomaterials. 4–6 hours after the inoculation, the serum-free medium was added to maintain cells nutrition in vitro and the nanoscaled vascularized tissue engineering bone was prepared and retained.

2.3.3. Rabbit Radius Bone Defect Model. 30 New Zealand white rabbits (male or female) have been prepared. Sodium pentobarbital (35 mg/kg) was used for intravenous anesthesia. The rabbits were fixed in supine position. The right forelimbs of rabbits were disinfected and then cut along the anterolateral part longitudinally. Periosteum was cut apart and the 1/3 part of radial bone in the upper was exposed. Then radial bone was sawn into sections about 15 mm to make bone defect, and then periosteum was completely resected. Finally, rabbit radius bone defect model was manufactured, and the male rabbits and female rabbis were raised separately.

2.3.4. Surgical Repair of Bone Defect Animal Model. Vascularized tissue engineering bone was implanted in the rabbit radius bone defect. Use alcohol on the wound for local disinfection every day within a week after the operation and inject 2 mL lincomycin to every rabbit.

2.3.5. Obtaining Animal Specimens after Ink Perfusion. The animals were killed, respectively, after 4, 8, and 12 weeks. The animals were under general anesthesia before obtaining specimens. Cut apart the rabbit, expose the heart, and inject ink-formaldehyde mixture (ink : formaldehyde = 6 : 1) about 10 mL into the left ventricle, until observing that the skin and mucous membranes of rabbit's face turn black. Obtain the specimens after 2 h. The specimens were placed into 10% formaldehyde solution for the latter histological examination.

2.4. Observation and Testing Indicators

2.4.1. General Observation. After surgery, the animal's diet, activity and other systemic conditions, local wound healing, and limb swelling were observed. Angiogenesis on the specimen surface and the materials degradation were observed after obtaining the specimens.

2.4.2. Histological Observation. Specimens had been decalcified for 15 days after being fixed with formaldehyde. Embed specimens in paraffin and slice with a slicing machine at the thickness of 20 μm for the observation of angiogenesis and osteogenesis.

2.4.3. Detection of the Degree of Vascularization. Three horizons of each slice from the ink perfusion specimens which were obtained at week 4, week 8, and week 12 were randomly selected. Ink image is collected and entered into a computer image analysis system; the ink color percentages of area occupied by the image were calculated to obtain the degree of vascularization.

2.4.4. X-Ray Examination. Take photos with the Philips 500 mAX ray machine in a small focus and shoot the film, at weeks 4, 8, and 12 after surgery. The exposure conditions were unified, at 45 Kv, 3–5 mAs. Callus formation and bone healing of bone defects area were observed.

3. Results

3.1. General Observation. The diet and activity of rabbits are normal after the surgery. The limbs were mildly swelling and then detumescence occured after 1 week. Except the four rabbits that died of unexplained diarrhea accidentally, all the other rabbits were surviving until the period required for the experiment. In addition, all the wounds of the rabbit were healing and the sutures were bit away by the rabbits themselves.

Four weeks after the surgery, all plants kept steady without position changing. There were fibrous connective tissue connecting together between the materials and radius bone. Complete fibrous tissue capsule formed on the surface of the implants, while the combination between the capsule and implants was loosened. A large number of blood vessels dyed black ink can be seen. Eight weeks after the surgery, the combination between the radius bone and the implants was stable, as well as the combination between capsule and implants. The area of blood vessels dyed black ink was more than 4 weeks ago. 12 weeks after the surgery, the combination between the radius bone and the implants became firm. The bounds between bone and implants were indistinct.

3.2. Histological Observation. 8, 8, and 12 specimens were obtained at week 4, week 8, and week 12. The ink perfusion tissue sections and conventional tissue sections occupied half, respectively, among the specimens obtained at different periods.

At week 4, it could be observed that fibrous connective tissue had grown inside the implant materials and separated the materials in the ink perfusion specimens. Most of the area of the ink perfusion specimens appeared in ink color. It was demonstrated that the new vessel had formed and had been dyed. Only the center of the specimens had not been dyed. It was demonstrated that new vessel had not formed at this part. A large moment of fibrous callus and osteoid had formed in the dyed part. The original shape of the implant materials had gradually disappeared and just only remained in the center of the material. Osteogenesis phenomenon had not been seen at week 4 (Figure 1(a)). New vessel could be seen in the conventional tissue sections, as well as the endothelial cells of the periphery vessel wall and a large number of erythrocytes in the blood vessel. A mass of fibroblasts, a number of lymphocytes, plasma cells, and neutrophils can be observed as well as osteoclasts and osteoblasts. Prototype materials had disappeared and materials had been replaced by fibrous osteotylus. A small amount of osteoid formed. New blood vessel could not be seen in the center of the conventional tissue sections as well as the bone repair phenomena. The original shape of the implant materials had been clear in the center of the conventional tissue sections (Figure 1(b)).

At week 8, it could be observed that more fibrous connective tissue had grown into the materials. New vessels had formed, as the center of the specimens turned black. Osteoid could be seen in most part of the ink perfusion pecimens (Figure 2(a)). Fibrous callus could be seen in the center of the conventional tissue sections. Osteoid could also be seen in the most part of the materials. A small amount of bone callus could be seen around the materials which had been divided. Monocytes, plasma cells, and lymphocytes had disappeared and been replaced by a number of fibroblasts, osteoblasts, and osteoclasts (Figure 2(b)).

At week 12, the ink color of the ink perfusion specimens had turned light and had been replaced by the red color of a large amount of osteoids, which formed recently in the ink perfusion group. All materials were already fully vascularized. Scattered new bone osteotylus, osteoid and a small amount of fibrous osteotylus existed at the same time. The newly formed bone callus gradually joined together to form a larger bone callus (Figure 3(a)). These phenomena could be seen even more clearly in the conventional slice. The bone lacunae and osteocyte could be observed in the bone osteotylus. Osteoclasts could be seen around the newly formed the bone osteotylus. It meant that new bone was forming when bone repaired and remodeled (Figure 3(b)).

3.3. Detection of the Degree of Vascularization. 13 ink perfusion specimens were obtained, respectively, in this experiment (4 specimens at week 4, 8 specimens at week 8, 5 specimens at week 12). Vascularized area gradually increased and then further increased to 100 percentages at week 12 (Table 1).

3.4. X-Ray Examination. X-ray examination was done as soon as the surgery was finished. It was successful to make

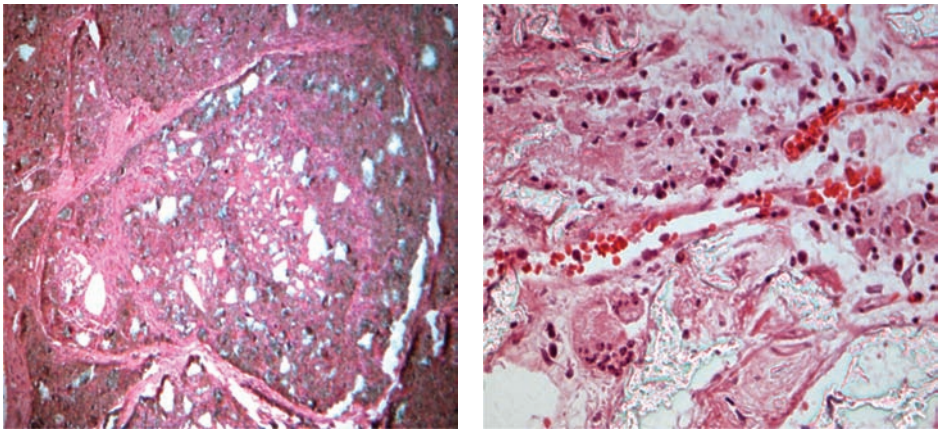

(a) (b)

Figure 1: Different tissue sections with different enlargement factors at week 4 ((a) 100 times enlarged ink perfusion tissue sections; (B) 400 times enlarged conventional tissue sections).

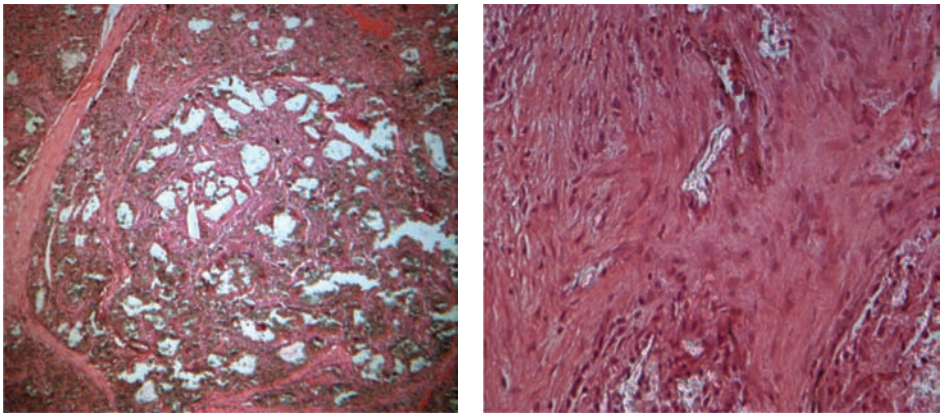

(a) (b)

Figure 2: Different tissue sections with different enlargement factors at week 8 ((a) 100 times enlarged ink perfusion tissue sections; (b) 400 times enlarged conventional tissue sections).

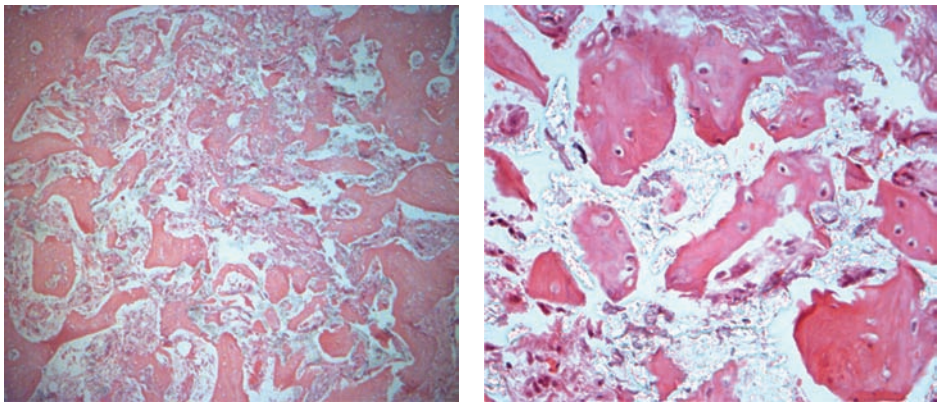

(a) (b)

Figure 3: Different tissue sections with different enlargement factors at week 12 ((a) 100 times enlarged ink perfusion tissue sections; (b) 400 times enlarged conventional tissue sections).

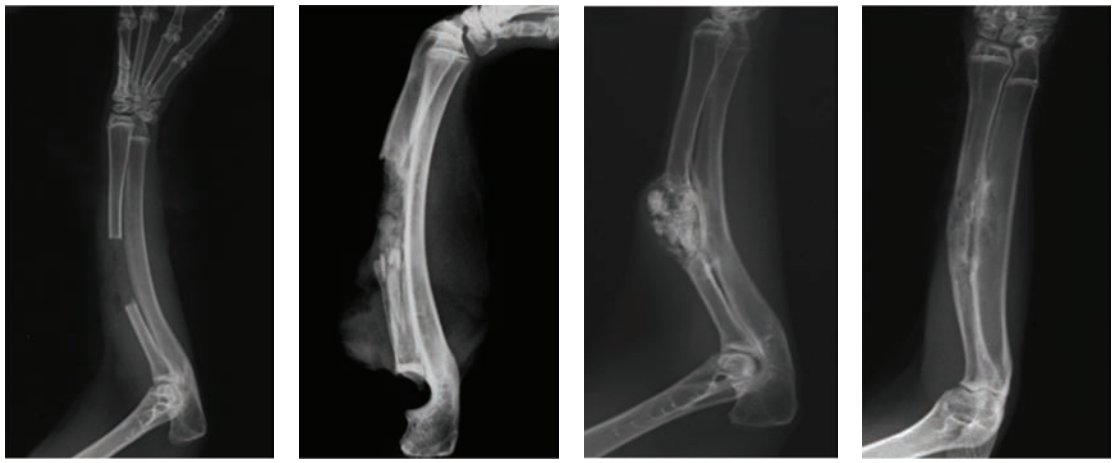

(a) (b) (c) (d)

Figure 4: X-ray image of the rabbits' radial bones taken at different periods. (a) X-ray image after making bone defect about 15 mm; (b) X-ray image at week 4; (c) X-ray image at week 8; (d) X-ray image at week 12.

Table 1: The degree of vascularization at different period.

4 w	8 w	12 w
85.13 ± 0.21	96.77 ± 0.24	100

bone defect about 15 mm at the upper one-third radial bones (Figure 4(a)).

The implants develop with low density. There were some high-density developments in the bone defect area. It meant that new bone had formed at week 4 (Figure 4(b)).

The high-density development caused by bone formation at week 8 turned larger than that at week 4 (Figure 4(c)). It could be seen that new bone formed in bone defect area and had connected the farther and the nearer side. The bone marrow cavity had formed in the newly formed bone at week 12 (Figure 4(d)).

4. Discussion

Bone grafting is the preferred method to treat bone defects [15, 16]. Vascularization of the graft determines whether the bone grafting is successful. In vivo nearly all tissues are supplied with nutrients and oxygen by a highly branched system of larger blood vessels, which are subdivided in the tissue into small capillaries. A good environment ensures the growth, differentiation, and proliferation of osteoblasts [4, 17, 18]. In the process of bone healing, mineral deposition is the main mechanism of blood flow control, rather than the physiological metabolic changes of periosteum. All in all, vascularization and osteogenic cells are closely related.

Current strategies for bone grafts including the use of autografts, allografts, and synthetic grafts have drawbacks. Bone tissue engineering provides a new way for regenerating bone tissues to repair or substitute damaged or diseased ones [19–24]. While the main limitation in engineering in vitro tissues is the lack of a sufficient blood vessel system, the vascularization, as well as the bone tissue engineering. Successful cell-based tissue engineering requires a rapid and thorough vascularization in order to ensure long-term implant survival and tissue integration [25, 26]. To rebuild the blood supply at the same time of building bone tissue engineering Is a main problem. The lack of adequate nutrition may have bad effect on the proliferation, differentiation, and secretion of seed cells in vitro environment and even cause the death of the seed cells, after the implantation of artificial bone. Thus, establishing blood transfer system as soon as possible can retain the osteogenesis advantage of artificial bone and bring more osteoblasts factor which can further promote the rapid regeneration of bone tissue.

The reconstruction of bone defects based on cell-seeded constructs requires a functional microvasculature that meets the metabolic demands of the engineered tissue. So, strategies that augment neovascularization need to be identified [27]. We propose an in vitro strategy consisting of the simultaneous culture of osteoblasts and endothelial cells on a collagen-based scaffold for the formation of prevascular structures, with the final aim of accelerating the establishment of a vascular bed in the implanted construct and supports the reformation of bone. In this paper, the vascularized tissue engineering bone cultured with vascular osteoblasts and endothelial cells was used as implant to repair the rabbit's radius bone defect. The ink perfusion method was used to study the angiogenesis and the relationship between angiogenesis and oteogenesis.

Ink was perfused into the left ventricle of rabbit. The tissue can only be dyed black at the existence of vessel. The ink color could be seen where new tissue formed, because there was no vessel in the materials we implant previously. The black area of ink perfusion specimens increased gradually as time passed. It meant that it was possible to vascularize the artificial bone cultured with vascular endothelial cells and that vascular endothelial cells were ideal seed cells for vascularization [28–30].

The size of the bone defect is directly related to the objectivity and reliability of the experiment. Hollinger and Kleinschmidt [31] proposed the concept of critical size of bone defects. Critical size of bone defects is the size that the bone defect cannot be self-healing without implants in experimental animals. The size of rabbit radius bone defect was based on this principle. It has been demonstrated that the rabbits can repair themselves with the size of bone defect which is less than 15 mm. Rabbit radius bone defect modeling was used in this experiment. Vascularized tissue engineering bone was implanted in this rabbit radius bone defect. Histological observation and X-ray examination were used to demonstrate the good ability to repair bone. The result showed that the HA/collagen composites were ideal extracellular matrix material and had a good biocompatibility in vivo. HA/collagen composites were promising to be an ideal bone substitute.

After scaffold implantation, the growth of capillaries into the porous construct may be too slow to provide adequate nutrients to the cells in the scaffold interior and this inhibits tissue formation in the scaffold core. It was found that the cell differentiation did not happen inside the tissue engineering bone constructed by implanted seed cells on the surface of materials. Vascularization and osteogenesis of the implant may be accelerated by using three-dimensional culture technology and culturing the seed cells inside the materials. Supporting nutrient and maintaining physiological function of tissue engineering bone in vivo were still a main problem. In short, the vascularization of tissue engineering bone will always be a task we should continue.

5. Conclusions

The present study demonstrates that the nanofiber reinforced HA/collagen composites cultured with osteoblasts and endothelial cells can induce vascularized bone tissue formation. The composites have a good biocompatibility in vivo and are promising to be an ideal bone substitute, which can be implanted as bone graft with inducing visualization and osteogenesis. However, because of the poor vascularization inside of scaffolds, further studies should investigate new strategies that can accelerate and improve the vascularization process in bone, where vascularization is a prerequisite to achieving optimal regeneration.

Conflict of Interests

The authors declare that they have no financial or personal relationship with any people or organization that may inappropriately influence their work; there is no professional or commercial interest of any kind in all the commercial identities mentioned in their paper.

References

[1] X. M. Li, Y. Yang, Y. B. Fan, Q. L. Feng, F. Z. Cui, and F. Watari, "Biocomposites reinforced by fibers or tubes, as scaffolds for tissue engineering or regenerative medicine," *Journal of Biomedical Materials Research A*, 2013.

[2] E. C. Novosel, C. Kleinhans, and P. J. Kluger, "Vascularization is the key challenge in tissue engineering," *Advanced Drug Delivery Reviews*, vol. 63, no. 4, pp. 300–311, 2011.

[3] J. Jang, O. Castano, and H. Kim, "Electrospun materials as potential platforms for bone tissue engineering," *Advanced Drug Delivery Reviews*, vol. 61, no. 12, pp. 1065–1083, 2009.

[4] X. Li, Q. Feng, W. Wang, and F. Cui, "Chemical characteristics and cytocompatibility of collagen-based scaffold reinforced by chitin fibers for bone tissue engineering," *Journal of Biomedical Materials Research B*, vol. 77, no. 2, pp. 219–226, 2006.

[5] X. M. Li, L. Wang, Y. B. Fan, Q. L. Feng, F. Z. Cui, and F. Watari, "Nanostructured scaffolds for bone tissue engineering," *Journal of Biomedical Materials Research A*, vol. 101, pp. 2424–2435, 2013.

[6] L. Cao, J. Wang, J. Hou et al., "Vascularization and bone regeneration in a critical sized defect using 2-N, 6-O-sulfated chitosan nanoparticles incorporating BMP-2," *Biomaterials*, vol. 35, pp. 684–698, 2014.

[7] X. M. Li, Y. Huang, L. S. Zheng et al., "Effect of substrate stiffness on the functions of rat bone marrow and adipose tissue derived mesenchymal stem cells in vitro," *Journal of Biomedical Materials Research A*, 2013.

[8] S. Fuchs, S. Ghanaati, C. Orth et al., "Contribution of outgrowth endothelial cells from human peripheral blood on in vivo vascularization of bone tissue engineered constructs based on starch polycaprolactone scaffolds," *Biomaterials*, vol. 30, no. 4, pp. 526–534, 2009.

[9] X. Li, H. Liu, X. Niu et al., "Osteogenic differentiation of human adipose-derived stem cells induced by osteoinductive calcium phosphate ceramics," *Journal of Biomedical Materials Research B*, vol. 97, no. 1, pp. 10–19, 2011.

[10] X. M. Li, L. Wang, Y. B. Fan, Q. L. Feng, and F. Z. Cui, "Biocompatibility and toxicity of nanoparticles and nanotubes," *Journal of Nanomaterials*, vol. 2012, Article ID 548389, 19 pages, 2012.

[11] X. M. Li, X. H. Liu, M. Uo, Q. L. Feng, F. Z. Cui, and F. Watari, "Investigation on the mechanism of the osteoinduction for calcium phosphate," *Bone*, vol. 43, pp. S111–S112, 2008.

[12] X. Li, X. Liu, W. Dong et al., "In vitro evaluation of porous poly(L-lactic acid) scaffold reinforced by chitin fibers," *Journal of Biomedical Materials Research B*, vol. 90, no. 2, pp. 503–509, 2009.

[13] X. M. Li, R. R. Cui, W. Liu et al., "The use of nano-scaled fibers or tubes to improve biocompatibility and bioactivity of biomedical materials," *Journal of Nanomaterials*, vol. 2013, Article ID 728130, 16 pages, 2013.

[14] X. M. Li and Q. L. Feng, "Dynamic rheological behaviors of the bone scaffold reinforced by chitin fibres," *Materials Science Forum*, vol. 475–479, pp. 2387–2390, 2005.

[15] X. Li, Q. Feng, X. Liu, W. Dong, and F. Cui, "Collagen-based implants reinforced by chitin fibres in a goat shank bone defect model," *Biomaterials*, vol. 27, no. 9, pp. 1917–1923, 2006.

[16] X. Li, Q. Feng, Y. Jiao, and F. Cui, "Collagen-based scaffolds reinforced by chitosan fibres for bone tissue engineering," *Polymer International*, vol. 54, no. 7, pp. 1034–1040, 2005.

[17] S. Checa and P. J. Prendergast, "Effect of cell seeding and mechanical loading on vascularization and tissue formation inside a scaffold: a mechano-biological model using a lattice approach to simulate cell activity," *Journal of Biomechanics*, vol. 43, no. 5, pp. 961–968, 2010.

[18] X. Li, H. Liu, X. Niu et al., "The use of carbon nanotubes to induce osteogenic differentiation of human adipose-derived

MSCs in vitro and ectopic bone formation in vivo," *Biomaterials*, vol. 33, no. 19, pp. 4818–4827, 2012.

[19] X. Li and Q. Feng, "Porous poly-L-lactic acid scaffold reinforced by chitin fibers," *Polymer Bulletin*, vol. 54, no. 1-2, pp. 47–55, 2005.

[20] X. M. Li, X. H. Liu, G. P. Zhang et al., "Repairing 25 mm bone defect using fibres reinforced scaffolds as well as autograft bone," *Bone*, vol. 43, pp. S94–S94, 2008.

[21] X. Li, Q. Feng, and F. Cui, "In vitro degradation of porous nano-hydroxyapatite/collagen/PLLA scaffold reinforced by chitin fibres," *Materials Science and Engineering C*, vol. 26, no. 4, pp. 716–720, 2006.

[22] X. Li, H. Gao, M. Uo et al., "Maturation of osteoblast-like SaoS2 induced by carbon nanotubes," *Biomedical Materials*, vol. 4, no. 1, Article ID 015005, 2009.

[23] X. Li, X. Liu, J. Huang, Y. Fan, and F. Cui, "Biomedical investigation of CNT based coatings," *Surface and Coatings Technology*, vol. 206, no. 4, pp. 759–766, 2011.

[24] X. Li, Y. Fan, and F. Watari, "Current investigations into carbon nanotubes for biomedical application," *Biomedical Materials*, vol. 5, no. 2, Article ID 022001, 2010.

[25] S. Ghanaati, R. E. Unger, M. J. Webber et al., "Scaffold vascularization in vivo driven by primary human osteoblasts in concert with host inflammatory cells," *Biomaterials*, vol. 32, no. 32, pp. 8150–8160, 2011.

[26] J. Rouwkema, N. C. Rivron, and C. A. van Blitterswijk, "Vascularization in tissue engineering," *Trends in Biotechnology*, vol. 26, no. 8, pp. 434–441, 2008.

[27] M. I. Santos, R. E. Unger, R. A. Sousa, R. L. Reis, and C. J. Kirkpatrick, "Crosstalk between osteoblasts and endothelial cells co-cultured on a polycaprolactone-starch scaffold and the in vitro development of vascularization," *Biomaterials*, vol. 30, no. 26, pp. 4407–4415, 2009.

[28] Z. Zhang, W. D. Ito, U. Hopfner et al., "The role of single cell derived vascular resident endothelial progenitor cells in the enhancement of vascularization in scaffold-based skin regeneration," *Biomaterials*, vol. 32, no. 17, pp. 4109–4117, 2011.

[29] X. Li, C. A. van Blitterswijk, Q. Feng, F. Cui, and F. Watari, "The effect of calcium phosphate microstructure on bone-related cells in vitro," *Biomaterials*, vol. 29, no. 23, pp. 3306–3316, 2008.

[30] X. Li, H. Gao, M. Uo et al., "Effect of carbon nanotubes on cellular functions in vitro," *Journal of Biomedical Materials Research A*, vol. 91, no. 1, pp. 132–139, 2009.

[31] J. O. Hollinger and J. C. Kleinschmidt, "The critical size defect as an experimental model to test bone repair materials," *The Journal of Craniofacial Surgery*, vol. 1, no. 1, pp. 60–68, 1990.